UNIVERSITY OF CALIFORNIA, SAN DIEGO

The Mechanics of SR protein Phosphorylation by the Splicing Kinases SRPK1 and Clk/Sty

A dissertation submitted in partial satisfaction of the

requirements for the degree Doctor of Philosophy

in

Biomedical Sciences

by

Jonathan Charles Hagopian

Committee in charge:

Professor Joseph Adams, Chair
Professor Xiang-Dong Fu, Co-Chair
Professor Pieter Dorrestein
Professor Gourisankar Ghosh
Professor Susan Taylor

2008

The dissertation of Jonathan Charles Hagopian is approved, and acceptable in quality and form for publication electronically and on microfilm:

_____

_____

_____

_____
Co-Chair

_____
Chair

University of California, San Diego

2008

TABLE OF CONTENTS

LIST OF FIGURES

ACKNOWLEDGMENTS

I thank my advisor, Dr. Joseph Adams, for giving me the opportunity to work in his lab. I deeply appreciate his constant mentorship, support, and enthusiasm for research.

I thank my co-advisor, Dr. Xiang-Dong Fu, for all of his efforts, which have grounded this work in sound biological principles.

I thank Dr. Pieter Dorrestein for taking interest in my project, and showing me the power of mass spectrometry.

I thank Dr. Gourisankar Ghosh for providing structural insights that are so critical for understanding this complex system.

I thank Dr. Susan Taylor for her great enthusiasm for science.

I thank Dr. Patricia Jennings for encouraging me to wear a bicycle helmet, like a good mother should.

I thank Dr. Palmer Taylor, Dr. Vivian Hook, and Dr. Tracy Handle for their recognition and support of my love for teaching.

I thank Dr. Mark Kamps, Dr. Ken Kaushansky, Dr. Rahul Jandial, Dr. Hoi Sang U, Dr. Christopher Kane, Dr. Tony Reid, and Dr. Paul Fanta for their mentorship during my HHMI "Med-Into-Grad" fellowship. Thank you HHMI.

I thank my lab mate Chen-ting Ma for always having my back.

I thank the UCSD Pharmacology Training Grant for four years of generous support. Thank you NIH.

I thank my wife Alison Metz Hagopian, my family, my friends, my dog Grace, and the Pacific Ocean for the joy they bring to my life.

The text of Chapter III is a reprint of the material as it appears in *The Journal of Biological Chemistry*, 2005, 280(50), 41761-8, Velazquez-Dones, A., Hagopian, J.C., Ma, C.T., Zhong, X.Y., Zhou, H., Ghosh, G., Fu, X.D., Adams, J.A. The dissertation author was a primary researcher and author of this publication. Additional text of Chapter III is a reprint of the material as it appears in *Molecular Biology of the Cell*, 2006, 17(2), 876-85, Ding, J.H., Zhong, X.Y., Hagopian, J.C., Cruz, M.M., Ghosh, G., Feramisco, J., Adams, J.A., Fu, X.D. The dissertation author was a collaborative researcher and co-author of this publication.

The text of Chapter IV is a reprint of the material as it appears in *The Journal of Molecular Biology*, 2008, 382(4), 894-909, Hagopian, J.C., Ma, C.T., Meade, B.R., Albuquerque, C.P., Ngo, J., Ghosh, G., Jennings, P.A., Fu, X.D., Adams, J.A. The dissertation author was the primary researcher and author of this publication.

The text of Chapter V is, in part, a reprint of the material as it appears in *Molecular Cell*, 2008, 29(5), 563-76, Ngo, J.C., Giang, N., Chakrabarti, S., Ma, C.T., Huynh, N., Hagopian, J.C., Dorrestein, P.C., Fu X.D., Adams, J.A., Ghosh, G. The dissertation author was a collaborative researcher and co-author of this publication.

VITA

EDUCATION

1991-1996	B.S., B.S., University of California, Santa Barbara
2003-2008	Ph.D., University of California, San Diego

HONORS AND AWARDS

2008	HHMI Med-Into-Grad Fellowship, Cancer Division
2003-2008	NIH Predoctoral Fellowship, UCSD Pharmacology Training Grant
2002-2003	Organization of American States Academic Fellowship
2000-2001	United States Fulbright Fellowship
1996	Distinction in Major / High Honors
1995-1996	HHMI Undergraduate Research Fellowship
1994	NSF Undergraduate Research Fellowship

TEACHING EXPERIENCE

2004-2008	Graduate Teaching Assistant, Graduate School of Pharmacy (UCSD)
1996	Undergraduate Teaching Assistant, Biological Sciences (UCSB)

RESEARCH EXPERIENCE

2003-2008	Laboratories of Dr. Joseph Adams and Dr. Xiang-Dong Fu Dept. of Pharmacology, Dept. of Cell and Molecular Medicine University of California, San Diego
2000-2003	Laboratory of Dr. Mariana Cabral de Oliveira Biological Sciences Institute University of Sao Paulo, Brazil
1997-2000	Laboratory of Dr. John Lew Dept. of Biomolecular Science and Engineering University of California, Santa Barbara
1995-1996	Laboratory of Dr. Daniel Morse Dept. of Biomolecular Science and Engineering University of California, Santa Barbara
1994	Tropical Field Station of Dr. Robert Warner Christiansted, St. Croix, U.S. Virgin Islands Dept. of Evolution, Ecology, and Marine Biology Universtiy of California, Santa Barbara

PUBLICATIONS

Hagopian, J.C., Ma, C.T., Meade, B.R., Albuquerque, C.P., Ngo, J., Ghosh, G., Jennings, P.A., Fu, X.D., Adams, J.A. "Adaptable Molecular Interactions Guide Phosphorylation of the SR Protein ASF/SF2 by SRPK1." *J Mol Biol.* 2008, 382(4):894-909.

Velazquez-Dones, A.*, Hagopian, J.C.*, Ma, C.T., Zhong, X.Y., Zhou, H., Ghosh, G., Fu, X.D., Adams, J.A. "Mass spectrometric and kinetic analysis of ASF/SF2 phosphorylation by SRPK1 and Clk/Sty." *J Biol Chem*. 2005, 280(50):41761-8. *co-first authorship

Ma, C.T., Velazquez-Dones A., Hagopian J.C., Ghosh G., Fu X.D., Adams J.A. "Ordered multi-site phosphorylation of the splicing factor ASF/SF2 By SRPK1." *J Mol Biol*. 2008, 376(1):55-68.

Ngo, J.C., Giang, N., Chakrabarti, S., Ma, C.T., Huynh, N., Hagopian, J.C., Dorrestein, P.C., Fu X.D., Adams, J.A., Ghosh, G. "A roving docking interaction is essential for sequential and processive phosphorylation of an SR protein by the SR protein kinase." *Mol Cell.* 2008, 29(5):563-76.

Lukasiewicz, R., Velazquez-Dones, A., Huynh, N., Hagopian, J., Fu, X.D., Adams, J., Ghosh, G. "Structurally unique yeast and mammalian serine-arginine protein kinases catalyze evolutionarily conserved phosphorylation reactions." *J Biol Chem*. 2007, 282(32):23036-43.

Ding, J.H., Zhong, X.Y., Hagopian, J.C., Cruz, M.M., Ghosh, G., Feramisco, J., Adams, J.A., Fu, X.D. "Regulated cellular partitioning of SR protein-specific kinases in mammalian cells." *Mol Biol Cell*. 2006, 17(2):876-85.

Hagopian, J.C., Reis, M., Kitajima, J.P., Bhattacharya, D., de Oliveira M.C. "Comparative analysis of the complete plastid genome sequence of the red alga *Gracilaria tenuistipitata var. liui* provides insights into the evolution of rhodoplasts and their relationship to other plastids." *J Mol Evol*. 2004, 59(4):464-77.

Hagopian, J.C., Nyvall, P., de Oliveira, M.C. "Purification of plastid DNA from an enriched rhodoplast fraction of the red alga *Gracilaria tenuistipitata*." *Plant Mol Biol Rep.* 2002, 20, 1-8.

Hagopian, J.C., Kirtley, M.P., Stevenson, L.M., Gergis, R.M., Russo, A.A., Pavletich, N.P., Parsons, S.M., Lew, J. "Kinetic basis for activation of cdk2/cyclinA by phosphorylation." *J Biol Chem*. 2000, 276: 275-80.

Stevenson, L.M., Deal, M.S., Hagopian, J.C., Lew, J. "Activation mechanism of cdk2/cyclinA: Role of cyclin binding versus phosphorylation." *Biochemistry* 2002, 41, 8528-34.

Prowse, C., Hagopian, J.C., Cobb, M.H., Ahn, N.G., Lew, J. "Catalytic reaction pathway for the mitogen-activated protein kinase ERK2." *Biochemistry* 2000, 39 (20): 6258-66.

ABSTRACT OF THE DISSERTATION

The Mechanics of SR protein Phosphorylation by the

Splicing Kinases SRPK1 and Clk/Sty

by

Jonathan Charles Hagopian

Doctor of Philosophy in Biomedical Science

University of California, San Diego

Professor Joseph Adams, Chair
Professor Xiang-Dong Fu, Co-Chair

The SR protein family of splicing factors plays critical roles in many facets of RNA metabolism such as constitutive and alternative splicing, mRNA export, and transcription. SR proteins are carefully regulated by phosphorylation in vivo. Phosphorylation and dephosphorylation events influence protein-protein interactions that determine SR protein localization and recruitment to and from active sites of transcription and translation in the cell. Phosphorylation of SR proteins is an important regulatory mechanism of gene expression at the post-transcriptional level. The SR proteins and the kinases that regulate them are linked to multiple neurodegenerative disease states and cancer. Therefore, detailed understanding of SR kinase catalysis with SR proteins is necessary to elucidate biological mechanisms of regulation and to provide a foundation for novel therapeutic modalities.

The finding that spacer deleted SRPK1 processively phosphorylates its substrate ASF/SF2 has important implications for the biological activity of this splicing factor in mammalian cells. We have reproduced this result with full-length

independently purified components in a novel efficient start-trap system that utilizes a catalytically inactive form of the kinase. We show that like SRPK1, phosphorylation of ASF/SF2 by Clk/Sty occurs in a processive manner. The SRPK1 spacer domain was found to have minimal contribution to kinetic and thermodynamic properties with its substrate. We determined that SRPK1 preferentially phosphorylates the N-terminal portion of the ASF/SF2 RS domain, and that SRPK1 and Clk/Sty cooperate to completely phosphorylate this region of the splicing factor.

To investigate the unusual high affinity of SRPK1 for its substrate, we analyzed multiple domains of ASF/SF2 by developing a competitive inhibition assay from which equilibrium dissociation constants could be determined in the form K_I. We discovered that the kinase makes low nano-molar contacts with residues in both the RRM and RS domains of ASF/SF2. The absence of additive thermodynamics in the context of SRPK1 interaction with full-length ASF/SF2 indicates that the kinase utilizes sub-optimal recognition of its substrate during catalysis to allow the flexibility required for poly-phosphorylation of the RS domain.

The final studies of this thesis employed high-resolution FT-ICRMS to refine our understanding of ASF/SF2 phosphorylation by SRPK1. We report that SRPK1 phosphorylates 14-15 residues of ASF/SF2, and that this endpoint did not change for RRM deletion constructs. We demonstrate mechanistic changes that reflect enzyme kinetics with an aggregated substrate. And finally, we show that the phospho-serine observed in the SRPK1ΔNS:ASF/SF2ΔRRM1 crystal structure was due to ATP contaminated AMPPNP. A result that significantly furthered insights gained from this complex structure.

Chapter I

General Introduction

A. Pre-mRNA splicing

The recent discovery that the human genome is composed of a surprisingly limited number of genes has made it clear that alternative splicing mechanisms are critical for the generation of a diverse proteome. It has been estimated that 75% of human genes are alternatively spliced mRNA variants (Modrek and Lee, 2002). Most eukaryotic proteins are coded by discontinuous genetic sequences called exons (Padgett et al., 1986; Sharp, 1985). As the gene is transcribed in the nucleus, non-coding sequences called introns are removed from pre-mRNA, by a catalytic complex called the spliceosome, to form mature mRNA that is subsequently transported to the cytoplasm for translation. Constitutive splicing occurs when all of the exons in a gene are brought together in a linear fashion to form a single gene product. The same gene can have its exons joined in different ways by the spliceosome to produce multiple gene products via alternative splicing (Figure 1.1).

Pre-mRNA splicing occurs co-transcriptionally in the nucleus at a macromolecular complex composed of many RNA and protein molecules known as the spliceosome (Proudfoot et al., 2002; Stojdl and Bell, 1999). The steps of spliceosome maturation occur in sequential phases that integrate the binding of small nuclear ribonucleoproteins (snRNPs: U1, U2, U4, U5, and U6) and many non-snRNPs (Figure 1.2). The great specificity of splice-site selection is mediated by many factors, including RNA consensus sequences at the 5', 3', and branch point sites. In the last decade it has become apparent that both the assembly of the spliceosome and selection of splice sites depend on the proper phosphorylation of a family of splicing factors

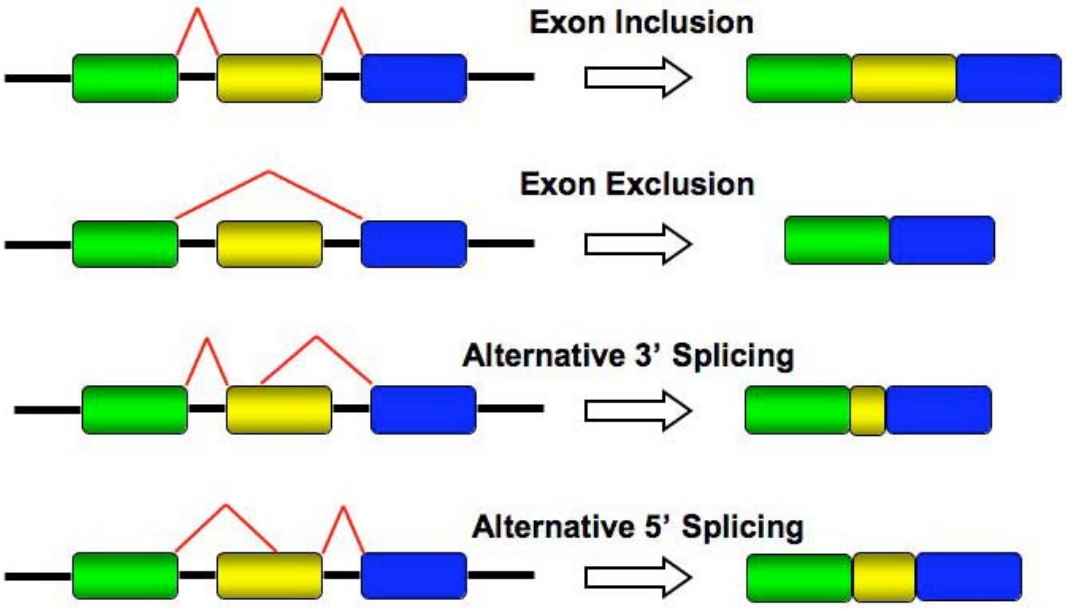

Figure 1.1 Alternative Splicing. Different forms of alternative splicing create diverse combinations of exons in mature mRNA transcripts to eventually expand the diversity of the proteome beyond that of the genome.

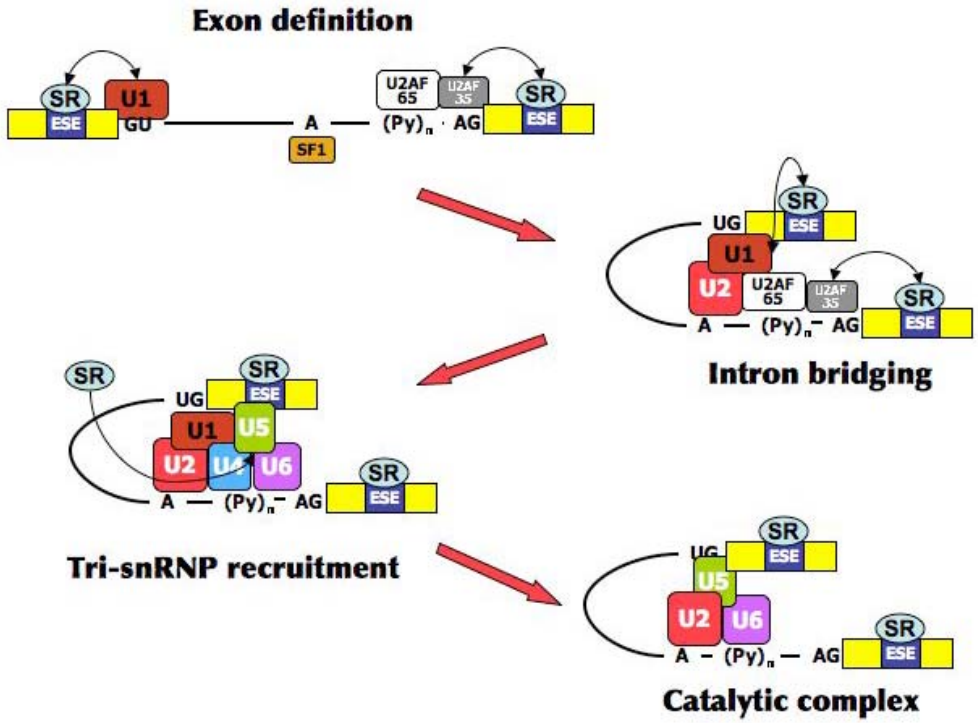

Figure 1.2 Spliceosome assembly. Spliceosome assembly involves sequential phases of snRNP recruitment mediated by SR protein splicing factors.

known as SR proteins (Misteli et al., 1998; Misteli and Spector, 1999; Modrek and Lee, 2002; Yeakley et al., 1999). Few genes have been shown to splice constitutively and alternatively in an RS domain independent manner (Zhu and Krainer, 2000). SR proteins have a unique modular structure with one or two N-terminal RNA recognition domains (RRMs) and a C-terminal RS domain composed of multiple arginine-serine dipeptide repeats. Phosphorylated SR proteins are believed to facilitate both 5' and 3' splice site recognition through interaction with the RS domain of the 70 kDa subunit of U1 and the 35 kDa subunit of the U2AF heterodimer (Jamison et al., 1995; Xiao and Manley, 1997, 1998). Phosphorylated SR proteins also facilitate subsequent steps of spliceosome assembly including intron bridging, recruitment of the U4/U5/U6 tri-snRNP to form the B complex, and splicing catalysis (Chew et al., 1999; Roscigno and Garcia-Blanco, 1995). The SR proteins influence alternative splicing by binding to exon splicing enhancer sequences (ESE), where they recruit the U2AF factor to weak 3' splice sites and antagonize the splice site silencing effects of heterogeneous nuclear ribonucleoproteins (hnRNPs) (Graveley, 2000). In addition to these important protein-protein interactions, RS domains of SR proteins have been shown to interact specifically with critical cis-acting elements in pre-mRNA in a phosphorylation dependent manner (Shen and Green, 2004; Shen et al., 2004) (Figure 1.3).

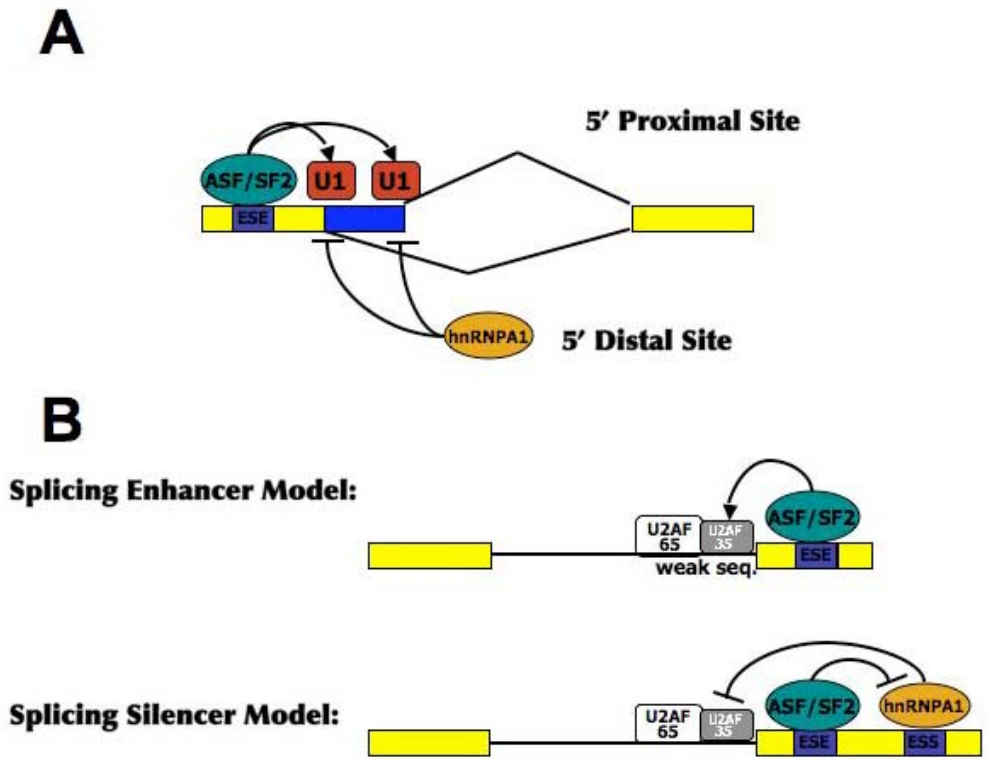

Figure 1.3 SR protein regulation of alternative splicing. Alternative splicing is influenced by the activity of SR protein splicing factors like ASF/SF2. A) 5' splice site selection is influenced by SR proteins bound to cis-acting elements known as exonic splicing enhancer (ESE) sequences in pre-mRNA. SR proteins bound to ESE's can direct the U1 snRNP to initiate spliceosome assembly at alternate 5' sites. B) 3' splice site selection is mediated in a similar fashion by SR proteins that can enhance recruitment of the U2AF factor to weak 3' splice sites and counteract the inhibitory effects of hnRNPA1.

B. SR Protein Localization

There are two well-established families of SR protein kinases in mammalian cells. The SRPKs are primarily localized in the cytoplasm, with a fraction detectable in the nuclei during interphase (Ding et al., 2006; Wang et al., 1999). SRPK1 was the original kinase determined to be capable of catalyzing the RS domain phosphorylation required for spliceosome assembly and activity (Gui et al., 1994b). It is now clear that SRPK phosphorylation of serine residues induces nuclear import of SR proteins by enhancing their affinity for the nuclear import receptor transportin-SR (Yun and Fu, 2000; Yun et al., 2003) (Figure 1.4). Once in the nucleus, SR proteins converge in complex structures called nuclear speckles. Speckles are thought to be dynamic centers of transcription and mRNA processing (Hall et al., 2006). SRPK overexpression affects the distribution of SR proteins in the nucleus, indicating that SRPKs can also influence SR protein activity beyond the cytoplasm (Ding et al., 2006; Gui et al., 1994a; Wang et al., 1998). In contrast to SRPKs, the Clk/Sty family (for cyclin-like kinase or serine/threonine/tyrosine kinase) are nuclear localized dual specificity kinases that were originally cloned as cyclin-like kinases by degenerate PCR (Ben-David et al., 1991; Howell et al., 1991). Clk/Sty was identified as an SR kinase when it was shown to interact with SR proteins in a two-hybrid screen (Colwill et al., 1996b). Clk/Sty was linked to splicing regulation in Drosophila studies, where the Clk/Sty ortholog was shown to phosphorylate endogenous SR proteins and mutations in the kinase altered specific alternative splicing events in the sex determination pathway (Du et al., 1998). Like SRPKs, overexpression of Clk/Sty in

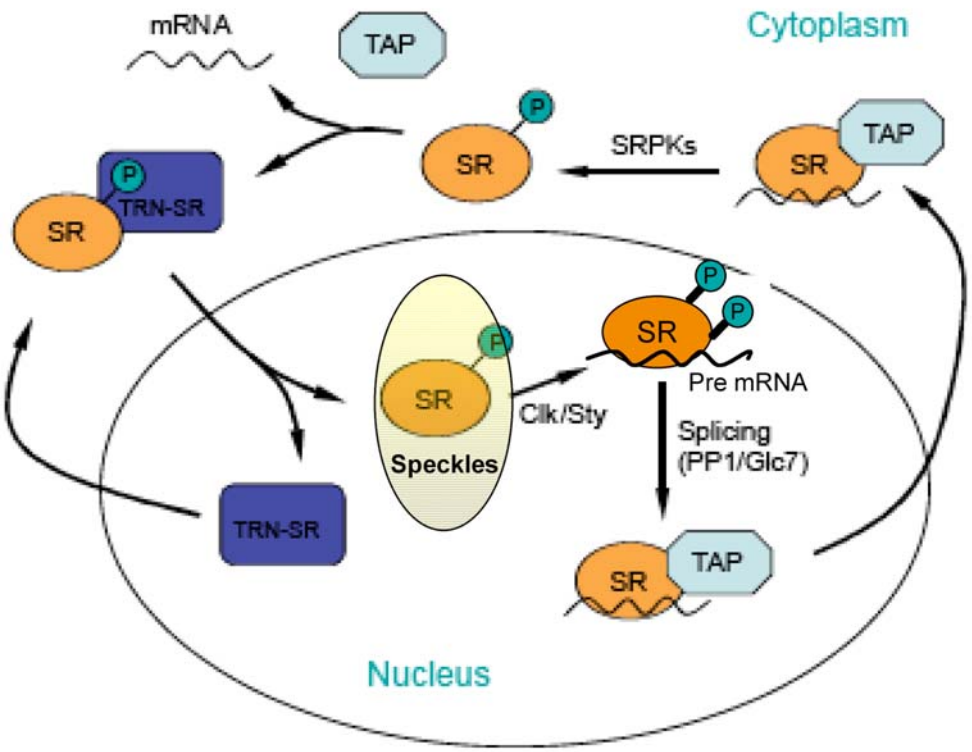

Figure 1.4 Regulation of SR protein localization and mRNA metabolism. SR protein phosphorylation states influence splicing factor localization and mRNA metabolism. Phosphorylation of SR proteins in the cytoplasm by SRPK1 enhances affinity for the nuclear import receptor transportin-SR (TRN-SR). Phosphorylation by SRPK1 and Clk/Sty in the nucleus induces relocalization from nuclear speckles. Dephosphorylation of SR proteins associated with mature mRNA enhances affinity with the nuclear export factor TAP.

mammalian cells causes the redistribution of SR proteins from nuclear speckles (Colwill et al., 1996b; Ngo et al., 2005).

While SR protein phosphorylation is necessary for spliceosome assembly on pre-mRNA, dephosphorylation is critical for splicing catalysis (Cao et al., 1997; Mermoud et al., 1992). Furthermore, it has been shown that a fraction of the dephosphorylated SR proteins remain associated with spliced mature mRNA and facilitate interactions with the mRNA export factor TAP (Huang et al., 2003; Huang and Steitz, 2001; Huang et al., 2004; Lai and Tarn, 2004) (Figure 1.4). In this way, SR proteins couple pre-mRNA splicing with mRNA export to the cytoplasm (Huang and Steitz, 2005). Once in the cytoplasm, these mRNA associated SR proteins are subject to regulatory processes in route to the ribosome where they have also been found to play a direct role in translation (Sanford et al., 2004). The cytoplasmic SRPKs are likely involved in such regulatory processes, including phosphorylation induced re-localization to the nucleus of these shuttling SR proteins.

C. The Splicing Kinases are Structurally and Catalytically Unique Enzymes

This thesis will focus on the kinases SRPK1 and Clk/Sty, which phosphorylate and regulate the SR protein family of splicing factors. SRPK1, its mammalian homolog SRPK2, and its yeast homolog Sky1 have unique features that distinguish them from other members of the kinase superfamily. All three have a kinase core that is divided by an autonomously folding insert domain sequence (Figure 1.5). These kinases only phosphorylate serine residues, never modify threonine residues, and are

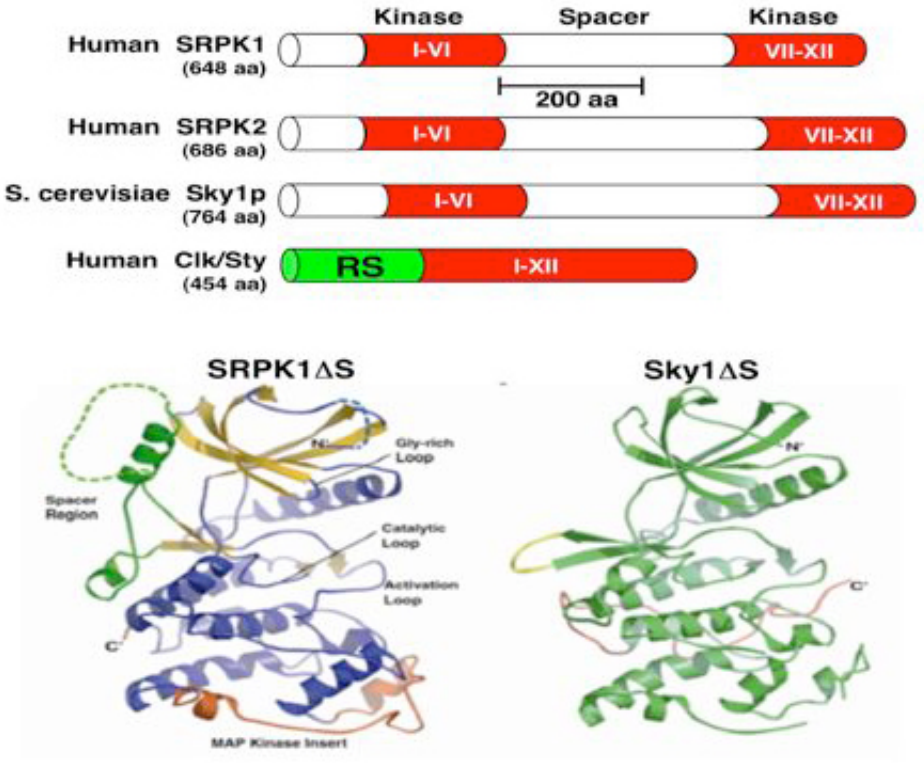

Figure 1.5 The SR protein kinases have a unique internal spacer domain. The SR protein kinase family are highly conserved from yeast to humans. Their kinase domains are separated by a unique independently folding spacer domain. The X-ray structure of SRPK1 and Sky1 without the insert domain (ΔS) revealed that the kinases adopt typical kinase folds (Ngo et al., 2005; Nolen et al., 2001).

constitutively active with no requirement for activation loop phosphorylation. The X-ray structure of SRPK1 and Sky1 without the insert domain (ΔS) revealed that the kinases adopt typical kinase folds (Ngo et al., 2005; Nolen et al., 2001) (Figure 1.5). The SRPK1 structure revealed a potential docking site that is an acidic pocket near the MAP kinase insert in the large C-terminal lobe (Ngo et al., 2005). It is thought that the docking site binds the linker region between the RS domain and RRM of the prototypical SR protein ASF/SF2 (Ngo et al., 2005). Kinetic analysis of a refolded heterodimeric complex of SRPK1ΔS and ASF/SF2, in start-trap assays with a peptide trap based on the Sky1 substrate Npl3, showed that polyphosphorylation of the SR protein is catalyzed in a processive manner (Aubol et al., 2003). In contrast to SRPK1, Clk/Sty is a dual-specificity kinase capable of phosphorylating serine, threonine, and tyrosine residues. The kinase is extensively autophosphorylated and contains an N-terminal domain that is enriched with arginine-serine dipeptides similar to the RS domain of SR proteins (Colwill et al., 1996a; Colwill et al., 1996b; Du et al., 1998; Prasad et al., 1999; Prasad and Manley, 2003). Both the SRPK and Clk/Sty family of kinases are constitutively active.

D. Processive Polyphosphorylation by Protein Kinases

Phosphorylation events regulate a full spectrum of functions in the cell. In many cases, modification of multiple residues on a single protein are necessary to induce physical changes that influence activity or binding events by other factors. The extent of phosphorylation on a protein can be very high. For example, the C-terminal domain of RNA polymerase II functions as a binding domain for several nuclear

factors and has been shown to have over 50 phosphorylated residues *in vivo* (Dahmus, 1996). Polyphosphorylation can be achieved by multiple kinases working on a common substrate, or single kinases that catalyze the phosphorylation of multiple residues on a protein. There are two distinct catalytic mechanisms by which a substrate can be modified at several residues by a single protein kinase. If catalysis occurs in a processive mechanism, the kinase binds and phosphorylates the multiple sites without releasing the substrate prior to completion (Figure 1.6). In a distributive mechanism, complete polyphosphorylation is achieved in distinct binding/catalytic events, where the kinase releases its substrate following each phosphorylation event (Figure 1.6).

Our group has recently demonstrated that SRPK1 processively phosphorylates multiple serine residues in the RS domain of ASF/SF2 (Aubol et al., 2003). This processive mechanism was discovered by the implementation of a novel start-trap assay. In this study, SRPK1 and ASF/SF2 were independently expressed in bacteria and co-purified as a heterodimeric complex. In the start-trap assay, progress curves were monitored following the addition of ATP(γ-P^{32}), both in the presence and absence of excess concentrations of a substrate mimetic inhibitor peptide based on the yeast protein phosphorylation site of NPL. For reactions initiated in the presence of inhibitor peptide, the mechanism of phosphorylation was determined by comparing the rate and endpoint of single-turnover phosphorylation to those observed in the absence of trap. If the mechanism of polyphosphorylation by SRPK1 were distributive, the reaction progress could be markedly slowed by the binding of inhibitor peptide

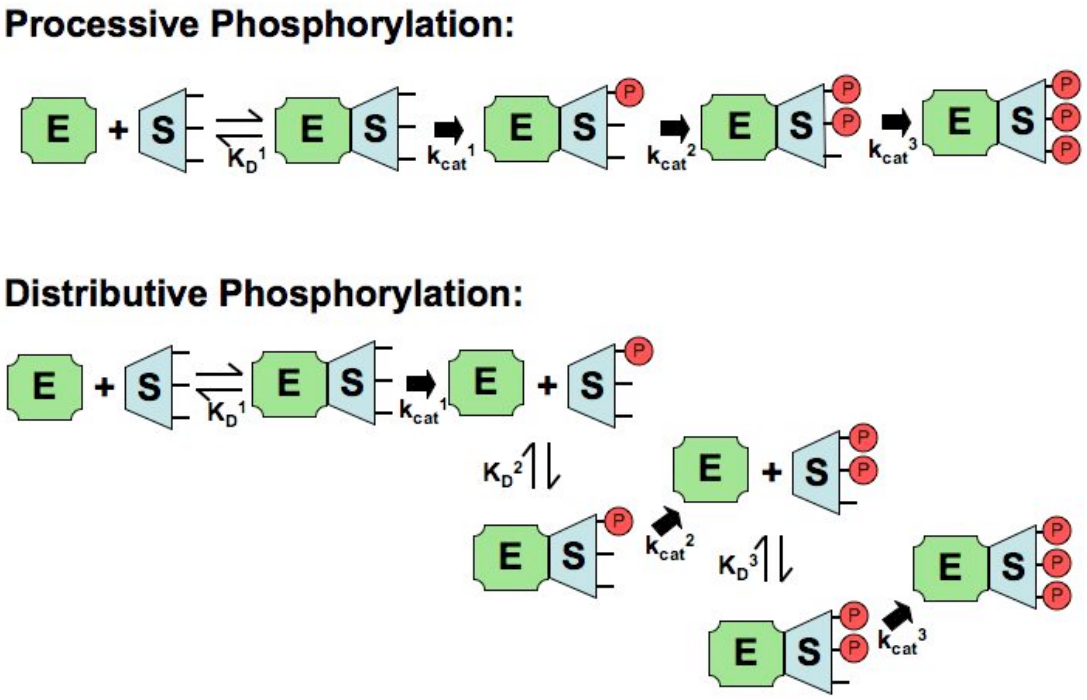

Figure 1.6 Processive vs. Distributive Phosphorylation. In a processive reaction, the initial binding event (thermodynamic properties characterized by K_D^1) is followed by multiple catalytic events occurring sequentially without dissociation. In the distributive reaction, each catalytic addition of phosphate to the substrate is followed by a dissociation event prior to subsequent binding events (characterized by distinct thermodynamic dissociation constants: K_D^2, K_D^3) and additional catalysis to eventually form the final product.

trap to the kinase following dissociation after initial phosphorylation of ASF/SF2. However, the inhibitor peptide did not significantly reduce the rate or endpoint of ASF/SF2 phosphorylation. This demonstrated that SRPK1 stays associated with ASF/SF2 throughout the multiple phosphorylation events on the RS domain as a processive kinase (Aubol et al., 2003).

Additional examples of processive phosphorylation have been reported in the literature. Cas (Crk-associated substrate) was discovered as a heavily tyrosine phosphorylated complex partner of Src and Crk in transformed cells (Matsuda et al., 1990; Reynolds et al., 1989; Sakai et al., 1994). Cas has a modular structure with a central domain, which functions as a substrate for Src composed of multiple YXXP motifs that can be phosphorylated by multiple tyrosine kinases (Bouton et al., 2001; Mayer et al., 1995; Ruest et al., 2001). The phosphorylated YXXP motifs function as ligands for the SH2 domains of various signaling proteins. Kinetic experiments have demonstrated that Src processively phosphorylates the YXXP motifs of Cas. The first evidence came from gel-shift analysis experiments (Pellicena and Miller, 2001). Fully phosphorylated Cas has significantly reduced mobility in SDS-PAGE gels. ATP(γ-P^{32}) phosphorylation reactions with catalytic concentrations of Src did not reveal intermediate migration states during the course of the reaction. The absence of intermediate phosphorylation states in excess of the Src concentration was consistent with a processive mechanism (Pellicena and Miller, 2001). Secondary evidence of Src processivity with Cas was demonstrated in pulse-chase experiments where the rate of Cas phosphorylation was monitored at varying enzyme concentrations. Because the rate of progression to generate a completely phosphorylated product was independent

of enzyme concentration, a processive mechanism was supported (Patwardhan et al., 2006). Other examples of processive phosphorylation include the lymphocyte-specific kinase (Lck) phosphorylation of the three tandem immunoacceptor tyrosine based activation motifs (ITAMs) in the ζ chain of TCR/CD3 (Lewis et al., 1997), the Abl tyrosine kinase phosphorylation of the RNA pol II CTD (Duyster et al., 1995), and the semi-processive phosphorylation of Pho4 transcription factor by the cyclin-CDK complex Pho80/Pho85 (Jeffery et al., 2001; Komeili and O'Shea, 1999).

E. SR Proteins and SR Protein Kinases in Disease and Tumorigenesis

A significant percentage of known mutations that affect RNA processing and cause human disease are driven by erroneous pre-mRNA splicing (Faustino and Cooper, 2003; Krawczak et al., 1992). For example, frontal dementia and Parkinsonism (FTDP) is caused by erroneous expression of multiple alternatively spliced isoforms of a microtubule-associated protein called tau (D'Souza et al., 1999; Hong et al., 1998). Amyotrophic lateral sclerosis (ALS) is linked to RNA processing defects of the glutamate transporter EAAT-2 in the brain (Lin et al., 1998). Myotonic dystrophy (MD) is linked to splicing defects in the protein kinase DMPK (Brook et al., 1992; Buxton et al., 1992; Fu et al., 1992; Mahadevan et al., 1992). Spinal muscular atrophy (SMA), the most common genetic cause of childhood mortality, is caused by splicing defects of the survival motor neuron gene involved in RNA processing (Coovert et al., 1997). In addition to multiple neurodegenerative diseases, links have been established between alternative splicing defects and neoplastic onset. An example is the glycoprotein receptor for hyaluronan, CD44. Despite diverse potential

for alternatively spliced gene products (over 30 mRNA's have been detected), metastatic clones of rat pancreatic adenocarcinoma cells express only a single splice variant that is believed to drive the disease (Gunthert et al., 1991). In nude mice, monoclonal antibodies against CD44 inhibit the proliferation of human melanoma cells (Guo et al., 1994). Evidence continues to accumulate that suggests these and other disorders result primarily from defects in the splicing machinery.

The SR protein family of splicing factors has elevated expression in numerous tumors (Fischer et al., 2004; Ghigna et al., 1998; Stickeler et al., 1999). The SR protein ASF/SF2 was recently shown to play a critical role in the maintenance of genomic stability (Li and Manley, 2005). SR proteins are likely to regulate the alternative splicing of various genes that are critical for cell survival, growth, and proliferation. It was recently established that ASF/SF2 directly influences the splicing of the proto-oncogene Ron, and that defective splicing regulation enhanced cell motility and invasion (Ghigna et al., 2005; Zerbe et al., 2004). Furthermore, it is well known that most genes involved in apoptosis express multiple isoforms, and that splice variants often exhibit opposite functions to either inhibit or stimulate apoptosis (Jiang and Wu, 1999; Wu et al., 2003). It is possible then that splicing defects could single handedly induce multiple hits that drive the development of cancer. Such findings implicate the regulators of alternative splicing in oncogenesis.

Recent research is now establishing this principle. ASF/SF2 was recently identified as a proto-oncogene, with over-expression in mammalian cells inducing a transforation phenotype (Karni et al., 2007). The mechanism of ASF/SF2 transformation appears to be multi-faceted with evidence for the promotion of

alternatively spliced isoforms of the BIN1 tumor supressor, and activation of the MNK2 and S6K1 kinases (Karni et al., 2007). ASF/SF2 was to activate mTORC1 in a manner that bypassed upstream Akt/PI3K signaling (Karni et al., 2008). Genetic knockout of SRPK1 in mice induced a cellular transformation phenotype in isolated embryonic fibroblasts (Fu, pers. comm.). It was previously reported that the proto-oncogene Akt and SRPK1 induce opposite effects on alternative splicing (Blaustein et al., 2005). Evidence is continuing to accumulate that implicate SRPK1 as a regulator of the Akt pathway, and a novel tumor suppressor gene (Fu, pers. comm.)

The complex process of pre-mRNA splicing is regulated by multiple protein-protein and protein-RNA interactions that direct complex formation and localization of numerous essential factors. Although our understanding of these processes at the molecular level is incomplete, it is clear that the phosphorylation of SR protein splicing factors by the SR kinases is of critical importance. Although much remains to be learned about the regulation of SR protein phosphorylation, the medical significance of understanding these processes is undeniable given the many known diseases associated with splicing errors, and the growing link between SR proteins, SR kinases, and cancer. As a result, the SR kinases have become promising targets for the treatment of human disease. Inhibitors have been developed that target the nucleotide-binding pocket of both SRPK1 and Clk/Sty (Fukuhara et al., 2006; Muraki et al., 2004). However, despite therapeutic successes with nucleotide-directed molecules like Gleevec, adequate selectivity remains a major limitation of this approach as it often causes adverse side effects. Targeting substrate docking motifs beyond the active site of SR kinases is a novel strategy for the design of drugs that affect splicing.

Elucidating the mechanisms of catalysis and substrate recognition by the SR kinases will advance our basic understanding of processes regulated by these enzymes, and provide a framework for applications aimed at modifying their activity in diseased cells.

F. Focus of Study

This project is primarily a study of SR protein kinase enzymology. We employed molecular biological and biochemical techniques to generate and purify proteins of interest for *in vitro* analyses of catalytic function. Thanks to a strong collaboration with Dr. Xiang-Dong Fu and Dr. Gourisankar Ghosh our efforts have been grounded in both biological and structural contexts. My work has focused on the kinetic properties of the mammalian splicing kinases SRPK1 and Clk/Sty, with emphasis on the former. Initial work in our lab had focused on kinetic analysis of a mutant form of SRPK1, which had its internal spacer domain deleted (SRPK1ΔS). The primary reason for this deletion was that the spacer domain was unstructured and hindered efforts to crystalize the protein for X-ray structural analysis. Interesting observations with the spacer deleted kinase included evidence of processive phosphorylation and unusually high affinity for its splicing factor substrate ASF/SF2. These initial kinetic studies were conducted on an enzyme-substrate complex that was co-purified for structural analysis. The general aims of my research were to study wild-type enzymes and analyze their properties with independently purified substrates to deepen our understanding of their catalytic relationships.

The primary goals of my research were as follows: 1) to assess the mechanistic and regiospecific properties of splicing factor phosphorylation by SRPK1 and Clk/Sty (Chapter 3). 2) to compare the spacer deleted and wild-type kinases to elucidate potential mechanisms explaining SRPK1 localization phenomena observed by my co-chair Dr. Xiang-Dong Fu (Chapter 3). 3) to dissect the determinants of the high affinity interaction between SRPK1 and ASF/SF2 in the context of structural data provided by our collaborator Dr. Gourisankar Ghosh (Chapter 4). 4) to employ powerful analyses by high resolution Fourier transform ion cyclotron resonance mass spectrometry (FT-ICRMS), with our collaborator Dr. Pieter Dorrestein, to refine our understanding of SRPK1 phosphorylation of ASF/SF2 and explain interesting observations within a recent crystal structure of an SRPK1:ASF/SF2 complex (Chapter 5).

Chapter II

Assay Development and

Sequence and Analysis of Investigated Proteins

A. Introduction

This thesis documents research efforts conducted to elucidate the kinetic properties of the mammalian SR protein kinases SRPK1 and Clk/Sty. I have utilized a variety of standard molecular biological and biochemical techniques to achieve our research goals. These techniques included bacterial plasmid preparation and cloning, site-directed mutagenesis, DNA sub-cloning, recombinant protein expression, protein purification, kinase assays, and mass spectrometric protein analysis. Details of these methods are reported in the respective chapters of this thesis. In addition, I have developed novel *in vitro* techniques to gain a more profound understanding of the mechanistic and thermodynamic properties of these kinases and their splicing factor substrates. In Chapter 3, I describe results generated from a novel start-trap assay designed to assess the mechanism of multisite phosphorylation of the RS domain of ASF/SF2. This assay employs active-site mutant kinases, incapable of phosphorylation (kinase-dead), as catalytic traps. The assays have several advantages over the original peptide inhibitor start-trap assay. In Chapter 4, I utilize a novel competition assay to efficiently measure the true dissociation binding constants for SRPK1 to multiple deletion constructs and mutant forms of the splicing factor ASF/SF2. These techniques and general methodology will be described in further detail here and within the respective chapters of this thesis.

B. Assay Development

1. The Kinase-Dead Enzyme Start-Trap Experiment for Mechanistic Analysis of Polyphosphorylation by SR Protein Kinases

Previous work in our lab showed that a spacer deleted mutant form of SRPK1 (ΔS) processively phosphorylates multiple serine residues in the ASF/SF2 RS domain (Aubol et al., 2003). In this study, SRPK1ΔS and ASF/SF2 were independently expressed in bacteria and co-purified as a heterodimeric complex. This processive mechanism was elucidated with the use of a start-trap assay. The experimental design was based on previous studies with the DNA polymerases. The processive nature of DNA replication was demonstrated in start-trap assays where reactions were initiated in the presence of excess amounts of DNA trap molecules chemically modified to prevent 3' extension. The degree to which chain elongation continued in the presence of trap was a measure of DNA polymerase processivity (McClure and Chow, 1980).

In the Aubol et al., 2003 start-trap assay, progress curves were monitored following the addition of ATP(γ-P^{32}), both in the presence and absence of excess concentrations of a substrate mimetic inhibitor peptide (YRTRDAPRERAPTR) that was synthesized based on the single phosphorylation site (underlined alanine residue was mutated from serine) of the yeast protein Npl3. The peptide was determined to competitively inhibit the phosphorylation of ASF/SF2, but because of the relatively low affinity of the peptide for SRPK1ΔS (K_I = 30 μM), high concentrations were necessary (20 mM) to significantly inhibit the reaction in trap-start assays where the trap was pre-equilibrated with the complex prior to start with ATP. For reactions

initiated with ATP in the presence of inhibitor peptide, the mechanism of phosphorylation was determined by comparing the rate and endpoint of single-turnover phosphorylation to those observed in the absence of trap. If the kinase processively phosphorylates the multiple serines on the substrate without dissociating (pathway 1, Figure 2.1A), the peptide trap will not interfere with reaction progress. However, if the kinase dissociates from its substrate after phosphorylation events in a distribute manner (pathway 2, Figure 2.1A), the peptide inhibitor will bind and trap the free enzyme significantly slowing the rate of the phosphorylation reaction. The observation that 20 mM peptide trap had no impact on the rate or endpoint of ASF/SF2 phosphorylation by SRPK1ΔS was strong evidence of a fully processive mechanism (Figure 2.1B) (Aubol et al., 2003).

Although the peptide trap based start-trap experiment was functional with the SRPK1ΔS:ASF/SF2 complex, the peptide inhibitor trap has several significant limitations that motivated us to develop a more efficient trapping system for the additional investigations of processive phosphorylation by splicing kinases. First, the peptide inhibitor has low affinity for SRPK1ΔS. As a result, concentrations of peptide as high as 20 mM were required to efficiently inhibit the reaction in trap-start control experiments. The use of such large concentrations of peptide in these start-trap and trap-start control experiments was proving to be very expensive. Second, we were concerned that such high concentrations of peptide could impact the solvent properties of buffers used in these kinetic experiments. Third, because the peptide was a relatively small molecule, we realize that it might not completely displace the kinase

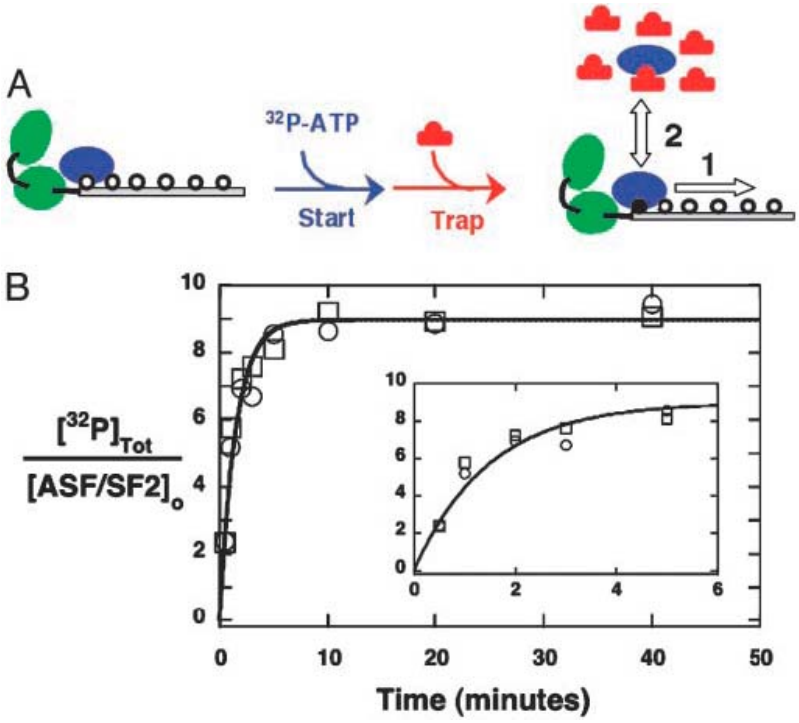

Figure 2.1 Peptide inhibitor start-trap experiment. A) Illustration of the theoretical differences of processive (pathway 1) and distributive (pathway 2) phosphorylation in the peptide inhibitor start-trap experiment. The RRMs of ASF/SF2 are represented in green attaced to the C-terminal RS doman depicted in grey. Unphosphorylated serine residues are open circles and the initial phosphorylation event is represented as a closesd circle. SRPK1ΔS is drawn in blue bound to the RS domain, and the peptide trap is shown in red. B) The progress curves of ASF/SF2 phosphorylation in the presence of 20 mM peptide trap overlaped the progress curve of ASF/SF2 phosphorylation with no trap present indicating a processive mechanism of phosphorylation (from Aubol et al., 2003).

from its protein substrate. One can imagine a situation where the peptide could bind the kinase near the active site and inhibit the reaction while the enzyme remained bound to its substrate by more distal contacts, thereby forming a trimeric complex. Inhibition in this case would not reflect a complete dissociation event and would generate erroneous results that indicate a distributive mechanism for a system that may in fact be quite processive (Figure 2.2). Finally, we wanted to develop an assay that could be used to study multisite phosphorylation by any protein kinase. While the Npl3 based peptide had a low affinity for SRPK1ΔS, it would be even lower for other kinases less conserved with the Sky1 kinase that phosphorylates the Npl3 protein *in vivo*. One of our immediate aims was to study the mechanism of ASF/SF2 phosphorylation by Clk/Sty, and we needed a new assay to do this.

The strategy we chose to pursue was to explore the trapping potential of kinase-inactive mutant enzymes. A conserved lysine residue in the active site that is critical for ATP binding is commonly mutated in cell biological systems to study phenotypic effects of catalytically inactive forms of protein kinases (Hannink and Donoghue, 1985). In theory, mutation of this internal residue should not alter substrate recognition by the kinase mediated by external docking interactions. We hypothesized that due to the high-affinity (K_D<100 nM) interaction between SRPK1 and ASF/SF2, the kinase-dead enzyme would have significant trapping capabilities in the low micro-molar range. Because the kinase-inactive trap will interact with the substrate at the same contact points as the active kinase, trapping in the start-trap assay will result in complete displacement of the kinase and rigorously demonstrate

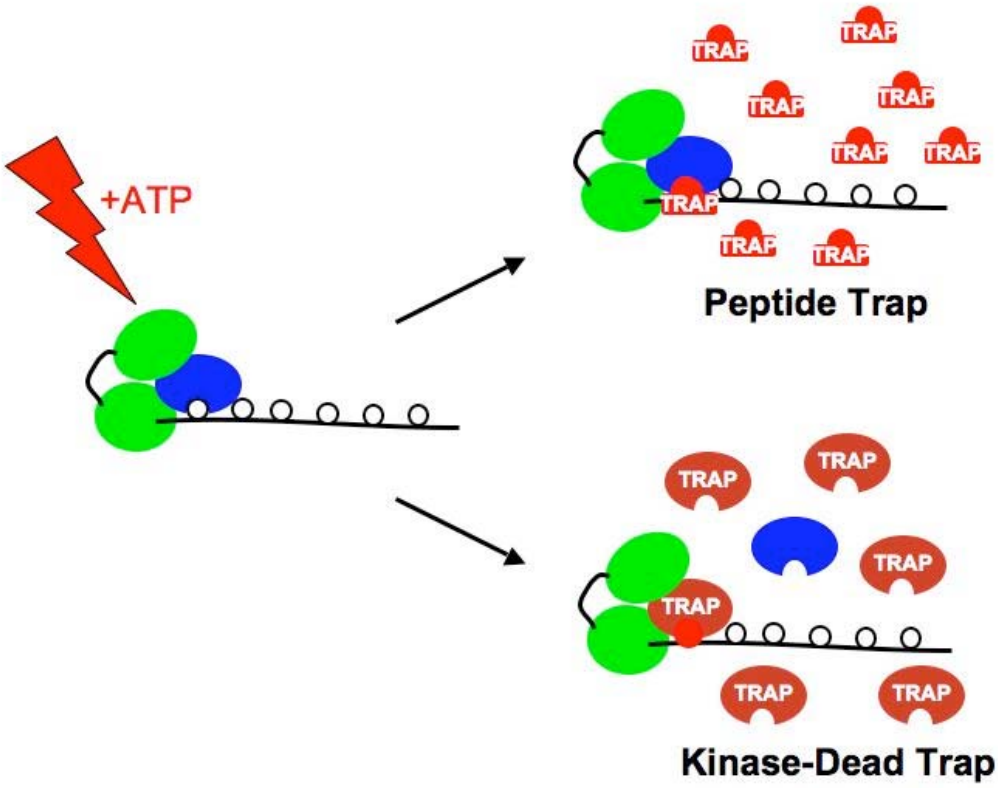

Figure 2.2 The peptide inhibitor trap vs. the kinase-dead enzyme trap. The peptide trap system has significant limitations that motivated the development of a more efficient trapping system including low affinity binding, expense, solvent effects, incomplete displacement, and non-universal application. The kinase-dead trapping system is effective at low micro-molar concentrations, completely displaces the kinase from its substrate, and can be applied to any kinase that phosphorylates its substrate at multiple residues.

dissociative properties consistent with distributive mechanisms. Finally, because all protein kinases can have a single lysine residue mutated in their active site to generate a kinase-inactive enzyme, this trapping system can be applied to investigate the processive nature of polyphosphorylation by any protein kinase. Chapter 3 of this thesis details the methodology of the kinase-dead start-trap assay and reports data generated for both SRPK1 and Clk/Sty. A kinase-inactive form of SRPK1 was generated by replacing lysine at position 109 with methionine. Replacing lysine at position 190 with methionine generated a kinase-inactive form of Clk/Sty. The kinase-dead trap was effective at 50 μM for both SRPK1 and Clk/Sty. The processive result obtained by (Aubol et al., 2003) for SRPK1ΔS purified as a complex with ASF/SF2 was corroborated for independently purified wild-type SRPK1 and ASF/SF2 in start-trap assays using kinase-inactive SRPK1. Surprisingly, Clk/Sty was found to processively phosphorylate the entire RS domain of ASF/SF2.

2. The Competition Assay Is an Efficient Kinetic Method for Determination of True Dissociation Constants for SRPK1 Substrates

Preliminary studies with the SRPK1ΔS:ASF/SF2 complex demonstrated an unusually high-affinity association for a kinase and its substrate (K_D = 50 nM) (Aubol et al., 2003). The dissociation constant for the complex was measured in a series of single-turnover reaction progress curves monitored by ^{32}P incorporation on ASF/SF2 isolated by SDS-PAGE separation for scintillation quantification. The reaction series involved the dilution of the SRPK1ΔS:ASF/SF2 complex in concentrations ranging

from 4 μM to 0.03 μM. The reactions conducted at high concentrations, 0.5 – 4 μM, had similar reaction rates that all fit rapid single exponential functions. This was an indication that the complex does not dissociate at concentrations above 0.5 μM, and the reaction is completed rapidly in the processive manner determined by start-trap experimentation. As the complex was diluted further, the progress curves shifted to biphasic functions with initial "fast" phase amplitudes that decreased in a positive correlation with complex concentration. The biphasic nature of the diluted complex progress curves was the result of SRPK1ΔS:ASF/SF2 complex dissociation and a direct reflection of the thermodynamic properties of the interaction. The initial fast phase represents the fraction of the complex that remains associated and processively phosphorylates ASF/SF2, while the slow secondary phase of the reaction represents the fraction of dissociated complex that require a binding step prior to catalysis (Aubol et al., 2003). The dissociation constant of the complex (K_D) was determined by analyzing the relative amplitude of the initial fast phase of the progress curves (representative of the fraction of enzyme bound to substrate: BF) as a function of enzyme concentration using Equation 1:

$$BF = \frac{K_d + [S]_o + [E]_o - \sqrt{(K_d + [S]_o + [E]_o)^2 - 4[S]_o[E]_o}}{2[S]_o} \qquad (1)$$

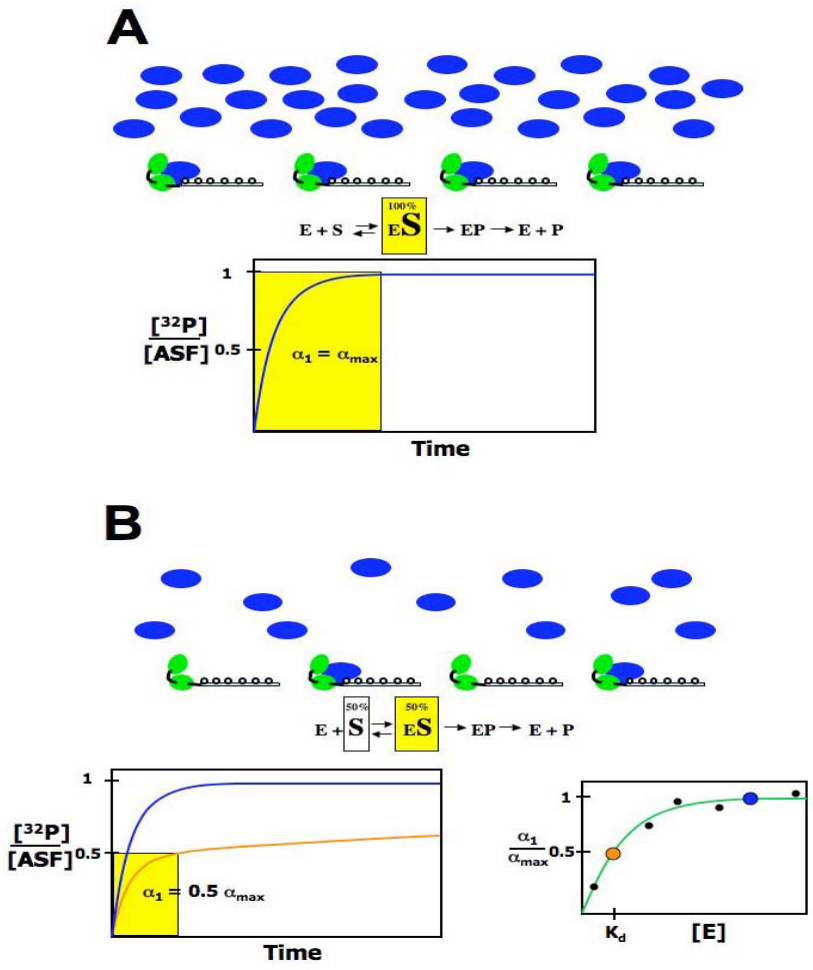

Figure 2.3 K_D determination by single-turnover kinetic analysis of SRPK1. A) At high enzyme concentrations (shown in blue), the substrate molecules (shown in green) are all bound in complex with enzyme. The resulting progress curve of the reaction initiated with ATP fits a single-exponential function with a maximal amplitude reflecting rapid processive phosphorylation (blue progress curve). B) As the enzyme concentration is decreased, the fraction of substrate bound to enzyme decreases. When the reaction is initiated in the presence of enzyme at a concentration equal to its dissociation constant (K_D), exactly half of the substrate molecules are bound to enzyme. The resulting reaction (orange progress curve) has an initial fast phase with an amplitude half that of the maximal observed at high concentrations. The plot of relative fast phase amplitude as a function of enzyme concentration can be fit to Equation 1 (above) to calculate the K_D of the interaction.

In Chapter 3 of this thesis we employed this single-turnover method to study the affinity of independently purified full length SRPK1 and Clk/Sty for ASF/SF2. Both of these kinases were shown to catalyze processive phosphorylation within the RS domain of ASF/SF2. Unlike the study with SRPK1ΔS:ASF/SF2 complex, ASF/SF2 concentrations were maintained at concentrations below the expected K_D of 50 nM for all SRPK1 and Clk/Sty concentrations studied. Figure 2.3 is a schematic representation of the single-turnover method.

In Chapter 4 of this thesis we set out to investigate the determinants of the high-affinity interaction between SRPK1 and ASF/SF2. This study required analysis of many mutant protein constructs of ASF/SF2. The single-turnover method for K_D determination described above is very labor intensive, requiring nearly a hundred data points to firmly establish a dissociation constant value for a single enzyme substrate pair. Furthermore, we expected that some deletion mutants of ASF/SF2 planned for this project would have altered mechanics with SRPK1 catalysis due to the absence of residues critical for interactions necessary for processive phosphorylation. Interpretation of the single-turnover experimental data would be confounded for substrates phosphorylated in a semi or non-processive manner. We needed an efficient method to analyze the binding affinities proteins independent of kinetic mechanism.

The strategy we employed utilized the principles of competitive inhibition in steady-state systems. Our experimental strategy was to generate sequential deletions from both the N and C-terminus of ASF/SF2 to identify domains critical for high-affinity binding to SRPK1. We expected that these deletion constructs would bind the

same regions of the kinase as full length ASF/SF2 in a way that would be mutually exclusive. Although deletion constructs that contained some portion of the RS domain would likely act as substrates for the kinase in reactions initiated in the presence of full length ASF/SF2, they would effectively function as inhibitors of ASF/SF2 phosphorylation. We could therefore monitor the decreasing initial velocity rates of ASF/SF2 phosphorylation by SRPK1 as a function of increasing competitor concentrations to assess the affinity of the competitor for SRPK1. The matter of critical importance for the viability of this assay system was to establish that the deletion construct competitors indeed bind SRPK1 in a mode that is competitive with full length ASF/SF2.

Figure 2.4 illustrates the fundamentals of competitive inhibition for the deletion construct analyses reported in Chapter 4. Competitive binding implies mutual exclusivity such that the binding of substrate, characterized by the thermodynamic equilibrium dissociation constant K_D, can only occur in the absence of competitor binding, characterized by its own thermodynamic equilibrium binding constant K_I (Figure 2.4A). To illustrate competitive mode binding for a competitor substrate, Michaelis Menton "V vs. S" plot experiments are conducted with SRPK1 and varying concentrations of ASF/SF2 both in the absence and presence of a fixed concentration of competitor substrate. The competitive substrate should only effect the apparent K_m of the SRPK1:ASF/SF2 "V vs. S" Plot, and not impact V_{max}. Data from these experiments can be presented as standard "V vs. S" or Double-Reciprocal Plots (Figure 2.4B). Once competitive mode binding has been established, the initial velocities of ASF/SF2 phosphorylation by SRPK1 can be monitored with single data

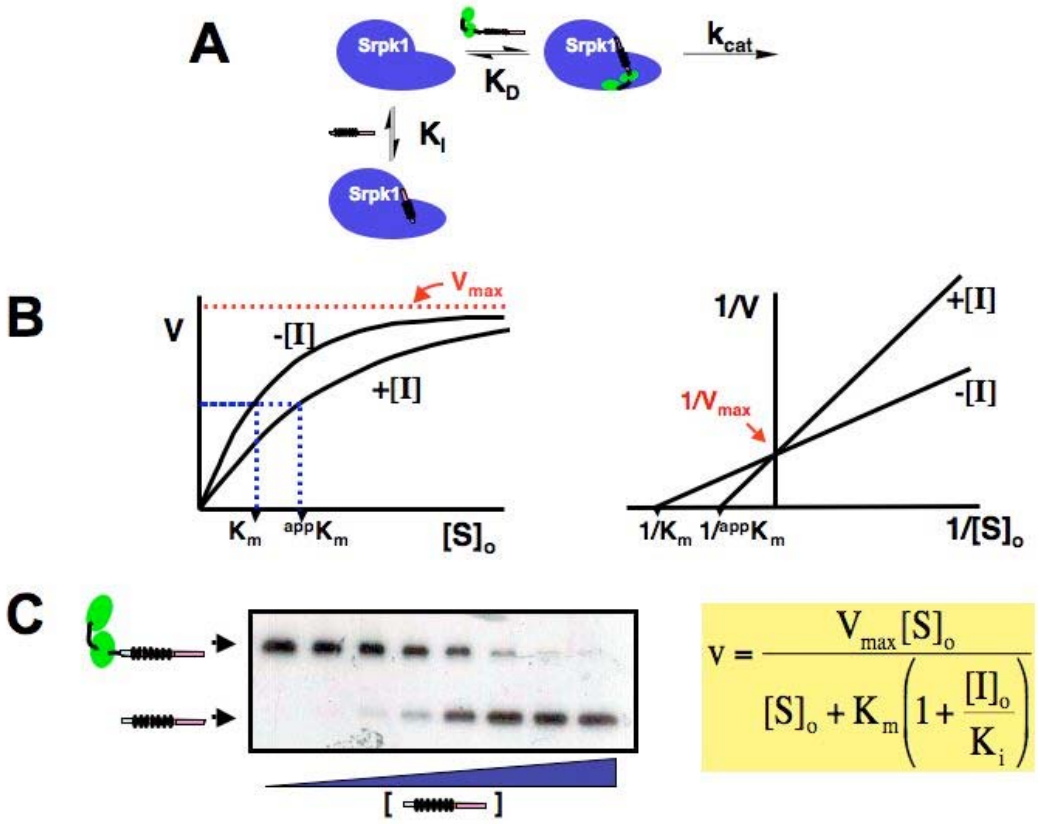

Figure 2.4 Competitive inhibition analysis of ASF/SF2 phosphorylation yields dissiociation constants for deletion constructs. A) Competitive inhibition by a secondary substrate that binds to SRPK1 in a mutually exclusive manner. B) "V vs. S" and Double-Reciprocal Plots of steady-state catalysis in the presence of a competitive inhibitor. V_{max} is unchanged in the presence of inhibitor because increasing substrate concentrations can "out compete" the inhibitor. K_m changes because in the presence of inhibitor it takes a higher concentration of substrate to achieve the half-maximal initial velocity. C) The decrease in initial velocity as a function of competitor substrate concentration is related to the K_m of the monitored substrate to calculate binding affinity of the competitor for SRPK1 as a true equilibrium dissociation constant, K_I.

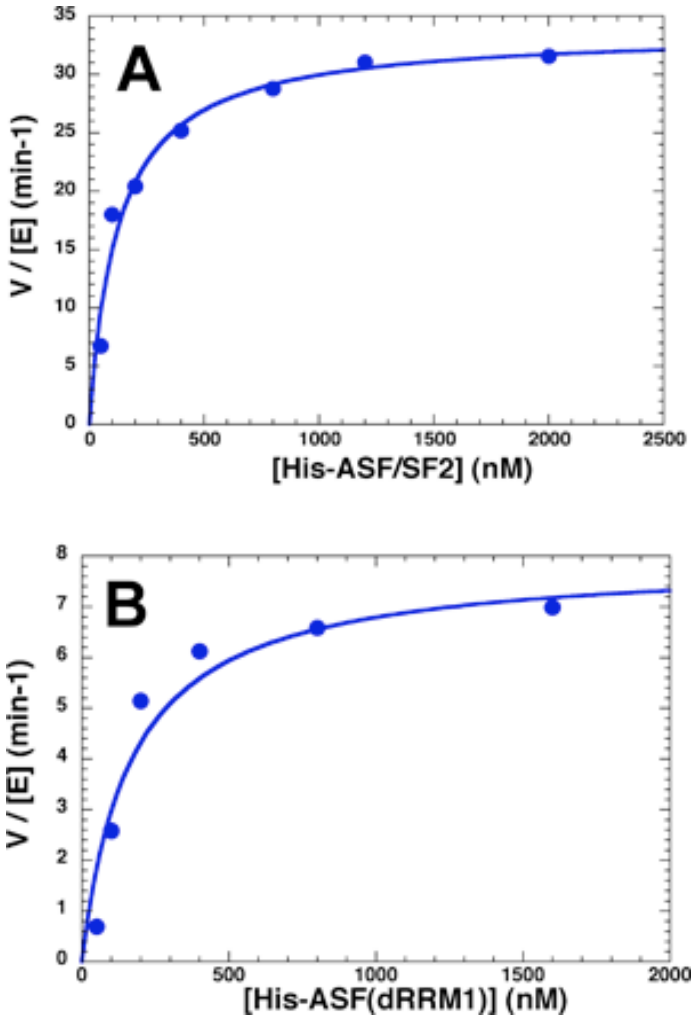

Figure 2.5 "V vs. S" plots for K_m analysis of SRPK1 with ASF/SF2 substrates. 2 nM SRPK1 was studied in assays with saturating concentrations of ATP and varying concentrations of ASF/SF2 substrates. Data were fit to the Michaelis-Menton equation to generate K_m values of 125 ± 24 nM for His-ASF/SF2 and 140 ± 55 nM for His-ASF(ΔRRM1). The K_m value for His-ASF/SF2 was used to calculate K_I's of deletion constructs, while the K_m value for His-ASF(ΔRRM1) was used to calculate K_I's of full length ASF/SF2 constructs.

points in the presence of increasing concentrations of competitor protein. The decrease in initial velocity as a function of competitor substrate concentration is related to the K_m of the monitored substrate (Figure 2.5) to calculate binding affinity of the competitor for SRPK1 as a true equilibrium dissociation constant, K_I (Figure 2.4C).

C. Sequence Analysis of Investigated Proteins

The majority of proteins investigated in this thesis were cloned, expressed, and purified as recombinant proteins in *E. coli* BL21-DE3 cells. The plasmid DNA clones for human SRPK1, murine Clk/Sty, and human ASF/SF2 were provided by Dr. Xiang-Dong Fu. All constructs used for protein expression, whether provided or generated by us were sequenced to eliminate the potential for unwanted spontaneous mutations from plasmid propagation. The plasmid type, monoisotopic mass, and translated protein sequence of all clones studied are listed here.

SRPK1 (pRSETa, 78963.34):

MRGSHHHHHHGMetASMTGGQQMGRDLYDDDDKDPSSRSAAGTMERKVLALQARKKRTKA
KKDKAQRKSETQHRGSAPHSESDLPEQEEEILGSDDDEQEDPNDYCKGGYHLVKIGDLFNGRY
HVIRKLGWGHFSTVWLSWDIQGKKFVAMKVVKSAEHYTETALDEIRLLKSVRNSDPNDPNRE
MVVQLLDDFKISGVNGTHICMVFEVLGHHLLKWIIKSNYQGLPLPCVKKIIQQVLQGLDYLHT
KCRIIHTDIKPENILLSVNEQYIRRLAAEATEWQRSGAPPPSGSAVSTAPQPKPADKMSKNKKK
KLKKKQKRQAELLEKRMQEIEEMEKESGPGQKRPNKQEESESPVERPLKENPPNKMTQEKLEE
SSTIGQDQTLMERDTEGGAAEINCNGVIEVINYTQNSNNETLRHKEDLHNANDCDVQNLNQES
SFLSSQNGDSSTSQETDSCTPITSEVSDTMVCQSSSTVGQSFSEQHISQLQESIRAEIPCEDEQEQE

HNGPLDNKGKSTAGNFLVNPLEPKNAEKLKVKIADLGNACWVHKHFTEDIQTRQYRSLEVLIG
SGYNTPADIWSTACMAFELATGDYLFEPHSGEEYTRDEDHIALIIELLGKVPRKLIVAGKYSKEF
FTKKGDLKHITKLKPWGLFEVLVEKYEWSQEEAAGFTDFLLPMLELIPEKRATAAECLRHPWL
NS

SRPK1ΔS (pET19b, 47177.24)

MGSSHHHHHHSSGLVPRGSHMERKVLALQARKKRTKAKKDKAQRKSETQHRGSAPHSESDL
PEQEEEILGSDDDEQEDPNDYCKGGYHLVKIGDLFNGRYHVIRKLGWGHFSTVWLSWDIQGK
KFVAMKVVKSAEHYTETALDEIRLLKSVRNSDPNDPNREMVVQLLDDFKISGVNGTHICMVFE
VLGHHLLKWIIKSNYQGLPLPCVKKIIQQVLQGLDYLHTKCRIIHTDIKPENILLSVNERRQVKIA
DLGNACWVHKHFTEDIQTRQYRSLEVLIGSGYNTPADIWSTACMAFELATGDYLFEPHSGEEY
TRDEDHIALIIELLGKVPRKLIVAGKYSKEFFTKKGDLKHITKLKPWGLFEVLVEKYEWSQEEA
AGFTDFLLPMLELIPEKRATAAECLRHPWLNS

His-ASF/SF2 (pET19b; 30377.45)

MGHHHHHHHHHHSSGHIDDDDKHMSGGGVIRGPAGNNDCRIYVGNLPPDIRTKDIEDVFYKY
GAIRDIDLKNRRGGPPFAFVEFEDPRDAEDAVYGRDGYDYDGYRLRVEFPRSGRGTGRGGGG
GGGGGAPRGRYGPPSRRSENRVVVSGLPPSGSWQDLKDHMREAGDVCYADVYRDGTGVVEF
VRKEDMTYAVRKLDNTKFRSHEGETAYIRVKVDGPRSPSYGRSRSRSRSRSRSRSRSNSRSRSY
SPRRSRGSPRYSPRHSRSRSRT

His-ASF/SF2Δ219 (pET19b, 27035.17)

MGHHHHHHHHHHSSGHIDDDDKHMSGGGVIRGPAGNNDCRIYVGNLPPDIRTKDIEDVFYKY
GAIRDIDLKNRRGGPPFAFVEFEDPRDAEDAVYGRDGYDYDGYRLRVEFPRSGRGTGRGGGG
GGGGGAPRGRYGPPSRRSENRVVVSGLPPSGSWQDLKDHMREAGDVCYADVYRDGTGVVEF
VRKEDMTYAVRKLDNTKFRSHEGETAYIRVKVDGPRSPSYGRSRSRSRSRSRSRSRS

His-ASF/SF2Δ196 (pET19b, 24345.75)

MGHHHHHHHHHHSSGHIDDDDKHMSGGGVIRGPAGNNDCRIYVGNLPPDIRTKDIEDVFYKY
GAIRDIDLKNRRGGPPFAFVEFEDPRDAEDAVYGRDGYDYDGYRLRVEFPRSGRGTGRGGGG
GGGGGAPRGRYGPPSRRSENRVVVSGLPPSGSWQDLKDHMREAGDVCYADVYRDGTGVVEF
VRKEDMTYAVRKLDNTKFRSHEGETAYIRVKVDG

His-ASF/SF2ΔRRM1 (pET15b, 18737.34)

MGSSHHHHHHSSGLVPRGSHMGGAPRGRYGPPSRRSENRVVVSGLPPSGSWQDLKDHMREA
GDVCYADVYRDGTGVVEFVRKEDMTYAVRKLDNTKFRSHEGETAYIRVKVDGPRSPSYGRSR
SRSRSRSRSRSRSNSRSRSYSPRRSRGSPRYSPRHSRSRSRT

His-ASF/SF2(116-248) (pET15b, 17671.80)

MGSSHHHHHHSSGLVPRGSHMSRRSENRVVVSGLPPSGSWQDLKDHMREAGDVCYADVYRD
GTGVVEFVRKEDMTYAVRKLDNTKFRSHEGETAYIRVKVDGPRSPSYGRSRSRSRSRSRSRSR
SNSRSRSYSPRRSRGSPRYSPRHSRSRSRT

His-ASF/SF2ΔRRM12 (pET15b, 9459.81)

MGSSHHHHHHSSGLVPRGSHMAYIRVKVDGPRSPSYGRSRSRSRSRSRSRSRSNSRSRSYSPRR
SRGSPRYSPRHSRSRSRT

His-ASF/SF2(RRM1) (pET15b, 12392.99)

MGSSHHHHHHSSGLVPRGSHMSGGGVIRGPAGNNDCRIYVGNLPPDIRTKDIEDVFYKYGAIR
DIDLKNRRGGPPFAFVEFEDPRDAEDAVYGRDGYDYDGYRLRVEFPR

His-ASF/SF2(RRM2) (pET15b, 19807.84)

MGSSHHHHHHSSGLVPRGSHMSGRGTGRGGGGGGGGGAPRGRYGPPSRRSENRVVVSGLPPS
GSWQDLKDHMREAGDVCYADVYRDGTGVVEFVRKEDMTYAVRKLDNTKFRSHEGETAYIR
VKVDGPRSPSYGRSRSRSRSRSRSRSRSNSRSRSYSPRRSRGSPRYSPRHSRSRSRT

ASF/SF2-His (pET28a; 28980.36)

MGMSGGGVIRGPAGNNDCRIYVGNLPPDIRTKDIEDVFYKYGAIRDIDLKNRRGGPPFAFVEFE
DPRDAEDAVYGRDGYDYDGYRLRVEFPRSGRGTGRGGGGGGGGGAPRGRYGPPSRRSENRV
VVSGLPPSGSWQDLKDHMREAGDVCYADVYRDGTGVVEFVRKEDMTYAVRKLDNTKFRSH
EGETAYIRVKVDGPRSPSYGRSRSRSRSRSRSRSRSNSRSRSYSPRRSRGSPRYSPRHSRSRSRTL
EHHHHHH

ASF/SF2ΔRRM1-His (pET28a, 17085.60)

MGSRRSENRVVVSGLPPSGSWQDLKDHMREAGDVCYADVYRDGTGVVEFVRKEDMTYAVR
KLDNTKFRSHEGETAYIRVKVDGPRSPSYGRSRSRSRSRSRSRSRSNSRSRSYSPRRSRGSPRYS
PRHSRSRSRTKLAAALEHHHHHH

ASF/SF2ΔRRM12-His (pET28a, 8873.62)

MGAYIRVKVDGPRSPSYGRSRSRSRSRSRSRSRSNSRSRSYSPRRSRGSPRYSPRHSRSRSRTKL
AAALEHHHHHH

ASF/SF2(RS12)-His (pET28a, 7929.07)

MGGPRSPSYGRSRSRSRSRSRSRSRSNSRSRSYSPRRSRGSPRYSPRHSRSRSRTKLAAALEHHH
HHH

ASF/SF2(RS2)-His (pET28a, 5182.63)

MGNSRSRSYSPRRSRGSPRYSPRHSRSRSRTKLAAALEHHHHHH

His-ASF/SF2(188-220) (pET15b, 6116.06)

MGSSHHHHHHSSGLVPRGSHMAYIRVKVDGPRSPSYGRSRSRSRSRSRSRSRSN

His-ASF/SF2(188-235) (pET15b, 7832.95)

MGSSHHHHHHSSGLVPRGSHMAYIRVKVDGPRSPSYGRSRSRSRSRSRSRSRSNSRSRSYSPRR
SRGSP

ASF/SF2(4M-ΔRS))-His (pET28a, 5182.63)

MGHHHHHHHHHHSSGHIDDDDKHMSGGGVIRGPAGNNDCRIYVGNLPPDIRTKDIEDVFYKY
GAIRDIDLKNRRGGPPFAFVEFEDPRDAEDAVYGRDGYDYDGYRLRVEFPRSGRGTGRGGGG
GGGGGAPRGRYGPPSRRSENRVVVSGLPPSGSAADLKDHMREAGDVCYADVYADGTGVVEF
VRKEDMTYAVRKLDNTKFRSHAGETAYIRVKVDGP

His-ASF/SF2_Block1 (pET15b, 29534.53)

MGSSHHHHHHSSGLVPRGSHMSGGGVIRGPAGNNDCRIYVGNLPPDIRTKDIEDVFYKYVAIR
DIDLKNRRGGPPFAFVEFEDPRDAEDAVYGRDGYDYDGYRLRVEFPRSGRGTGRGGGGGGGG
GAPRGRYGPPSRRSENRVVVSGLPPSGSWQDLKDHMREAGDVCYADVYRDGTGVVEFVRKE
DMTYAVRKLDNTKFRSHEGETAYIAVAVDGPASPSYGASASRSRSRSRSRSRSNSRSRSYSPRR
SRGSPRYSPRHSRSRSRT

His-ASF/SF2_Block2 (pET15b, 29982.57)

MGHHHHHHHHHHSSGHIDDDDKHMSGGGVIRGPAGNNDCRIYVGNLPPDIRTKDIEDVFYKY
GAIRDIDLKNRRGGPPFAFVEFEDPRDAEDAVYGRDGYDYDGYRLRVEFPRSGRGTGRGGGG
GGGGGAPRGRYGPPSRRSENRVVVSGLPPSGSWQDLKDHMREAGDVCYADVYRDGTGVVEF
VRKEDMTYAVRKLDNTKFRSHEGETAYIRVKVDGPRSPSYGRSRSASASASASASASNSRSRS
YSPRRSRGSPRYSPRHSRSRSRT

His-ASF/SF2_Block3 (pET15b, 30067.64)

MGHHHHHHHHHHSSGHIDDDDKHMSGGGVIRGPAGNNDCRIYVGNLPPDIRTKDIEDVFYKY
GAIRDIDLKNRRGGPPFAFVEFEDPRDAEDAVYGRDGYDYDGYRLRVEFPRSGRGTGRGGGG
GGGGGAPRGRYGPPSRRSENRVVVSGLPPSGSWQDLKDHMREAGDVCYADVYRDGTGVVEF
VRKEDMTYAVRKLDNTKFRSHEGETAYIRVKVDGPRSPSYGRSRSRSRSRSRSRSRSNSASASY
SPAASAGSPRYSPRHSRSRSRT

His-ASF/SF2_Block4 (pET15b, 30067.64)

MGHHHHHHHHHHSSGHIDDDDKHMSGGGVIRGPAGNNDCRIYVGNLPPDIRTKDIEDVFYKY
GAIRDIDLKNRRGGPPFAFVEFEDPRDAEDAVYGRDGYDYDGYRLRVEFPRSGRGTGRGGGG
GGGGGAPRGRYGPPSRRSENRVVVSGLPPSGSWQDLKDHMREAGDVCYADVYRDGTGVVEF
VRKEDMTYAVRKLDNTKFRSHEGETAYIRVKVDGPRSPSYGRSRSRSRSRSRSRSRSNSRSRSY
SPRRSRGSPAYSPAHSASASAT

His-ASF/SF2_Block1/2 (pET15b, 29585.26)

MGHHHHHHHHHHSSGHIDDDDKHMSGGGVIRGPAGNNDCRIYVGNLPPDIRTKDIEDVFYKY
GAIRDIDLKNRRGGPPFAFVEFEDPRDAEDAVYGRDGYDYDGYRLRVEFPRSGRGTGRGGGG
GGGGGAPRGRYGPPSRRSENRVVVSGLPPSGSWQDLKDHMREAGDVCYADVYRDGTGVVEF

VRKEDMTYAVRKLDNTKFRSHEGETAYIAVAVDGPASPSYGASASASASASASASASNSRSRS
YSPRRSRGSPRYSPRHSRSRSRT

His-ASF/SF2_Block2/3 (pET15b, 29557.25)

MGHHHHHHHHHHSSGHIDDDDKHMSGGGVIRGPAGNNDCRIYVGNLPPDIRTKDIEDVFYKY
GAIRDIDLKNRRGGPPFAFVEFEDPRDAEDAVYGRDGYDYDGYRLRVEFPRSGRGTGRGGGG
GGGGGAPRGRYGPPSRRSENRVVVSGLPPSGSWQDLKDHMREAGDVCYADVYRDGTGVVEF
VRKEDMTYAVRKLDNTKFRSHEGETAYIRVKVDGPRSPSYGRSRSASASASASASASNSASAS
YSPAASAGSPRYSPRHSRSRSRT

His-ASF/SF2_Block3/4 (pET15b, 29642.32)

MGHHHHHHHHHHSSGHIDDDDKHMSGGGVIRGPAGNNDCRIYVGNLPPDIRTKDIEDVFYKY
GAIRDIDLKNRRGGPPFAFVEFEDPRDAEDAVYGRDGYDYDGYRLRVEFPRSGRGTGRGGGG
GGGGGAPRGRYGPPSRRSENRVVVSGLPPSGSWQDLKDHMREAGDVCYADVYRDGTGVVEF
VRKEDMTYAVRKLDNTKFRSHEGETAYIRVKVDGPRSPSYGRSRSRSRSRSRSRSRSNSASASY
SPAASAGSPAYSPAHSASASAT

Additional SR proteins subcloned from mammalian expression vector pBABE into pET28a for bacterial expression:

SC35-His (pET28a, 27079.03)

MSYGRPPPDVEGMTSLKVDNLTYRTSPDTLRRVFEKYRRVGDVYIPRDRYTKESRGFAFVRFH
DKRDAEDAMDAMDGAVLDGRELRVQMARYGRPPDSHHSRRGPPPRRYGGGGYGRRSRSPRR
RRRSRSRSRSRSRSRSRSRYSRSKSRSRTRSRSRSTSKSRSARRSKSKSSSVSRSRSRSRSRSRS
PPPVSKRESKSRSRSKSPPKSPEEEGAVSSKLAAALEHHHHHH

SRp38-His (pET28a, 32857.63)

MGSRYLRPPNTSLFVRNVADDTRSEDLRREFGRYGPIVDVYVPLDFYTRRPRGFAYVQFEDVR
DAEDALHNLDRKWICGRQIEIQFAQGDRKTPNQMKAKEGRNVYSSSRYDDYDRYRRSRSRSY
ERRRSRSRSFDYNYRRSYSPRNSRPTGRPRRSRSHSDNDRFKHRNRSFSRSKSNSRSRSKSQPKK
EMKAKSRSRSASHTKTRGTSKTDSKTHYKSGSRYEKESRKKEPPRSKSQSRSQSRSRSKSRSRS
WTSPKSSGHKLAAALEHHHHHH

SRp40-His (pET28a, 32821.08)

MGSGCRVFIGRLNPAAREKDVERFFKGYGRIRDIDLKRGFGFVEFEDPRDADDAVYELDGKEL
CSERVTIEHARARSRGGRGRGRYSDRFSSRRPRNDRRNAPPVRTENRLIVENLSSRVSWQDLKD
FMRQAGEVTFADAHRPKLNEGVVEFASYGDLKNAIEKLSGKEINGRKIKLIEGSKRHSRSRSRS
RSRTRSSSRSRSRSRSRSRKSYSRSRSRSRSRSRSKSRSVSRSPVPEKSQKRGSSSRSKSPASVDR
QRSRSRSRSRSVDSGNKLAAALEHHHHHH

hTra2α-His (pET28a, 34088.75)

MGSDVEENNFEGRESRSQSKSPTGTPARVKSESRSGSRSPSRVSKHSESHSRSRSKSRSRSRRHS
HRRYTRSRSHSHSHRRRSRSRSYTPEYRRRRSRSHSPMSNRRRHTGSRANPDPNTCLGVFGLSL
YTTERDLREVFSRYGPLSGVNVVYDQRTGRSRGFAFVYFERIDDSKEAMERANGMELDGRRIR
VDYSITKRAHTPTPGIYMGRPTHSGGGGGGGGGGGGGGGRRRDSYYDRGYDRGYDRYEDY
DYRYRRSPSPYYSRYRSRSRSRSYSPRRYKLAAALEHHHHHH

hTra2β-His (pET28a, 35221.35)

MGSDSGEQNYGERESRSASRSGSAHGSGKSARHTPARSRSKEDSRRSRSKSRSRSESRSRSRRS
SRRHYTRSRSRSRSHRRSRSRSYSRDYRRRHSHSHSPMSTRRRHVGNRANPDPNCCLGVFGLSL
YTTERDLREVFSKYGPIADVSIVYDQQSRRSRGFAFVYFENVDDAKEAKERANGMELDGRRIR
VDFSITKRPHTPTPGIYMGRPTYGSSRRRDYYDRGYDRGYDDRDYYSRSYRGGGGGGGGWRA
AQDRDQIYRRRSPSPYYSRGGYRSRSRSRSYSPRRYKLAAALEHHHHHH

SRp75-His (pET28a, 58251.13)

MGPRVYIGRLSYQARERDVERFFKGYGKILEVDLKNGYGFVEFDDLRDADDAVYELNGKDLC
GERVIVEHARGPRRDGSYGSGRSGYGYRRSGRDKYGPPTRTEYRLIVENLSSRCSWQDLKDY
MRQAGEVTYADAHKGRKNEGVIEFVSYSDMKRALEKLDGTEVNGRKIRLVEDKPGSRRRRSY
SRSRSHSRSRSRSRHSRKSRSRSGSSKSSHSKSRSRSRSGSRSRSKSRSRSQSRSRSKKEKSRSPSK
DKSRSRSHSAGKSRSKSKDQAEEKIQNNDNVGKPKSRSPSRHKSKSKSRSRSQERRVEEEKRGS
VSRGRSQEKSLRQSRSRSRSKAGSRSRSRSRSKSKDKRKSRKRSREESRSRSRSRSKSERSRKRG
SKRDSKAGSSKKKKKEDTDRSQSRSPSRSVSKEREHAKSESSQREGRGESENAGTNQETRSRSR
SNSKSKPNLPSESRSRSRKSASKTRSRSKSRSRSASRSPSRSRSRSHSRSKLAAALEHHHHHH

SC35_RSdomain (pET28a, 15596.34)

MGSRRGPPPRRYGGGGYGRRSRSPRRRRRSRSRSRSRSRSRSRSRYSRSKSRSRTRSRSRSTSKS
RSARRSKSKSSSVSRSRSRSRSRSRSRSRSPPPVSKRESKSRSRSKSPPKSPEEEGAVSSKLAAALEH
HHHHH

SRp38_RSdomain (pET28a, 20674.45)

MGYSSSRYDDYDRYRRSRSRSYERRRSRSRSFDYNYRRSYSPRNSRPTGRPRRSRSHSDNDRFK
HRNRSFSRSKSNSRSRSKSQPKKEMKAKSRSRSASHTKTRGTSKTDSKTHYKSGSRYEKESRK
KEPPRSKSQSRSQSRSRSKSRSRSWTSPKSSGHKLAAALEHHHHHH

SRp40_RSdomain (pET28a, 13199.04)

MGKIKLIEGSKRHSRSRSRSRSRTRSSSRSRSRSRSRSRKSYSRSRSRSRSRSRSKSRSVSRSPVPE
KSQKRGSSSRSKSPASVDRQRSRSRSRSRSVDSGNKLAAALEHHHHHH

SRp55_RSdomain (pET28a, 21038.26)

MGRLIEDKPRTSHRRSYSGSRSRSRSRRRSRSRSRRSSRSRSRSISKSRSRSRSRSKGRSRSRSKG

RKSRSKSKSKPKSDRGSHSHSRSRSKDEYEKSRSRSRSRSPKENGKGDIKSKSRSRSQSRSNSPL

PVPPSKARSVSPPPKRATSRSRSRSRSKSRSRSRSSSRDKLAAALEHHHHHH

Chapter III

Kinetic Analysis of ASF/SF2

Phosphorylation by SRPK1 and Clk/Sty

A. Abstract

Assembly of the spliceosome requires the participation of SR proteins, a family of splicing factors rich in arginine-serine dipeptide repeats. The repeat regions (RS domains) are polyphosphorylated by the SRPK and Clk/Sty families of kinases. The two families of kinases have distinct enzymatic properties, raising the question of how they may work to regulate the function of SR proteins in RNA metabolism in mammalian cells. We found that SRPK1 was responsible for efficient phosphorylation of a short stretch of amino acids in the N-terminal portion of the RS domain of ASF/SF2 while Clk/Sty was able to transfer phosphate to all available serine residues in the RS domain, indicating that SR proteins may be phosphorylated by different kinases in a stepwise manner. Both kinases bind with high affinity and use processive catalytic mechanisms to achieve either restrictive or complete RS domain phosphorylation. These findings have important implications on the regulation of SR proteins in vivo by the SRPK and Clk/Sty families of kinases.

B. Introduction

It is estimated that more than one-half of human genes are alternatively spliced (Modrek and Lee, 2002). Although many of these genes may contain only a few splice variants, a few have been shown to possess thousands (Black, 2000; Graveley, 2001; Modrek and Lee, 2002). RNA splicing occurs in the nucleus at a macromolecular complex composed of many RNA and protein molecules known as the spliceosome (Akker et al., 2001; Stojdl and Bell, 1999). In the last decade it has become apparent that both the assembly of the spliceosome and selection of splice sites depend on the

proper phosphorylation of a family of splicing factors known as SR proteins (Modrek and Lee, 2002). The SR proteins are so named because they have long stretches of arginine-serine dipeptide repeats in RS domains. Phosphorylation leads to translocation of the SR protein from the cytoplasm to the nucleus (Koizumi et al., 1999; Lai et al., 2001) and recruitment of the SR proteins from sites of nuclear storage in speckles to nascent transcripts for splicing (Colwill et al., 1996; Duncan et al., 1998; Gui et al., 1994a). Phosphorylated SR proteins are believed to facilitate both 5' and 3' splice site recognition through interaction with the RS domain in U1-70 K (a component of the U1 small nuclear ribonucleoprotein) and the U2AF heterodimer (Jamison et al., 1995; Xiao and Manley, 1997, 1998). More recently, RS domains were shown to interact directly with critical cis-acting elements in pre-mRNA (Shen and Green, 2004; Shen et al., 2004). In addition to their functions in the spliceosome, SR proteins are also shown to play a role in the export of processed mRNA from the nucleus to the cytoplasm for translation. Two shuttling SR proteins, ASF/SF26 and 9G8, have been shown to conduct the export of mRNA through interactions with a nuclear export factor, TAP (Huang et al., 2003; Huang and Steitz, 2001; Lai and Tarn, 2004). Hypophosphorylation of these SR proteins promotes interaction with TAP suggesting that transport may require splicing factor dephosphorylation. These shuttling SR proteins were also found to play a direct role in translation in the cytoplasm (Sanford et al., 2004).

Although it is clear that SR proteins can be polyphosphorylated in the RS domain regions by the SRPK and Clk/Sty families of protein kinases (Caceres and Krainer, 1993; Koizumi et al., 1999), the specificity and mechanism of SR protein

phosphorylation by these kinases is still poorly understood. We previously reported that SRPK and Clk/Sty have distinct substrate specificity and enzymatic kinetics in phosphorylating SR proteins (Colwill et al., 1996). More recently, we demonstrated that SRPK1 uses a processive catalytic mechanism to phosphorylate the prototypical SR protein ASF/SF2 (Aubol et al., 2003). This finding is interesting, because it indicates that SRPK1 makes a single encounter with ASF/SF2 and catalyzes the ATP-dependent phosphorylation of the RS domain without dissociating from the substrate. This unusual mechanism is prompted, in part, by a high affinity interaction between the enzyme and splicing factor (K_d = 50 nM) (Aubol et al., 2003). Once the SRPK1-ASF/SF2 complex is formed it dissociates very slowly in comparison to a fast forward rate for RS domain phosphorylation. Although a processive mechanism for serine phosphorylation is unique, it has been shown that the phosphorylation of tyrosine residues can occur in a similar manner. For instance, the tyrosine kinase Src phosphorylates Cas at numerous sites using a processive mechanism where no phosphotyrosine intermediates are released prior to complete phosphorylation of the substrate (Pellicena and Miller, 2001). In this case, it is thought that the SH2 domain of Src serves as a molecular tether for multiple rounds of tyrosine phosphorylation in the substrate, thereby, accounting for the absence of intermediate phosphoforms. In contrast, SRPK1 appears to use a unique docking site to anchor SR protein substrates near the catalytic site (Ngo et al., 2005).

In this present study mass spectrometric and kinetic methods were used to determine how the SRPK and Clk/Sty families of protein kinases modify sequences in the RS domain of ASF/SF2. The results reveal that the RS domain in ASF/SF2 is not a

random sequence with Arg-Ser repeats as the only recognizable feature. Instead, the RS domain can be divided into two subdomains, one of which was efficiently phosphorylated by SRPK1. In contrast, Clk/Sty was capable of transferring phosphate to all available serines in the RS domain. The phosphorylation of these subdomains appears to occur through similar catalytic mechanisms. Both SRPK1 and Clk/Sty can phosphorylate the RS domain using processive mechanisms. Interestingly, SRPK1 phosphorylates only the N-terminal portion of the RS domain before dissociating, whereas Clk/Sty can stay attached and phosphorylate the entire RS domain.

SR protein phosphorylation is a critical regulatory mechanism for these unique splicing factors. The distinct cellular partitioning of the SR kinases in the nucleus and cytoplasm are likely regulated by signaling pathways to modulate phosphorylation states of SR proteins in different regions of the cell. The unique SRPK spacer domain separating its bipartite catalytic core plays an important role in its cellular localization by restricting the kinase to the cytoplasm. Removal of the spacer causes a quantitative translocation to the nucleus dependent on the kinase activity of SRPK1 (Ding et al., 2006). Furthermore, a cell cycle signal induced nuclear translocation of the full-length kinase at the G2/M boundary (Ding et al., 2006).

The requirement for an enzymatically active kinase to enter the nucleus is consistent with previous biochemical studies demonstrating the spacer-deleted SRPKs maintain catalytic activity (Aubol et al., 2003; Ngo et al., 2005; Nolen et al., 2001). It has been unclear, however, whether deletion of the spacer further activates the kinase or modulates other biochemical aspects of the kinase because many kinases translocate to the nucleus upon activation (Cyert, 2001). We therefore set out to conduct detailed

kinetic characterization of full-length and spacer-deleted SRPK1 using ASF/SF2 as a substrate.

C. Results

1. Phosphorylation Kinetics of ASF/SF2 by SRPK1 and Clk/Sty

The phosphorylation of ASF/SF2 by multiple kinases was evaluated by excising ^{32}P-labeled bands from SDS-PAGE gels corresponding to the phosphorylated forms of the substrate. The SRPK1 reaction is accompanied by a time-dependent increase in band intensity for ASF/SF2 as previously described (Aubol et al., 2003). The Clk/Sty reaction is accompanied by both an increase in band intensity and a small change in migration state of ASF/SF2 on the gel as described previously (Prasad and Manley, 2003). Data in Figure 3.1A shows that both SRPK1 and Clk/Sty catalyze rapid ASF/SF2 phosphorylation in single turnover experiments ([E] > [ASF/SF2]). Although SRPK1 could only phosphorylate 8-10 sites as previously shown (Aubol et al., 2003; Gui et al., 1994b), Clk/Sty was able to modify ~20 sites, a value reflecting all available serines in the RS domain of ASF/SF2 (Figure 3.1A). Because this radioactive incorporation assay requires precise determinations of substrate concentration, we used MALDI-TOF mass spectrometry to obtain substrate-independent measurements of phosphoryl content. Figure 3.1 (B and C) displays the spectra of ASF/SF2 with SRPK and Clk/Sty before and after treatment with ATP. The M+1 peak for ASF/SF2 increases to a higher mass/charge in the presence of both kinases consistent with ATP-dependent phosphorylation. For SRPK1, an increase of 845 mass units was observed, consistent with the incorporation of 10 phosphates per

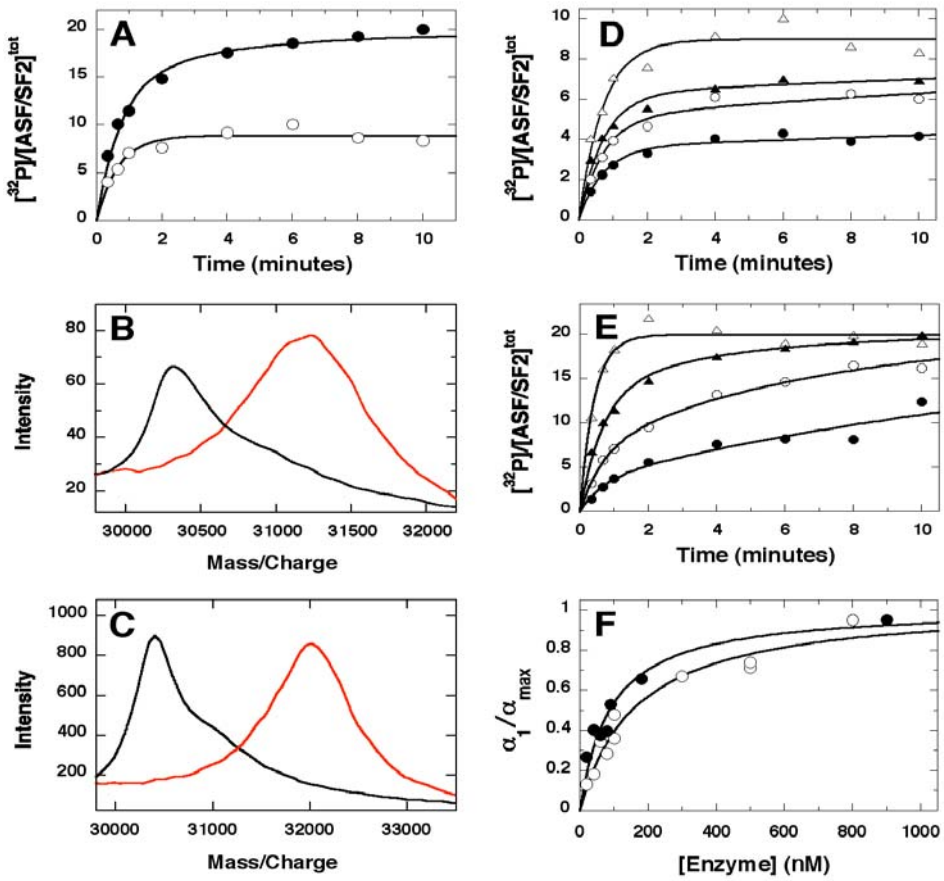

Figure 3.1 Kinetics of ASF/SF2 phosphorylation by SRPK1 and Clk/Sty. A) Progress curves for ASF/SF2 (20 nM) phosphorylation using 0.9 mM SRPK1 (●) and 0.5 mM Clk/Sty (o). The SRPK1 reaction is fit to a single exponential with an amplitude and a rate constant of 9 sites and 1.5 min^{-1}, respectively. The Clk/Sty reaction is fit to a double exponential with rate constants of 1.4 and 0.29 min^{-1} and amplitudes of 14 and 6 sites, respectively. B) MALDI-TOF spectra of ASF/SF2 with SRPK1. ASF/SF2 (10 mM) is mixed with SRPK1 (10 mM) for one hour in the absence and presence of ATP (3 mM). The maximum for the M+1 peak increases from 30,351 in the absence of ATP (black) to 31,196 in the presence of ATP (red). C) MALDI-TOF spectra of ASF/SF2 with Clk/Sty. ASF/SF2 (10 mM) is mixed with Clk/Sty (10 mM) for one hour in the absence and presence of ATP (3 mM). The maximum for the M+1 peak increases from 30,370 in the absence of ATP (black) to 32,087 in the presence of ATP (red). D) Progress curves for ASF/SF2 phosphorylation as a function of SRPK1. ASF/SF2 (20 nM) is phosphorylated using 60 (●), 90 (o), 180 (▲), and 900 (Δ) SRPK1. The data at 60, 90 and 180 nM SRPK1 were fit to double exponential functions with amplitudes for the fast phase of 3.6, 5.1, and 6.3, respectively, and a common fast phase rate constant of 1.4 min^{-1}. The maximum amplitude change in all plots is 9 sites. The data at 900 nM SRPK1 were fit to a single exponential function with an amplitude of 9 and a rate constant of 1.4 min^{-1}. E) Progress curves for ASF/SF2 phosphorylation as a function of Clk/Sty. ASF/SF2 (20 nM) is phosphorylated using 40 (●), 100 (o), 500 (▲), and 800 nM (Δ) Clk/Sty. The data at 40, 100, 500 and 800 nM Clk/Sty were fit to double exponential functions with amplitudes for the fast phase of 3.6, 6.9, 14 and 18, respectively, and a common fast phase rate constant of 1.4 min^{-1}. The maximum amplitude change in all transients is 20. F) Affinity of ASF/SF2 for SRPK1 and Clk/Sty. Amplitudes of the initial, fast phase in the progress curves normalized to the total amplitude change are plotted as a function of total SRPK1 (●) and Clk/Sty (o) concentration. The data are fit using equation (1) to obtain K_d values of 80 ± 20 nM for SRPK1 and 160 ± 33 nM for Clk/Sty.

substrate molecule (Figure 1B). In contrast, Clk/Sty treatment resulted in a large mass shift (1720 mass units), consistent with the incorporation of 22 phosphates (Figure 1C).

2. Dissociation Constants of SRPK1 and Clk/Sty

Because SRPK1 and Clk/Sty exhibit differential phosphorylation patterns, we sought to determine whether this unique specificity is linked to the stabilities of the enzyme-substrate complexes. To determine the affinities of both kinases for ASF/SF2, single turnover profiles were monitored as a function of total enzyme concentration.For both kinases, the phosphorylation kinetics of ASF/SF2 is biphasic at lower enzyme concentrations (Figure 3.1, D and E), a phenomenon observed previously for SRPK1 (Aubol et al., 2003). All progress curves approach a common end point defined by the total number of phosphorylation sites accessible by the kinase. In contrast, the kinetic profiles approximate single exponential transients that quickly reach an end point at high SRPK1 and Clk/Sty concentrations (>500 nM). The rate constants for the fast phases are similar in value and do not vary significantly over a wide range of enzyme concentrations (1-2 min^{-1}). The amplitude of the first phase is used as an estimate of the initial concentration of the enzyme-substrate complex, and its enzyme dependence can then be used to determine the K_d values for both SRPK1 and Clk/Sty (Fig. 3.1F). Fitting the normalized amplitude data to Equation 1 provides K_d values of 80 and 160 nM for SRPK1 and Clk/Sty.

3. SRPK1 Phosphorylates the N-terminal Region of the ASF/SF2 RS Domain

Having observed that SRPK1 phosphorylates approximately 10 residues on ASF/SF2, we next set out to determine which region of ASF/SF2 is targeted by the kinase. Using Quickchange mutagenesis, we inserted stop codons following residue 196 and 219 of our plasmid construct (Figure3.2A). These mutations gave rise to ASF/SF2 C-terminal deletion constructs that were lacking the entire RS domain (ASF/SF2Δ196) or the C-terminal portion of the RS domain (ASF/SF2Δ219). Protein concentrations were determined by Bradford analysis and A_{280} measurements, and the deletion mutants were compared to full length ASF/SF2 in ATP(γ-P^{32}) phosphorylation assays with SRPK1. In standard phosphorylation assays, 300 nM of SRPK1 was incubated with 1 μM of the respective ASF/SF2 protein constructs prior to reaction initiation with ATP(γ-P^{32}). SRPK1 did not phosphorylate the ASF/SF2Δ196 protein, demonstrating that SRPK1 does not phosphorylate the RRM domains of ASF/SF2, and has specificity for the RS domain (Figure 3.2B). Interestingly, the ASF/SF2Δ219 construct was phosphorylated to nearly the same extent as full length ASF/SF2 (Figure 3.2B). This result indicates that SRPK1 preferentially phosphorylates the N-terminal portion of the RS domain.

4. Stepwise Phosphorylation of ASF/SF2 By SRPK1 and Clk/Sty

The finding that SRPK1 and Clk/Sty differentially phosphorylate the RS domain in ASF/SF2 raises an interesting question as to whether these two kinases could act synergistically on the same substrate. In light of our previous finding that SRPK1 and Clk/Sty could each form stable complexes with ASF/SF2, we asked

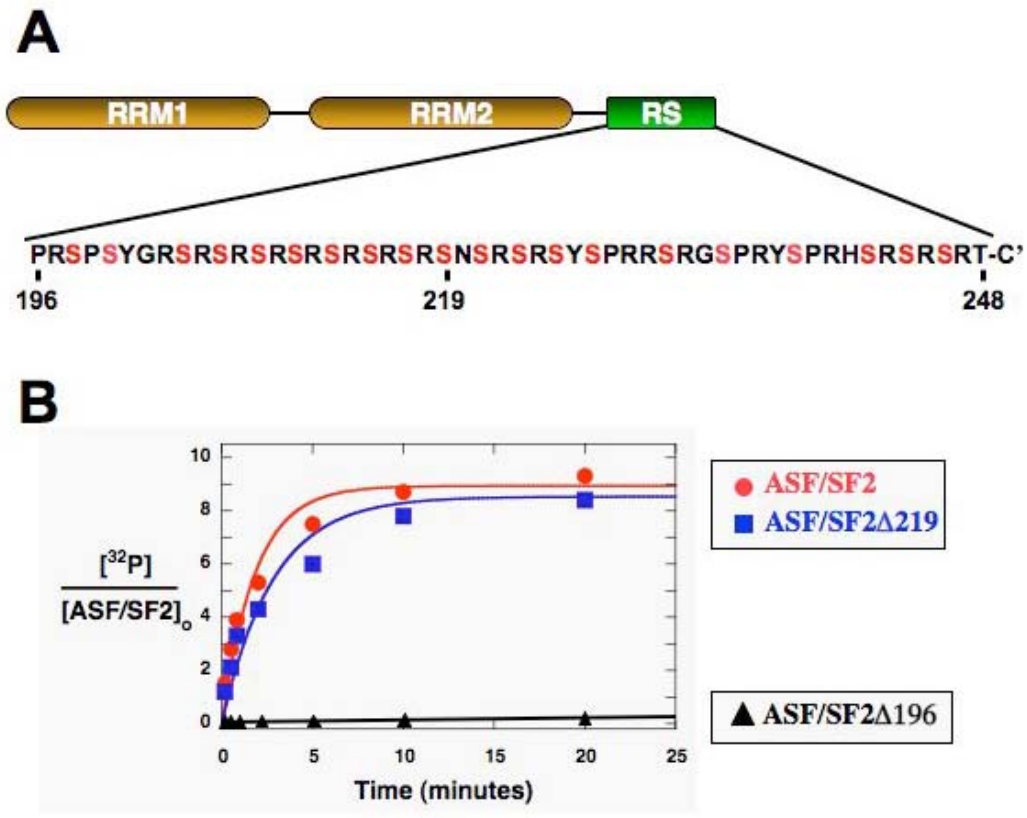

Figure 3.2 SRPK1 phosphorylates the N-terminal portion of the ASF/SF2 RS domain. (A) ASF/SF2 has two RRMs and a C-terminal RS domain. (B) C-terminal deletion constructs were studied as SRPK1 substrates. SRPK1 phosphorylates the 1-219 construct to nearly the same extent as full length ASF/SF2. The 1-196 construct is not phosphorylated by SRPK1.

whether Clk/Sty could still catalyze phosphorylation in the presence of SRPK1. These experiments were performed using equal concentrations of both Clk/Sty and SRPK1 so that either kinase can effectively compete with the other for ASF/SF2 if a common binding site is used. As shown in Figure 3.3A, after pre-phosphorylation of ASF/SF2 with SRPK1, an equivalent amount of Clk/Sty was added (300 nM) and found to phosphorylate the remaining sites in the RS domain. In contrast, the addition of an equivalent amount of SRPK1 (300 nM) after prephosphorylation with Clk/Sty led to no significant increase in phosphoryl content (Figure 3.3B). Thus, prephosphorylation of ASF/SF2 by SRPK1 does not impair additional phosphorylation by Clk/Sty when equivalent amounts of enzyme are used. To determine whether or not the binding of one kinase could antagonize the other at higher concentrations, inhibition studies were performed using excess amounts of an inactive version of SRPK1 (kdSRPK1) that contains a Lys to Met mutation in the ATP binding site. Using a 50-fold molar excess of kdSRPK1 (50 μM), the phosphorylation of ASF/SF2 by Clk/Sty (1 μM) was effectively reduced to a small background reaction, consistent with the trapping of about 98% of the total substrate. The initial velocities for ASF/SF2 phosphorylation are 50 and 1.3 sites/min in the absence and presence of kdSRPK1. Overall, these findings suggest that SRPK1 antagonizes the action of Clk/Sty when present at high concentrations but allows complete and rapid phosphorylation of the RS domain when the enzyme concentrations are equivalent.

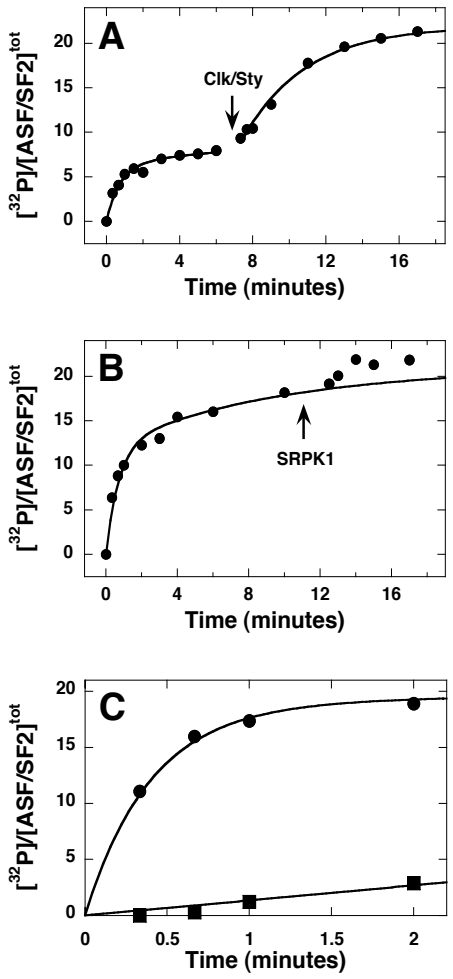

Figure 3.3 Step-wise phosphorylation of ASF/SF2 by SRPK1 and Clk/Sty. A) Clk/Sty doping of SRPK1-phosphorylated ASF/SF2. SRPK1 (300 nM) and ASF/SF2 (40 nM) are allowed to react for 7 minutes before one equivalent of Clk/Sty (300 nM) is then added. The SRPK1 reaction is fit to a double exponential function with a maximum phosphoryl content of 9 sites whereas the Clk/Sty addition phase is fit to a single exponential function with a maximum phosphoryl content of about 22 sites. B) SRPK1 doping of Clk/Sty-phosphorylated ASF/SF2. Clk/Sty (300 nM) and ASF/SF2 (40 nM) are allowed to react for 11 minutes before one equivalent of SRPK1 (300 nM) is then added. The Clk/Sty reaction is fit to a double exponential function with a maximum phosphoryl content of 20 sites whereas the SRPK1 addition phase increases the phosphoryl content to only about 21 sites. C) kdSRPK1 displacement of Clk/Sty from ASF/SF2. Clk/Sty (1 mM) and ASF/SF2 (200 nM) are preequilibrated for 5 minutes in the absence (●) and presence (■) of kdSRPK1 (50 mM) before addition of ATP. In the absence of kdSRPK1, the data are fit to a single exponential function with a rate constant and amplitude of 2.5 min^{-1} and 20 sites, respectively. The data in the presence of kdSRPK1 are fit to a line function with a slope of 1.3 sites/min.

5. Processive Phosphorylation of ASF/SF2 by SRPK1

We showed previously that SRPK1 catalyzes ASF/SF2 phosphorylation in a processive manner in a pre-formed enzyme-substrate complex (Aubol et al., 2003). To extend this analysis to a more natural kinase-substrate system, we determined whether processive phosphorylation is a result of the method of complex preparation. To perform these studies, we combined native SRPK1 and ASF/SF2 without a re-folding step and determined whether this complex could be processively phosphorylated in start-trap experiments. In this experiment, the reaction is initiated with ATP (start) and simultaneously mixed with excess kdSRPK1 (trap). The experiment is performed under single turnover conditions where the SRPK1 concentration (1 μM) is 12-fold above the K_d for the complex ensuring that very little free ASF/SF2 is present at the time of start. If any phosphorylated forms of ASF/SF2 are generated and released from SRPK1 as expected in a distributive mechanism, kdSRPK1 will trap them and inhibit the reaction. However, if the reaction is processive, kdSRPK1 will not influence the progress curve. As shown in Figure 3.4A, kdSRPK1 does not impact the phosphorylation of ASF/SF2 when added at the time of start in keeping with a processive reaction. In comparison, addition of kdSRPK1 to the complex prior to start with ATP leads to profound inhibition of the reaction progress curve indicating that kdSRPK1 is an effective trap for ASF/SF2. These data indicate that SRPK1 naturally catalyzes processive phosphorylation of ASF/SF2 within the time frame of the reaction.

6. Clk/Sty Catalyzes Processive Phosphorylation of the Entire RS Domain

Because Clk/Sty phosphorylates ASF/SF2 to a greater extent than SRPK1, we wondered whether the complete modification of the RS domain could occur in a processive manner. To test for this possibility, we performed start-trap experiments using excess amounts of a kinase inactive form of Clk/Sty (kdClk/Sty) as a trapping agent for the detection of any free ASF/SF2. As shown in Figure 3.4B, when added at reaction start, kdClk/Sty did not affect the reaction rate or end point for the Clk/Sty-catalyzed reaction. The efficiency of the trap was verified by demonstrating that kdClk/Sty could effectively inhibit the reaction when added to the complex prior to start. The initial velocity of the progress curve is lowered from 40 sites/min in the absence of kdClk/Sty to 1.1 sites/min in the presence of pre-equilibrated kdClk/Sty, a rate change corresponding to a trapping efficiency of 97%. These findings indicate that the absence of inhibition in the start-trap experiment is not the result of poor binding of the inactive kinase trap. Overall, these findings suggest that Clk/Sty is capable of processively phosphorylating the entire RS domain.

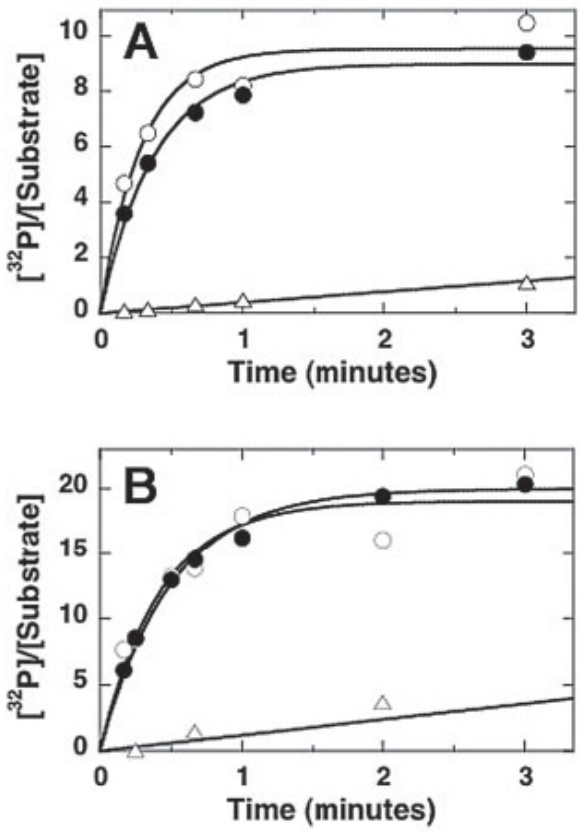

Figure 3.4 Mechanism of ASF/SF2 phosphorylation by SRPK1 and Clk/Sty. A, processive phosphorylation of ASF/SF2 by SRPK1. SRPK1 (1 μM) and ASF/SF2 (200 nM) are preequilibrated in the absence (●) and presence (Δ) of kdSRPK1 (50 μM) for 5 min before reaction initiation with ATP. The start-trap experiment is performed by pre-equilibrating SRPK1 (1 μM) and ASF/SF2 (200 nM) for 5 min before the simultaneous addition of ATP and 50 μM kdSRPK1 (o). The control (no kdSRPK1) and start-trap data are fit to a single exponential function with amplitudes of 9 and 9.5 sites, respectively, and rate constants of 3.4 and 2.6 min-1, respectively. When SRPK1 and ASF/SF2 are pre-equilibrated with kdSRPK1 for 5 min prior to reaction initiation with ATP, ASF/SF2 phosphorylation follows a linear time dependence with a slope of 0.4 sites/min. B, processive phosphorylation of ASF/SF2 by Clk/Sty. Clk/Sty (1 μM) and ASF/SF2 (150 nM) are pre-equilibrated in the absence (●) and presence (Δ) of kdClk/Sty (29 μM) for 5 min before reaction initiation with ATP. The start-trap experiment is performed by pre-equilibrating Clk/Sty (1 μM) and ASF/SF2 (150 nM) for 5 min before the simultaneous addition of ATP and 29 μM kdSRPK1 (o). The control (no kdClk/Sty) and start-trap data are fit to a single exponential function with rate constants of 2 and 2.3 min-1, respectively, and a common amplitude of 20 sites. When Clk/Sty and ASF/SF2 are pre-equilibrated with kdClk/Sty for 5 min prior to reaction initiation with ATP, ASF/SF2 phosphorylation follows a linear time dependence with a slope of 1.1 sites/min.

7. Sequential Phosphorylation of RS Domain Segments By Clk/Sty

To determine whether Clk/Sty could sequentially phosphorylate portions of the RS domain, we analyzed the gel shift associated with ASF/SF2 phosphorylation. Unlike the SRPK1 reaction, the phosphorylation of ASF/SF2 by Clk/Sty occurs with a detectable gel shift in the phosphorylated species (inset to Figure 3.5). A fast migrating species (lower) is populated early in the progress curve (~0.3 min) followed by the production of a slower migrating species (upper). The appearance and disappearance of the lower band were fitted to Equation 2,

$$L = L_{max} \times \frac{k_1}{(k_2 - k_1)}\left[\exp(-k_1 \times t) - \exp(-k_2 \times t)\right] \quad (2)$$

where L is the concentration of incorporated ^{32}P normalized to the total ASF/SF2 concentration at any time t, L_{max} is the maximum phosphoryl content of the lower band, and k_1 and k_2 are the rate constants controlling the production and disappearance of the lower band. The time dependence for the generation of the upper band was fitted to Equation 3,

$$U = U_{max} \times \frac{\left[1 - k_2\exp(-k_1 \times t) - k_1\exp(-k_2 \times t)\right]}{(k_2 - k_1)} \quad (3)$$

where U is the concentration of incorporated ^{32}P normalized to the total concentration of ASF/SF2 at any time t, U_{max} is the phosphoryl content of the upper band, and k_1 and k_2 are defined as in Equation 2. Equations 2 and 3 are adapted from a previous study

(Gutfreund, 1995). As shown in Figure 3.5, the appearance of the lower and upper bands follow a classic sequential reaction pattern where the lower (hypophosphorylated) species forms rapidly (3 – 6 min^{-1}) and then disappears at the same rate constant as the formation of the upper (hyperphosphorylated) species (~1min^{-1}). The total incorporation of ^{32}P into both bands (dotted line in Figure 3.5) approximates a single exponential relationship (1.5 min^{-1}) as observed previously under similar reaction conditions (Figure 3.1E). The rapid production of the lower band and the lag in the generation of the upper band is consistent with the sequential phosphorylation of two regions in the RS domain of ASF/SF2. Finally, it is worth noting that this sequential determination implies an ordered succession of phosphorylation events but does not refer to whether this occurs in a processive or distributive manner. Rather, processivity is established in start-trap experiments and is independent of reaction sequence determination (Figure 3.4).

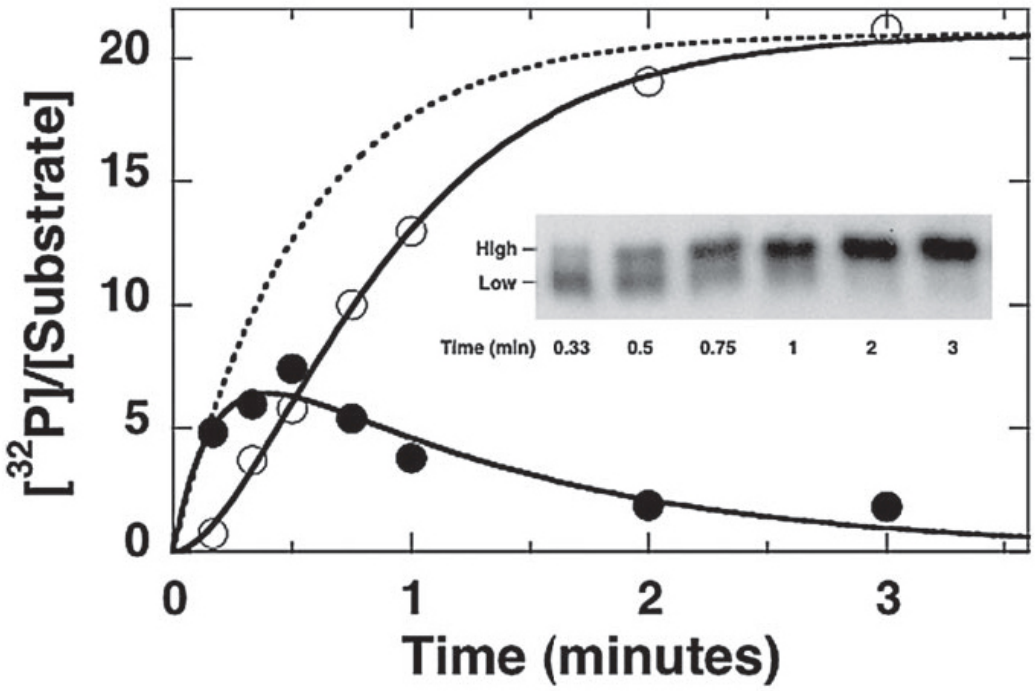

Figure 3.5 Sequential phosphorylation of ASF/SF2 phosphorylation by Clk/Sty. Clk/Sty (1 μM) and ASF/SF2 (0.2 μM) are pre-equilibrated before reaction initiation with ATP. Bands corresponding to the fast migrating (lower) and the slow migrating (upper) forms of ASF/SF2 are individually excised from the gel (inset) and the concentration of ^{32}P incorporated (normalized to the total substrate concentration) is plotted against reaction time. The data for the lower and upper bands are fit to Equations 2 and 3. For the lower band, values of 5.6 $\pm$ 2.4 min $^{-1}$, 0.80 $\pm$ 0.26 min^{-1}, and 8.8 1.7 sites were obtained for k1, k2, and Lmax, respectively. For the upper band, values of 3.3 $\pm$ 0.71 min^{-1}, 1.4 0.26 min^{-1}, and 21 $\pm$ 0.3 sites are obtained for k_1, k_2, and U_{max}, respectively.

8. Contribution of SRPK1 Spacer Domain to Catalysis and Affinity for ASF/SF2

In steady-state kinetic assays (Figure 3.6A), the spacer increased the turnover number (k_{cat}) by a factor of 2 (5 versus 10 min^{-1}), but had no impact on the K_m for ASF/SF2 (K_m of ~200 nM). In single turnover reactions (i.e., [E] >> K_d), the single exponential rate constants for ASF/SF2 phosphorylation differed by approximately three-fold (Figure 3.6B), further indicating the spacer enhances substrate turnover by a small but real amount. Whether the spacer altered the interaction between the kinase and ASF/SF2 was unclear from steady-state kinetic analyses because K_m is an apparent dissociation constant and does not commonly measure the real affinity of the substrate and enzyme. Because of these limitations, we directly measured the K_d for ASF/SF2 based on single turnover experiments. As shown in Figure 3.6C, the single exponential transient for ASF/SF2 was clearly biphasic at lower enzyme concentrations because of the dissociation of the kinase-substrate complex near or below the K_d value. The initial phase reflects the phosphorylation of ASF/SF2 in the enzyme-substrate complex, whereas the slower phase reflects the phosphorylation of ASF/SF2 upon recombination of the free enzyme and substrate. We measured the relative amplitude of the initial phase to the total amplitude as a function of enzyme concentration, and utilize Equation 1 below to calculate K_d values of 20 and 80 nM for full-length and spacer-deleted SRPK1 (Figure 3.6D). Based on this data, we concluded the spacer does not hinder ASF/SF2 phosphorylation but rather enhances the stability of the complex by approximately four fold. These observations suggest the translocation of the spacer-deleted SRPK1 is not the result of large changes in binding or catalytic properties imposed by the removal of the spacer sequence.

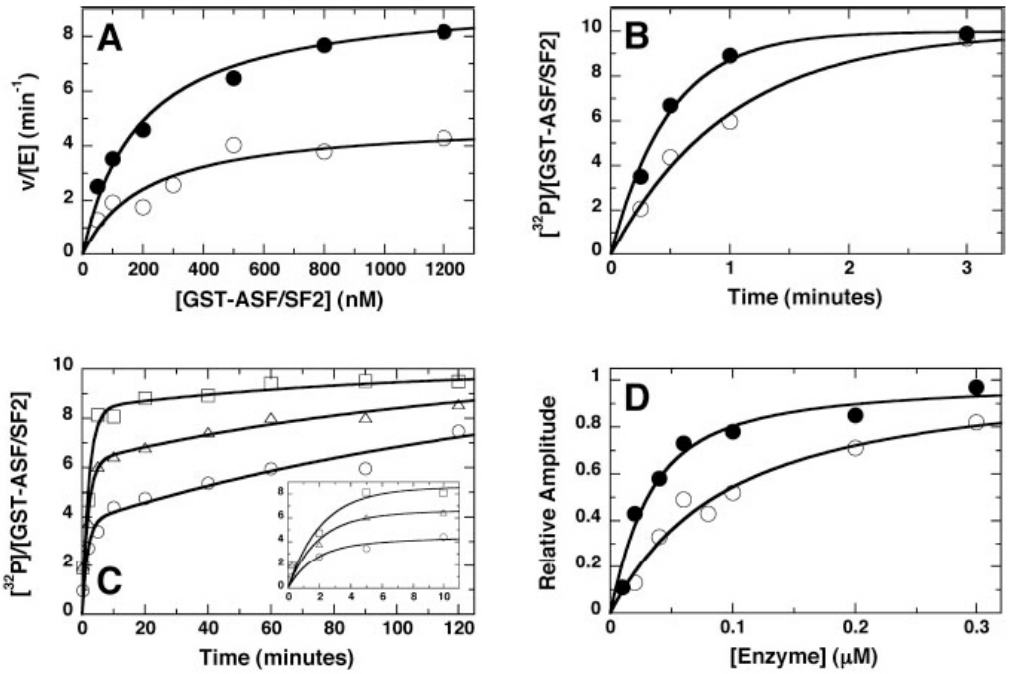

Figure 3.6 Effects of the SRPK1 spacer on the phosphorylation kinetics of ASF/SF2. Steady-state kinetics (A). Initial velocities were measured as a function of varying GST-ASF/SF2 using SRPK1 (•) and K1-ΔS (). For SRPK1, k_{cat} and K_m are 9.5 ± 0.5 min^{-1} and 190 ± 40 nM, respectively, and for K1-ΔS, k_{cat} and K_m are 4.9 ± 0.4 min^{-1} 210 ± 60 nM, respectively. and Single-turnover kinetics (B). GST-ASF/SF2 (200 nM) was preequilibrated with 1 μM SRPK1 (•) and K1-ΔS (o) and allowed to react with [^{32}P]ATP for varying periods of time. Data were fit to a single exponential function to obtain rate constants of 2.5 and 0.9 min^{-1} for SRPK1 and K1-ΔS. Enzyme-dependent single turnover kinetics (C). GST-ASF/SF2 (10 nM), preequilibrated with 50 nM (o), 150 nM (Δ), and 360 nM (□) K1-ΔS, was mixed with [γ-^{32}P]ATP for varying periods of time, and the number of sites phosphorylated was determined and expressed as a ratio of ^{32}P-incorporated and the total GST-ASF/SF2 concentration. The amplitudes of the first kinetic phase are 3.7, 6.2, and 8 at 50, 150, and 360 nM K1-ΔS, respectively. Determination ofK_d values for SRPK1 and K1-ΔS (D). The amplitudes of the first phases in single turnover experiments were normalized to the reaction endpoints and plotted against the total concentrations of SRPK1 (•) and K1-ΔS(o). A quadratic function was used to obtain *K* values of 20 ± 6 and 80 ± 14 nM for SRPK1 and K1-ΔS, respectively.

D. Discussion

In the present study, we characterized representatives of two major kinase families involved in post-translational modification of SR proteins. Enzyme-dependent single turnover data show that both kinases bind with similar affinities to ASF/SF2 (Figure 3.1). By kinetic methods, we found that Clk/Sty is able to transfer phosphates to the majority of serine residues in the RS domain, whereas SRPK1 is restricted to a block of arginine/serine (RS) repeats in the N-terminal half of the RS domain, demonstrating clear regiospecificity between the two kinases (Figures 3.1 and 3.2). The observation is consistent with previous phosphopeptide mapping, showing that the RS domain phosphorylated by Clk/Sty appears to give rise to a much more complicated phosphopeptide pattern than that by SRPK1 (Colwill et al., 1996). These findings can now be used to explain some unexpected reactivities of SR proteins from other species. For example, the Drosophila ASF/SF2 ortholog dASF was shown to be a substrate for Clk/Sty, but not for SRPK1 (Allemand et al., 2001). Sequence comparisons reveal that the first block of RS repeats in ASF/SF2 that are phosphorylated by SRPK1 is substituted with a glycine-tract in dASF, thereby, abolishing the SRPK1 sites but still preserving the Clk/Sty sites. The relaxed specificity of Clk/Sty-mediated phosphorylation indicates that this family of kinases may play a broad regulatory role in RNA metabolism in mammalian cells.

1. Partial Phosphorylation of the RS Domain By SRPK1

Although SRPK1 phosphorylates up to ten serines in the N-terminal portion of the RS domain, the kinetic transient associated with this modification is monophasic at

high enzyme concentration. This raises the compelling question of how SRPK1 accomplishes multisite phosphorylation over a confined polypeptide stretch without introducing complex multiphase kinetics. Two mechanisms can be invoked to account for this phenomenon. First, SRPK1 may not distinguish between these sites and consequently may phosphorylate them randomly in a tight complex with ASF/SF2. Such a mechanism would require considerable flexibility in the RS domain so that all sites are equally accessible to the kinase and, thus, kinetically indistinguishable. Second, SRPK1 may phosphorylate these residues in a sequential manner with the initial site representing the slow step in the overall reaction. In this mechanism, the RS domain may be more rigidly held in place so that SRPK1 starts at one locus and then phosphorylates in a single direction (either N- or C-terminal) until the entire block of residues is modified. The placement of a slow phosphorylation step early in the reaction cycle allows the overall reaction to appear monophasic, satisfying the observed single exponential kinetic traces at high enzyme concentrations (Figures 3.1 and 3.4). At this time, it is difficult to ascertain which mechanism predominates, because it is unclear whether the SRPK1-catalyzed reaction has a defined directionality or is random. Nonetheless, given the electrostatic changes expected in the RS domain upon modification, it is more likely that phosphorylation would affect interaction of the RS domain with the active site of SRPK1 and, thus, give rise to more complex multiphase kinetic behavior. Given this potential limitation, we suspect that SRPK1 is most likely to catalyze sequential, processive phosphorylation with an initial, rate-limiting priming step.

2. Modifying the Entire RS Domain without Enzyme Dissociation

Clk/Sty is not only capable of phosphorylating the entire RS domain of ASF/SF2, but it also accomplishes this feat using a processive pathway. Thus, Clk/Sty can remain attached to ASF/SF2 for a longer period of time, extending an otherwise regiospecific reaction and including all blocks of Arg-Ser repeats. Although it is not clear at this time whether either Clk/Sty or SRPK1 uses a preferred directionality for this modification, time-dependent gel shift assays suggest that regions of the RS domain are phosphorylated in sequential manners. For Clk/Sty an early phospho-intermediate is populated in the active site before conversion to the fully phosphorylated form. This early form is generated at a faster rate than the fully mature species, thus, establishing two identifiable blocks of Clk/Sty modification. Interestingly, Clk/Sty is capable of switching between these two phosphorylation blocks without dissociating from the SR protein.

3. Cellular Control of Phosphorylation Specificity

The current data indicate that Clk/Sty and SRPK1 can phosphorylate SR proteins sequentially but not simultaneously. Although Clk/Sty modifies additional residues in ASF/SF2 in the presence of equal amounts of SRPK1, an imbalance in the SRPK1 concentration can inhibit phosphorylation of the RS domain, because one kinase antagonizes the action of the other (Figure 3.3). The cell avoids this potential conflict by anchoring the SRPK family of kinases in the cytoplasm (Cao et al., 1997) and restricting the Clk/Sty family of kinases to the nucleus (Colwill et al., 1996). We have shown previously that the spatial control of SRPKs is achieved via a spacer

within the conserved kinase core. Deletion of this spacer has little effect on the kinase activity but results in a quantitative shift of the kinase to the nucleus. These and other findings (Colwill et al., 1996; Prasad et al., 1999; Wang et al., 1998) are consistent with a model in which the SRPK family is largely involved in SR protein import into the nucleus, whereas nuclear-anchored Clk/Sty serves as a mediator for SR protein utilization in the nucleus. Unlike SRPK1, Clk/Sty has much broader substrate specificity so the full potential of this enzyme family in splicing control is likely to be more complex. The methods outlined in this report to accurately assess phosphoryl content, regiospecificity of modification, and kinetic pathways are important for understanding the role of these SR proteins and their regulatory kinases in splicing regulation.

4. Signals in the Spacer for Cytoplasmic Localization of SRPK1

It is clear that the spacer in the kinase plays a key regulatory role. Our kinetic analysis indicates that removal of the spacer modestly increased the stability of the kinase-substrate complex, which may contribute to nuclear import of the spacer-deleted kinase via a potential piggy-back mechanism. This model is consistent with the observation that overexpression of ASF/SF2 increased nuclear localization of the full-length kinase in transfected cells (Ngo et al., 2005). However, the ASF/SF2 induced shift was not as quantitative as we detected with the spacer-deleted kinase. Thus, although a modest enhancement of the kinase-substrate stability may have helped nuclear translocation of the kinase upon the removal of the spacer, it is unlikely to count for the quantitative shift observed. Furthermore, it is unlikely that SR protein

synthesis and/or shuttling are significantly elevated at the end of the G2-phase to massively induce the nuclear translocation of the endogenous kinase.

E. Experimental Procedures

1. Expression and Purification of Recombinant Proteins

Construction of pET19b-ASF/SF2 containing the ASF/SF2 coding sequence with a 10xHis tag at the N terminus was constructed by inserting the PCR products of this gene in-frame into the NdeI and BamH1 sites of pET19b vector for expressing in Escherichia coli. All mutant constructs were generated using the QuikChangeTM mutagenesis kit (Stratagene, La Jolla, CA) A kinase-inactive form of SRPK1 (kdSRPK1) was generated by replacing Lys at position 109 with Met and was previously described (Yeakley et al., 1999). A kinase-inactive form of Clk/Sty (kdClk/Sty) was constructed by replacing Lys at position 190 with Met.

The plasmids for wild-type and mutant forms of His-tagged ASF/SF2 were transformed into the BL21(RIL) E. coli strain, and the cells were then grown at 37 °C in LB broth supplemented with 100 μg/ml ampicillin. Protein expression was induced with 0.1 mM isopropyl 1-thio--D-galactopyranoside at room temperature for 5 h. Cells were then pelleted and lysed by French Press using 10 ml of lysis buffer (0.1 M MOPS, 10 mM Tris-HCl, pH 8.0, 0.3 M NaCl, 10% glycerol, 1 mM phenylmethylsulfonyl fluoride). The insoluble fraction was collected by centrifugation at 14,000 rpm for 15 min, washed twice with lysis buffer containing 2 M urea, and then resuspended in denaturing buffer (lysis buffer containing 8 M urea) for 30 min at room temperature. The soluble fraction, collected by centrifugation at 14,000 rpm for

15 min, was applied to a 1.5-ml Ni^{2+}-Sepharose column and washed with denaturing buffer containing 20 mM imidazole. The protein was re-folded by passing decreasing concentrations of urea through the column (8, 6, 4, 2, 1, and 0 M urea). The re-folded protein was eluted with 40 ml of elution buffer (0.1 M MOPS, 10 mM Tris-HCl, 0.3 M NaCl, and 10% glycerol, pH 3.0).

Clk/Sty was expressed from a pRSETA plasmid construct in E. coli BL21-DE3 pLysS and induced with 0.8 mM isopropyl 1-thio--D-galactopyranoside for 5 h at room temperature. Cells were lysed by French Press in 50 mM NaH_2PO_4 (pH 7.8), 500 mM NaCl, 10 mM Imidazole, and 1 mM phenylmethylsulfonyl fluoride. The soluble fraction was loaded onto a Ni2+-Sepharose column, washed thoroughly with the same buffer containing 40 mM imidazole, and eluted with 300 mM imidazole. The eluted protein was dialyzed against 50 mM NaH_2PO_4 (pH 7.8), 10 mM NaCl, 1 mM EDTA, and 1 mM dithiothreitol, concentrated to 1 ml with Amicon 30-kDa MWCO spin columns, loaded onto a 2-ml Q-column by fast protein liquid chromatography (Amersham Biosciences) in the same buffer, and eluted within a shallow NaCl gradient. A single peak was collected, dialyzed against 50 mM MOPS (pH 7.6), 500 mM NaCl, 20% glycerol, 1 mM EDTA, and 1 mM dithiothreitol, and stored at -80 °C.

SRPK1 was expressed from a pRSETa plasmid construct transformed into E. coli. BL21(DE3) cells. Cells were cultured in 2 liters of LB (100μg/ml Ampicillin) , grown to an $O.D._{600}$ of 0.5 and induced with 0.4 mM IPTG for 6 hours at RT. Cell pellets were lysed by sonication in 20 mM MES pH 6.5, 50 mM NaCl, 20% glycerol, and 1 mM PMSF. The soluble fraction was loaded onto a Q-sepharose column equilibrated with lysis buffer and washed with 150 mL of lysis buffer. The flow

through of the sample was combined with the wash and the NaCl concentration was increased to 500 mM. Imidazole was added to a final concentration of 5 mM and the solution was loaded onto a Ni-NTA column washed with 20 mM MES pH 6.5, 500 mM NaCl, 20% glycerol, and 5 mM imidazol followed by another wash with 40 mM imidazole. The protein was eluted with 30 ml of buffer containing 250 mM imidazole. The elution was dialysed 1000 fold in 20 mM MES pH 6.5, 500 mM NaCl, 5% glycerol, and 1 mM DTT. The protein was concentrated with an Amicon-50 centrifugation concentrator to ~ 5 mg/ml. Aliquots were flash frozen in liquid nitrogen, and stored at -80 °C.

2. Phosphorylation Reactions

The phosphorylation of ASF/SF2 by SRPK1 and Clk/Sty was carried out in the presence of 50 mM MOPS (pH 7.0), 10 mM free Mg^{2+}, 5 mg/ml bovine serum albumin, and [^{32}P]ATP (600-1000 cpm $pmol^{-1}$) at 23 °C unless otherwise stated. Reactions were initiated with the addition of [^{32}P]ATP (250 μM) in a total reaction volume of 20 μl and then were quenched with 10 μl of SDS-PAGE loading buffer. A portion of each quenched reaction (20 μl) was loaded onto a 10% SDS-PAGE gel. Dried gels were then exposed with Kodak imaging film (Biomax MR), and protein bands corresponding to phosphorylated ASF/SF2 were excised and counted on the ^{32}P channel in liquid scintillant. Control experiments, specific activity determination, and time-dependent product concentrations were determined as previously described (Aubol et al., 2003).

3. Data Analysis

Progress curve data for ASF/SF2 phosphorylation were plotted as a ratio of incorporated phosphate and the total substrate concentration as a function of time and were fit to either a single- or double-exponential function unless otherwise stated. In the latter case, the amplitude of the first phase (1) represents the fraction of sites phosphorylated in the enzyme-substrate complex. The fraction of bound substrate was then calculated from the ratio of 1 and the total amplitude (tot) (Fraction bound = 1/tot). The dissociation constant for the enzyme-substrate complex (K_d) was determined by plotting the fraction bound as a function of $[E]_o$ and fitting the curve to

Equation 1:

$$BF = \frac{K_d + [S]_o + [E]_o - \sqrt{(K_d + [S]_o + [E]_o)^2 - 4[S]_o[E]_o}}{2[S]_o} \qquad (1)$$

where BF is the fraction bound, and $[S]_o$ and $[E]_o$ are the total concentrations of ASF/SF2 and SRPK1. Experiments were typically performed using fixed $[S]_o$ and varying $[E]_o$.

The text of Chapter III is a reprint of the material as it appears in *The Journal of Biological Chemistry*, 2005, 280(50), 41761-8, Velazquez-Dones, A., Hagopian, J.C., Ma, C.T., Zhong, X.Y., Zhou, H., Ghosh, G., Fu, X.D., Adams, J.A. The dissertation author was a primary researcher and author of this publication. Additional text of Chapter III is a reprint of the material as it appears in *Molecular Biology of the Cell*, 2006, 17(2), 876-85, Ding, J.H., Zhong, X.Y., Hagopian, J.C., Cruz, M.M., Ghosh, G., Feramisco, J., Adams, J.A., Fu, X.D. The dissertation author was a collaborative researcher and co-author of this publication.

Chapter IV

Adaptable Molecular Interactions Guide

Phosphorylation of the SR Protein ASF/SF2 by SRPK1

A. Abstract

The SR (arginine-serine rich) protein ASF/SF2 (also called human alternative splicing factor), an essential splicing factor, contains two functional modules consisting of tandem RNA recognition motifs (RRMs; RRM1–RRM2) and a C-terminal arginine-serine repeat region (RS domain, a domain rich in arginine-serine repeats). The SR-specific protein kinase (SRPK) 1 phosphorylates the RS domain at multiple serines using a directional (C-terminal-to-N-terminal) and processive mechanism—a process that directs the SR protein to the nucleus and influences protein–protein interactions associated with splicing function. To investigate how SRPK1 accomplishes this feat, the enzyme–substrate complex was analyzed using single-turnover and multi-turnover kinetic methods. Deletion studies revealed that while recognition of the RS domain by a docking groove on SRPK1 is sufficient to initiate the processive mechanism, continued processive phosphorylation in the presence of building repulsive charge relies on the fine-tuning of contacts with the RRM1–RRM2 module. These data indicate that SRPK1 uses stable, yet highly flexible protein–protein interactions to facilitate both early and late phases of the processive phosphorylation of SR proteins.

B. Introduction

The splicing of precursor mRNA (pre-mRNA) is essential for proteome diversity and many cellular regulatory processes, but is also associated with numerous diseases when mistakes are propagated into themature spliced mRNA (Faustino and Cooper, 2003; Hagiwara, 2005; Karni et al., 2007; Venables, 2006). Splicing occurs in

a macromolecular complex known as the spliceosome, a dynamic assembly of five small nuclear ribonucleoproteins and many protein cofactors (Graveley, 2000). An important family of splicing cofactors are the SR proteins (splicing factors containing arginine-serine repeats), so named because they contain a C-terminal domain composed largely of arginine-serine dipeptide repeats (RS domain, a domain rich in arginine-serine repeats). In addition to these repetitive sequences, SR proteins contain one or two N-terminal RNA recognition motifs (RRMs) that are essential for recognition of exonic enhancer sequences in pre-mRNA (Blencowe, 2000; Liu et al., 2000; Zhu et al., 2001). The SR proteins play roles in both constitutive and alternative splicing (Krainer et al., 1990; Krainer and Maniatis, 1985). While SR proteins are critical for the early stages of spliceosome assembly during the establishment of the proper 5′ and 3′ splice sites in the premRNA, (Kohtz et al., 1994; Wu and Maniatis, 1993) they are also thought to connect spliced mRNA to RNA export machinery and to modulate protein translation in the cytoplasm (Huang et al., 2004; Lai and Tarn, 2004; Sanford et al., 2004). SR proteins are now becoming recognized as potentially important targets for cancer therapy, as the prototypical SR protein ASF/SF2 (also called human alternative splicing factor) was recently identified as a protooncogene with the observation that it is overexpressed in many tumors and transforms immortalized rodent fibroblasts by altering the splicing pattern of critical tumor-suppressor and cell-cycle-regulatory genes (Karni et al., 2007).

Phosphorylation of the RS domains of SR proteins is important for the biological function of these splicing factors at several levels. The SR-specific protein kinase (SRPK) 1 phosphorylates multiple sites in the RS domain of the SR protein

ASF/SF2, a modification that promotes binding to an import receptor (transportin-SR) and delivers ASF/SF2 to the nucleus (Duncan et al., 1998; Koizumi et al., 1999; Lai et al., 2001; Yun and Fu, 2000). SRPK1 and its homolog, SRPK2, are unique among the serine kinases in that they will not phosphorylate threonine and that their kinase cores are bisected by a large insert domain (approximately 250 aa) (Wang et al., 1998) While its function is not fully understood, the insert domain localizes the kinase to the cytoplasm, where it can modify and support regulated nuclear entry of SR proteins (Ding et al., 2006). Once in the nucleus, the phosphorylated RS domain of ASF/SF2 assists in the interaction of the SR proteins with U1-70K (a component of the U1 small nuclear ribonucleoprotein) and the U2AF heterodimer at the 5′ and 3′ splice sites, respectively (Kohtz et al., 1994; Wu and Maniatis, 1993). A second family of protein kinases typified by Clk/Sty further alters the phosphoryl content of ASF/SF2 and impacts spliceosomal function as both hypophosphorylation and hyperphosphorylation of ASF/SF2 by this kinase can inhibit in vitro splicing reactions (Prasad et al., 1999). While some SR proteins are exclusively localized to the nucleus, others such as ASF/SF2 and 9G8 are shuttling SR proteins, since they can move from the nucleus to the cytoplasm in a phosphorylation-dependent manner. It has been demonstrated that dephosphorylation of the shuttling SR proteins ASF/SF2 and 9G8 facilitates binding to the nuclear export protein TAP (Huang et al., 2004).

In previous studies, we showed that SRPK1 modifies the N-terminal portion of the RS domain (RS1) of ASF/SF2 using a processive mechanism in which the enzyme stays attached for about eight cycles of rapid serine phosphorylation before releasing the splicing factor (Aubol et al., 2003; Velazquez-Dones et al., 2005). SRPK1

performs this feat using an ordered mechanism in which the kinase initiates phosphorylation at the center of the RS domain near the RS1/RS2 boundary (Figure 4.1A) and attaches phosphates onto serines moving in a general C-terminal-to-N-terminal direction (Ma et al., 2008). We recently solved an X-ray structure for SRPK1 with a monophosphorylated form of ASF/SF2 lacking RRM1 and RS2 (Ngo et al., 2008). Although portions of the RS1 segment are not visible in this model, several important features that help define the enzyme–substrate interface are now apparent. First, the N-terminal portion of RS1 (N′-RS1) resides in a docking groove made up of a long electronegative channel in the large lobe of SRPK1 (Figure 4.1B). This interaction would place the C-terminal portion of RS1 in the active site for initial phosphorylation near the RS1/RS2 boundary. Second, although RRM1 is not present in the structure, RRM2 makes three well-defined interactions with SRPK1, including one contact with two residues from the glycine-rich loop and several additional contacts in helices αD and αF (Figure 4.1B). Third, an electropositive pocket is positioned to interact with a phosphoserine from the substrate. The presence of this phosphoserine supports the experimental finding that the kinase initiates phosphorylation near the C-terminus of RS126 and suggests that nearby phosphoserines in the RS domain may be stabilized by this electropositive pocket as the reaction progresses.

In cases where X-ray structures are now available, the addition of a single phosphate does not induce large changes in the conformation of the enzyme–substrate complex. For example, no significant changes in the kinase domain of protein kinase A or in its bound substrate are observed upon phosphorylation of a single serine in the

active site (Madhusudan et al., 1994). Such observations raise the question of how protein kinases might accommodate a sequential phosphorylation reaction where the substrate must ‘slide’ through the active site. Glycogen synthase kinase-3 (GSK3) catalyzes polyphosphorylation of its protein substrates using an electropositive pocket that recognizes P+4 phosphoserines and imposes a Cterminal-to-N-terminal phosphorylation direction (Fiol et al., 1990). Although the X-ray structure of the SRPK1-ASF/SF2 complex reveals potentially important contacts for the initiation of phosphorylation near the RS1/RS2 border, how sequential phosphorylation events are facilitated in the RS1 segment of the RS domain while the substrate remains bound is not known. In this present study, we address the role of three critical groups of contacts made between the enzyme and the substrate that could be important for controlling reaction dynamics. We found that SRPK1 uses its electronegative docking groove to grip the N-terminal end of RS1, thereby initiating processive and directional phosphorylation that begins near the RS1/RS2 border. Contacts made between the kinase and the RRMs are not essential for initial recognition and early stages of the processive reaction, but instead play a vital role, in conjunction with the electropositive pocket, in facilitating the rate and processive modification of later serines in the reaction. Overall, the data indicate that SRPK1 uses multiple choreographed contacts to provide both flexibility and stability for the RS domain as it traverses the active site.

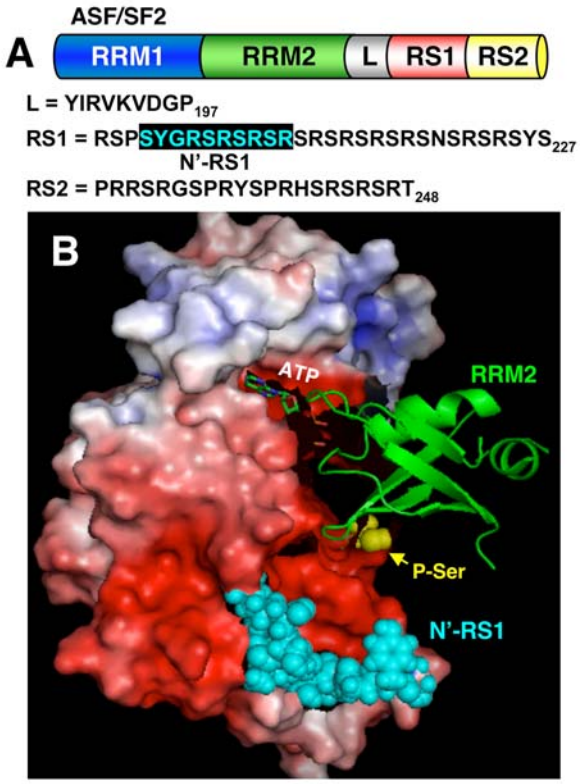

Figure 4.1 Structural features of the SRPK1:ASF/SF2 complex. (A) ASF/SF2 domain organization and C-terminal sequences. The RS domain is composed of RS1 and RS2 segments where the former is phosphorylated by SRPK1. L is a linker segment separating the RS domain from the canonical RRM. (B) X-ray structure of SRPK1 in complex with a truncated form of ASF/SF2 bound. SRPK1 lacking the insert domain is shown with an electrostatic surface where red represents negative charge and blue represents positive charge. The truncated ASF/SF2 lacks RRM1 and residues 221-248. A portion of RS1 (N'-RS1) is visible in the binary complex whereas the preceding sequence (PRSP) and residues 211-219 are disordered. The linker segment is the final β strand of RRM2. A dipeptide containing a phosphoserine that interacts with the P+2 pocket in SRPK1 comes form one of the serines in the C-terminal portion of RS1.

C. Results

1. RS domain is Sufficient for High-Affinity Binding of ASF/SF2

To define core structural elements involved in high-affinity ASF/SF2 binding, we made a series of N-terminal deletions in the substrate (Figure 4.2A). These deletion constructs were made with a common C-terminal His tag. To measure binding affinities of these constructs, we used a competition assay in which the phosphorylation rate of a fixed amount of ASF/SF2-His (50 nM) is monitored as a function of varying concentrations of a competing substrate. Since the assay is performed under low phosphorylation levels (<10%), the inhibitory parameters of the competitor substrate (K_I) reflect the binding affinity of its unphosphorylated form. The inhibition of ASF/SF2-His phosphorylation is shown in Figure 4.2B as a function of increasing competitors ASF (ΔRRM1)-His and ASF(ΔRRM12)-His. The time dependent phosphorylation of ASF/SF2-His is presented as relative velocity plotted against the total competitor concentration. The apparent K_I values are then converted to true K_I values using Eq. (1) and the K_m for the fixed substrate. The K_I for ASF/SF2-His was measured using a fixed amount of ASF (ΔRRM1)-His and varying amounts of wild-type protein (K_I=90 nM). In general, removal of the RRMs, including the linker segment between RRM2 and RS1, did not reduce binding affinity by more than two fold (legend to Figure 4.2B).

To ensure that removal of the RRMs does not impact binding mode, we performed steady-state kinetic analyses using varying amounts of ASF/SF2-His and varying fixed amounts of an RRM-deleted substrate. In double-reciprocal plots, we showed that ASF(RS12)-His, the most dramatic deletion, functioned as a competitive

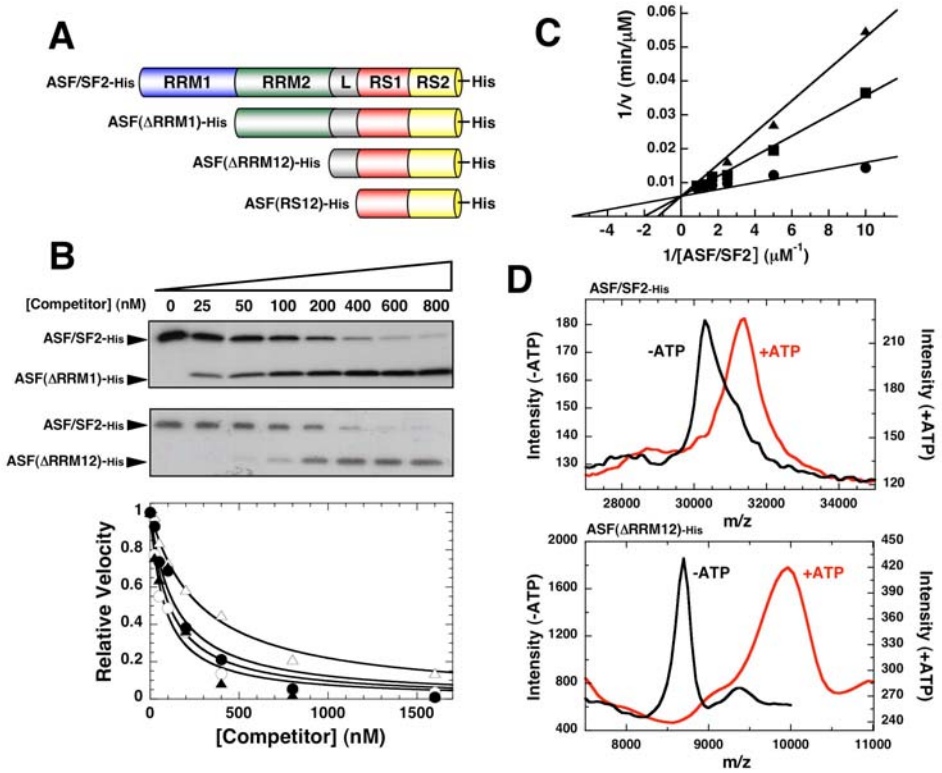

Figure 4.2 Effects of N-terminal deletions on the binding of ASF/SF2. (A) Deletion Mutants. All deletion constructs contain a C-terminal His_6 tag. (B) Competition assay. Phosphorylation of ASF/SF2-His (50 nM) is monitored as a function of varying concentrations of competitor substrates (0-1600 nM) using 100 μM ^{32}P-ATP. ASF(ΔRRM1)-His is the fixed substrate when the competitor is ASF/SF2-His. Relative velocities are plotted against total ASF/SF2-His (●), ASF(ΔRRM1)-His (○), ASF(ΔRRM12)-His (▲), and ASF(RS12)-His (△) concentrations and fitted to equation (1) to obtain true K_I values of 93 ± 14, 54 ± 5, 70 ± 15, and 190 ± 13 nM, respectively. (C) Double reciprocal plot of initial velocity versus varying ASF/SF2-His concentration using 0 nM (●), 100 nM (■) and 200 nM (▲) ASF(ΔRRM12)-His, respectively. (D) MALDI-TOF spectra of ASF/SF2-His and ASF(ΔRRM12)-His with SRPK1 in the absence and presence of 100 μM ATP. The increase in mass is consistent with the phosphorylation of about 14 sites for ASF/SF2-His and ASF(ΔRRM12)-His.

inhibitor of ASF/SF2-His phosphorylation (Figure 4.2C), suggesting that the wild type and RRM-deleted substrate bind in a similar manner. To demonstrate that domain removal did not impact RS domain positioning in the active site, the phosphoryl contents of the substrates were measured using matrix-assisted laser desorption ionization time-of-flight (MALDI-TOF) analyses. As shown in Figure 4.2D, removal of both RRMs did not impair phosphorylation compared to wild type (14 sites). MALDI-TOF spectra of all N-terminal deletion constructs are shown in Figure 4.3. Finally, to control for any potential effects of the affinity label, we studied the binding of N-terminally tagged forms of ASF(ΔRRM1), ASF(ΔRRM12), and wild-type substrate and found that they display K_I values similar to those of the C-terminally tagged substrates (data not shown). Overall, the combined data indicate that the RS domain is sufficient for high-affinity binding to SRPK1.

2. RS Domain can Initiate, but not Sustain, Processive Phosphorylation

The above deletion analyses indicate that the RRMs may not participate in the phosphorylation mechanism. To determine whether the RRMs could modulate SR protein phosphorylation, we performed kinetic analyses of several mutants lacking eitherRRM1 [ASF(ΔRRM1)], RRM2 [ASF(ΔRRM2)], or both RRMs [ASF(ΔRRM12)]. In single-turnover experiments, SRPK1 rapidly attaches about 12 phosphates onto ASF/SF2 (4 min^{-1}) and then adds two phosphates in a much slower phase (0.13 min^{-1}) (Figure 4.4A). Removal of either RRM1 or both RRMs lowers the amplitude and increases the rate of this initial phase. In comparison, removal of RRM2 does not affect the amplitude but does increase the rate constant for the initial phase.

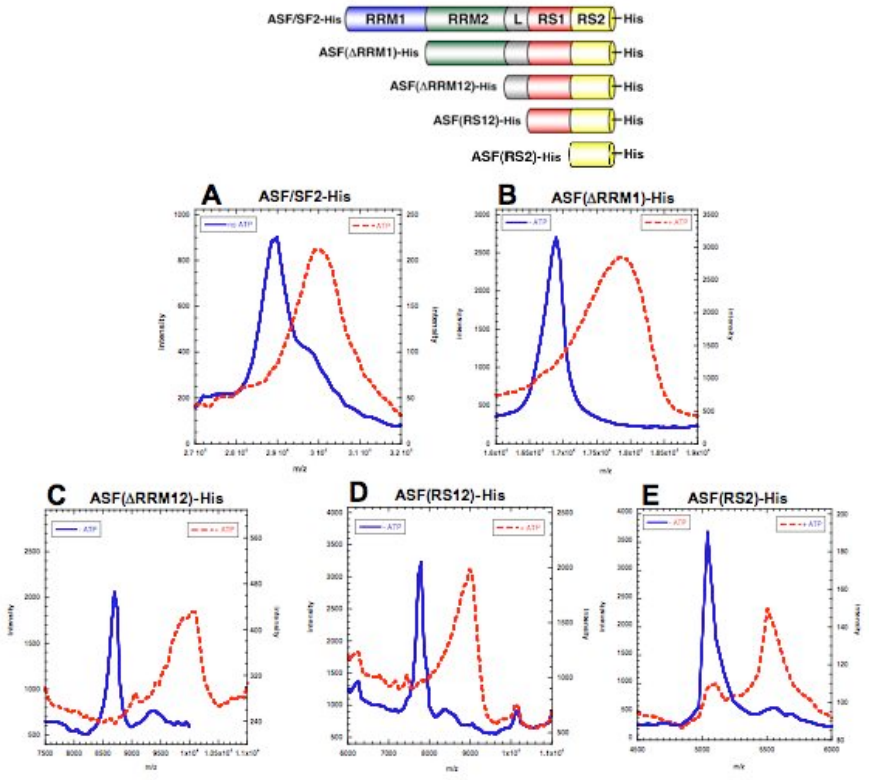

Figure 4.3 Effects of N-terminal deletions on ASF/SF2 phosphorylation endpoints by SRPK1. (A) The full length ASF/SF2 construct had a mass shift from 28,900 to 30,000 Da., consistent with ~14 phosphorylation sites. (B) The ASF(ΔRRM1) construct had a mass shift from 16,890 to 18,000 Da., consistent with ~14 phosphorylation sites. (C) The ASF(ΔRRM12) construct had a mass shift from 8,744 to 9,900 Da., consistent with ~15 phosphorylation sites. (D) The ASF(RS12) construct had a mass shift from 7,780 to 9,000 Da., consistent with ~15 phosphorylation sites. (E) The ASF(RS2) construct had a mass shift from 5,190 to 5,600 Da., consistent with ~5 phosphorylation sites.

Taken together, the kinetic data indicate that the RRMs are not necessary for efficient phosphorylation of the RS domain.

To determine whether the RRMs influence processivity, we performed start–trap experiments (Figure 4.4B). In this assay, SRPK1 (1 μM) is pre-equilibrated with substrate (250 nM) prior to the addition of [^{32}P]ATP (100 μM) in the absence and in the presence of excess kinase-inactive SRPK1 (kdSRPK1), which contains a single Lys-to-Met substitution in the ATP binding site (Velazquez-Dones et al., 2005). If phospho-intermediates are released from the active site, as expected in a non-processive (i.e., distributive) reaction, kdSRPK1 will bind them and inhibit reaction progress. Thus, the number of serines modified prior to reaction inhibition reflects the extent of processive phosphorylation. For ASF/SF2, ASF(ΔRRM1), ASF(ΔRRM2), and ASF(ΔRRM12), SRPK1 attaches about eight, six, seven, and three phosphates, respectively, prior to dissociation and reaction inhibition by kdSRPK1 (Figure 4.4B–F). To ensure that kdSRPK1 can trap free phospho-intermediates, a trap–start control experiment, in which kdSRPK1 is added prior to the addition of [^{32}P]ATP, is employed. Since kdSRPK1 substantially inhibits the initial reaction velocity in these experiments, the inability to trap early phospho-intermediates in start–trap experiments is not due to poor binding of the trapping agent. The low linear rates in the trap–start experiments reflect a small level of substrate not trapped by kdSRPK1 and is used as background in fitting the amplitude of the start–trap experiments. Overall, the data imply that the RRMs, while not necessary for binding and initial processivity, are important for maintaining processive phosphorylation of ASF/SF2 in the later phase of the reaction (i.e., after the first three serines).

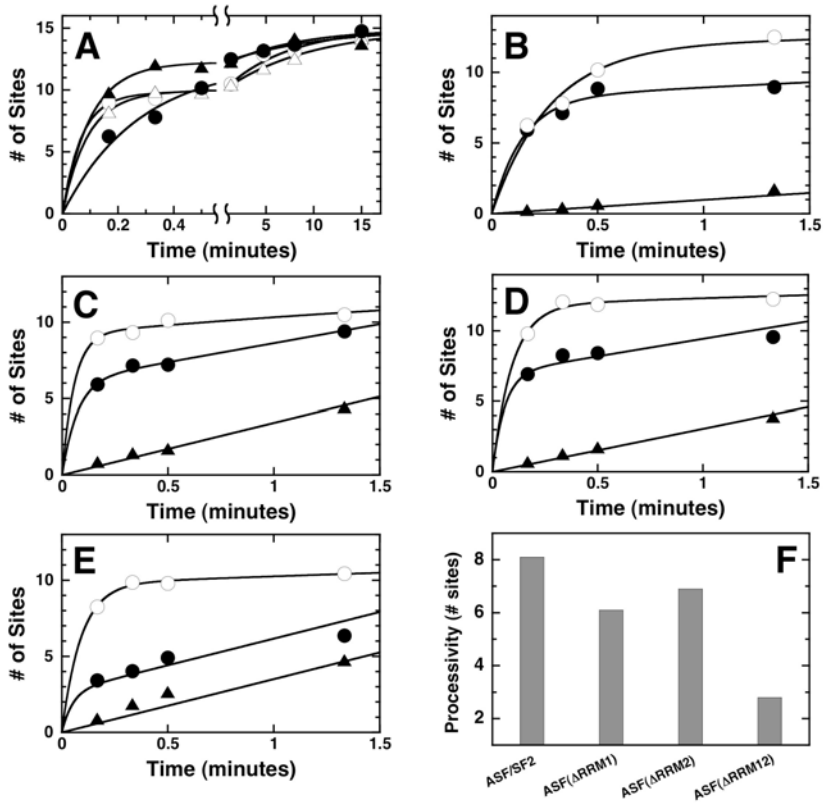

Figure 4.4 Kinetic investigation of ASF/SF2 lacking one or both RRMs. (A) Single turnover progress curves. SRPK1 (1 μM) is incubated with 250 nM of ASF/SF2 (●), ASF(ΔRRM1) (○), ASF(ΔRRM2) (▲) and ASF(ΔRRM12) (△) and the reaction is initiated with the addition of 100 μM ^{32}P-ATP. The data are fit to a double exponential equation with rate constants of 3.7 and 0.13 min^{-1} and amplitudes of 12 and 2 phosphates for ASF/SF2, rate constants of >10 and 0.11 min^{-1} and amplitudes of 10 and 4 phosphates for ASF(ΔRRM1), rate constants of >10 and 0.15 min^{-1} and amplitudes of 12 and 2 phosphates for ASF(ΔRRM2), and rate constants of >10 and 0.12 min^{-1} and amplitudes of 10 and 4 phosphates for ASF(ΔRRM12). (B-E) Start-trap experiments. SRPK1 (1 μM) is pre-equilibrated with 250 nM of ASF/SF2 (B), ASF(ΔRRM1) (C), ASF(ΔRRM2) (D), and ASF(ΔRRM12) (E) and then allowed to react with 100 μM ^{32}P-ATP in the absence (○) and presence (start-trap) (●) of 30 μM kdSRPK1 added at the time of reaction start. In control experiments (trap-start), kdSRPK1 is added prior to reaction start (▲). Start-trap data are fit to single exponentials followed by linear functions. Amplitudes are lowered from 12 to 8.1 sites for ASF/SF2, from 10 to 6.1 sites for ASF(ΔRRM1), from 12 to 6.9 sites for ASF(ΔRRM2) and from 9.7 to 2.8 sites for ASF(ΔRRM12) in the absence and presence of kdSRPK1. Trap-start experiments are fit to linear functions with slopes of 1, 1.6, 3.0 and 3.5 sites/min for ASF/SF2, ASF(ΔRRM1), ASF(ΔRRM2) and ASF(ΔRRM12), respectively. (F) Effects of deletion on processivity. Amplitudes (# sites) in start-trap experiments in (B-E) are plotted in the bar graph.

3. High-Affinity ASF/SF2 Binding is Resistant to RS Domain Charge Alterations

Since the RS domain is sufficient for high-affinity binding of unphosphorylated ASF/SF2 (Figure 4.2), we next addressed which regions in the domain constitute this binding. We made charge-to-Ala substitutions in seven individual blocks encompassing the entire RS domain and linker segment of ASF/SF2 (Figure 4.5A). Based on MALDI-TOF analyses, the mutant proteins were substrates for SRPK1, with Blocks 1 through 4 and Blocks 2/3 and 3/4 being phosphorylated to a similar level as ASF/SF2 (~14 sites) (Figure 4.6). Block 1/2 was phosphorylated at a lower extent (8 sites), suggesting that large removal of positive charge in RS1 has some impact on phosphoryl content (Figure 4.6). Blocks 1 through 4 bind with high affinity to SRPK1 in competition assays, suggesting that ASF/SF2 can tolerate five to six consecutive charge replacements anywhere in the RS domain without impacting binding affinity (Figure 4.5B). However, larger charge mutations had a significant impact on binding mode. Unlike the smaller block mutants, the larger block mutations were not capable of completely inhibiting this reaction (Figure 4.5C). For example, although Blocks 1/2, 2/3, and 3/4 initially lowered the phosphorylation rate of ASF(ΔRRM1) in a concentration-dependent manner similar to other mutants, 76%, 57%, and 20% of the activity remained at high competitor concentrations, respectively. These results are consistent with partial competitive inhibition29 and suggest that SRPK1 can bind well to the larger block mutants and still support the phosphorylation of ASF(ΔRRM1), the control substrate. This mode of inhibition is

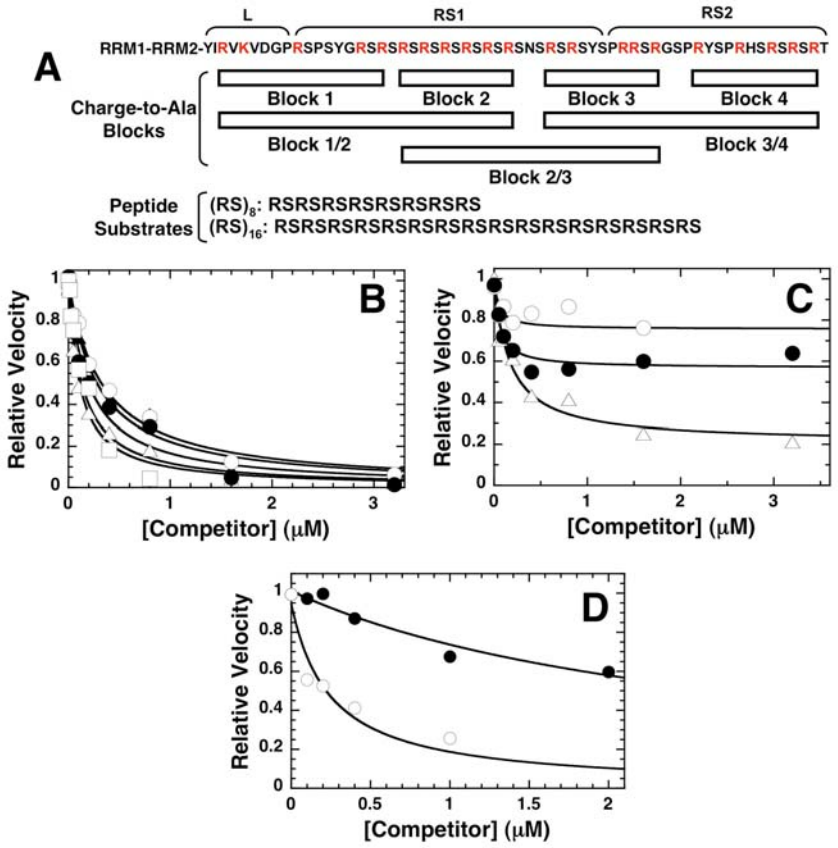

Figure 4.5 Effects of RS domain charge on ASF/SF2 binding. (A) Mutant and peptide substrates. Charge-to-Ala block mutations are made in the RS domain of ASF/SF2. Peptide substrates contain 8 and 16 Arg-Ser repeats. (B) Relative velocities for the phosphorylation of ASF(ΔRRM1) (50 nM) are plotted as a function of varying wt-ASF/SF2 (□), Block1 (●), Block 2 (○), Block 3 (▲), Block 4 (△) and fit to equation (1) to obtain K_I values of 90 ± 11, 130 ± 20, 220 ± 20, 190 ± 20, and 73 ± 10, respectively. (C) Relative initial velocities for the phosphorylation of ASF(ΔRRM1) (50 nM) are plotted as a function of varying Block 1/2 (○), Block 2/3 (●), and Block 3/4 (△) and fit to equation (2) to obtain K_I values of 40 ± 30, 45 ± 30, and 120 ± 30 nM, respectively, and αK_I values of 60 ± 40, 100 ± 40, and 800 ± 360, respectively. (D) Relative velocities for the phosphorylation of ASF/SF2 (50 nM) are plotted as a function of varying $(RS)_8$ (●) and $(RS)_{16}$ (○) and fit to equation (1) to obtain K_I values of 1.8 ± 0.22 and 0.16 ± 0.041 μM.

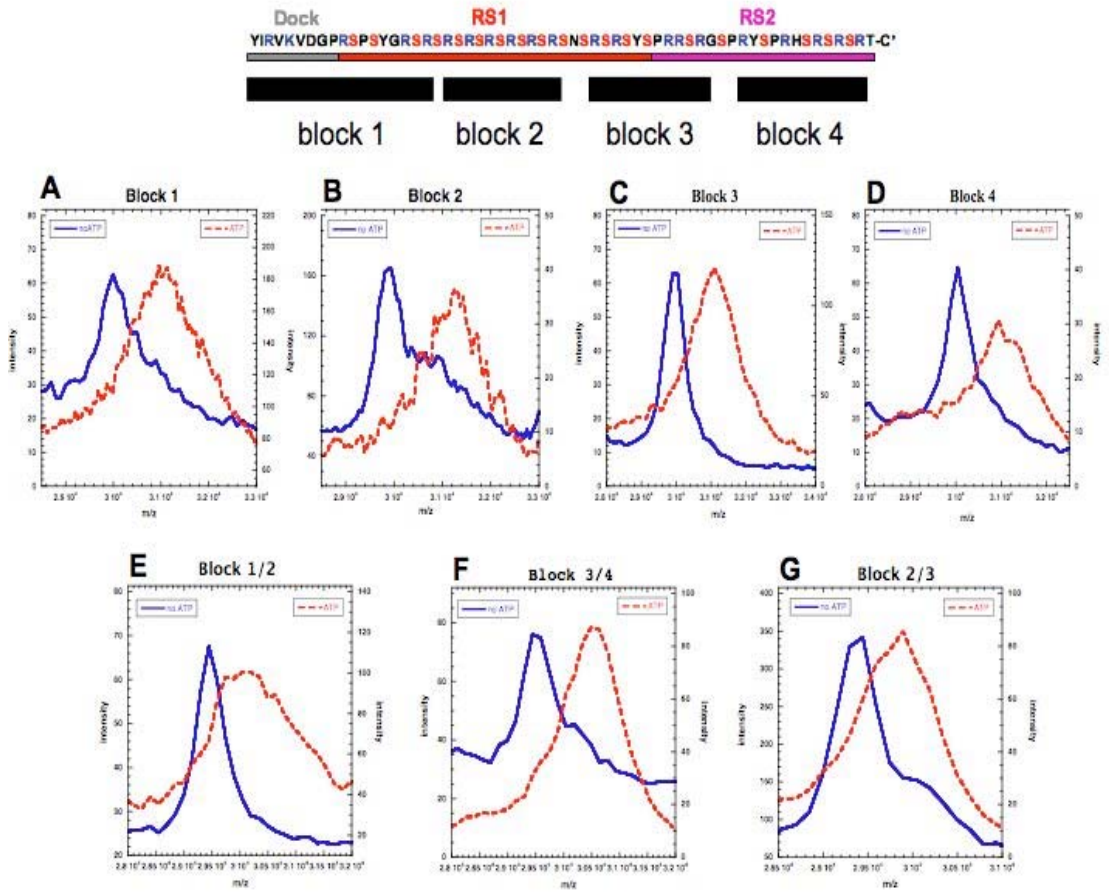

Figure 4.6 Effects of RS domain charge on ASF/SF2 phosphorylation endpoints by SRPK1. (A) The Block 1 construct had a mass shift from 30,100 to 31,300 Da., consistent with ~15 phosphorylation sites. (B) The Block 2 construct had a mass shift from 30,000 to 31,200 Da., consistent with ~15 phosphorylation sites. (C) The Block 3 construct had a mass shift from 30,000 to 31,200 Da., consistent with ~15 phosphorylation sites. (D) The Block 4 construct had a mass shift from 30,160 to 31,300 Da., consistent with ~15 phosphorylation sites. (E) The Block 1/2 construct had a mass shift from 29,457 to 30,100 Da., consistent with ~8 phosphorylation sites. (F) The Block 3/4 construct had a mass shift from 29,600 to 30,600 Da., consistent with ~13 phosphorylation sites. (G) The Block 2/3 construct had a mass shift from 29,300 to 30,000 Da., consistent with ~9 phosphorylation sites.

shown in Scheme 1:

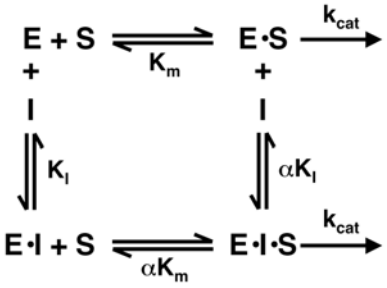

where S is ASF(ΔRRM1) and I is one of the large block mutants. The data are fitted to Eq. (2) for partial competitive inhibition to obtain K_I and αK_I values of 40 and 60 nM for Block 1/2, 45 and 100 nM for Block 2/3, and 120 and 800 nM for Block 3/4, respectively. Overall, the results indicate that the block mutants, although lacking many positively charged residues (5–11 Arg/Lys), can still bind with high affinity to SRPK1, as evident in low K_I values.

Since the RS domain can accommodate numerous charge changes with minimal impact on affinity, we investigated the phosphorylation of simple Arg-Ser peptides [$(RS)_8$ and $(RS)_{16}$] to determine a minimum number of arginines necessary for high-affinity binding. In competition studies, we found that while (RS)8 binds with greatly reduced affinity (K_I = 1.6 μM), $(RS)_{16}$ binds with a K_I close to that for ASF/SF2 (Figure 4.5D). For $(RS)_{16}$, the ability to lower the velocity of ASF(ΔRRM1) phosphorylation to near zero indicates that this peptide does not use a partial competitive mechanism (Figure 4.5D). In contrast, we found no plateau with $(RS)_8$ in the velocity-versus competitor plot up to 4 μM, with no evidence for partial competitive inhibition. The data indicate that while SRPK1 can recognize an Arg-Ser

stretch of eight repeats, high-affinity binding requires more positively charged residues. Overall, the combined data indicate that while the RS domain is sufficient for high-affinity binding, regions outside this domain are likely to contribute to binding when charge in the RS domain is removed.

4. Redundant Binding Determinants Revealed Through C-terminal Deletions

Although the N-terminal deletions suggest that the RS domain is the principal component for high affinity binding of ASF/SF2 (Figure 4.2), its affinity is highly resilient to large charge changes (Figure 4.5). To investigate whether regions in the RRMs also contribute to binding (therefore explaining this resiliency), we studied RS domain mutants (Figure 4.8A). If the RS domain contains all necessary residues for initial ASF/SF2 binding, then ASF(ΔRS) should bind very poorly, if at all. Interestingly, we found that ASF(ΔRS2) and ASF(ΔRS) bind with K_I values that are only two fold higher than that for wild-type ASF/SF2 (Figure 4.8B). Unlike the large charge block mutants, these deletions lower the velocity to near zero. Although ASF(ΔRS) is not a substrate for SRPK1 as expected, ASF(ΔRS2) is phosphorylated at 12 sites based on MALDI-TOF analyses (Figure 4.9). Since the RRM1–RRM2 module is not necessary for binding, we investigated the binding mode of ASF(ΔRS). In steady-state kinetic analyses, ASF(ΔRS) behaves as a competitive inhibitor against wild-type ASF/SF2 (Figure 4.8C), suggesting that the two molecules occupy common binding sites on SRPK1. These findings indicate that the RRM1–RRM2 domain pair in wild-type ASF/SF2 is bound to SRPK1 and that ASF(ΔRS) can compete for regions in the enzyme that bind these domains, indirectly displacing the RS domain. Finally,

although ASF(ΔRS2) is phosphorylated to a slightly lower extent than wild-type ASF/SF2, SRPK1 processively phosphorylates about eight serines, in line with the wild-type substrate (Figure 4.8C). These findings suggest that while the RS domain is sufficient for high-affinity interactions, other surfaces on SRPK1 have the capacity to bind the RRMs to compensate for partial loss of high-affinity binding mediated by the RS domain.

Since a construct lacking the RS domain, ASF(ΔRS), could readily inhibit ASF/SF2 phosphorylation, we next investigated whether the individual RRMs are capable of binding to SRPK1. We designed two deletion constructs that express only RRM1 [ASF(RRM1)] or RRM2 with the linker segment [ASF(RRM2)] (Figure 4.8A) and measured their abilities to inhibit ASF/SF2 phosphorylation in the competition assay. Unlike the high-affinity RRM1–RRM2 construct, ASF(RRM1) and ASF(RRM2) bind poorly to SRPK1, displaying elevated K_I values of 1.6 and 6.3 μM—values that are between 18-fold and 73-fold higher than that for the full-length substrate. These data indicate that the high affinity of the RRM1–RRM2 construct relies not on the presence of one RRM but on the presence of both RRMs. To investigate whether RRM1 could interact directly with SRPK1 or simply stabilize the conformation of RRM2 and its interactions with the enzyme, we made four alanine substitutions in RRM2 (W134, Q135, E184, and R154) that constitute the SRPK1–

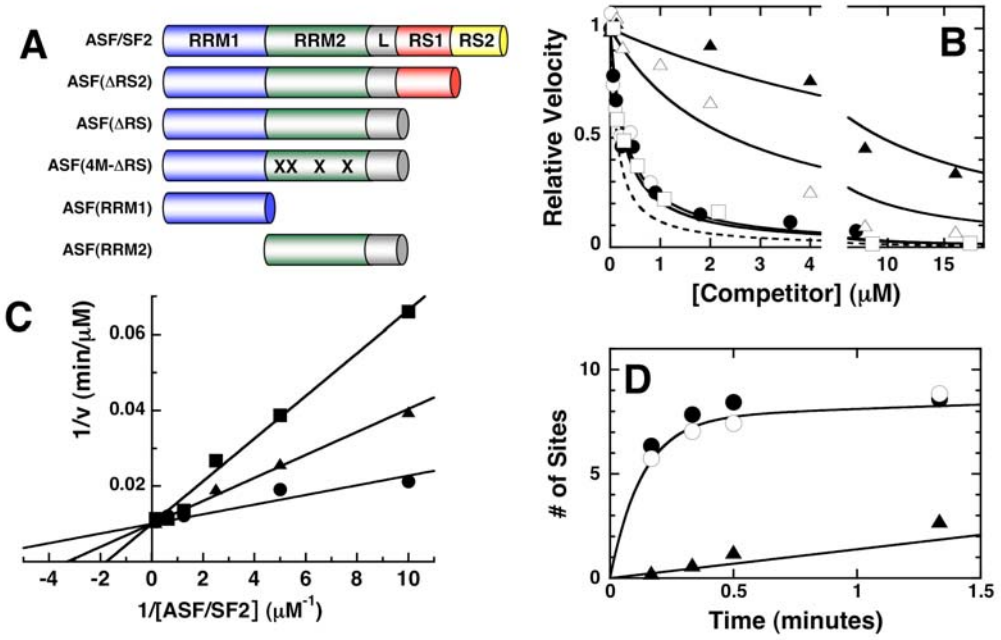

Figure 4.7 C-terminal deletion analyses of ASF/SF2. (A) Deletion constructs. (B) Competition assay. Phosphorylation of ASF/SF2 (50 nM) is monitored as a function of varying concentrations of competitor substrates (0-16 μM) using 100 μM ^{32}P-ATP. Relative initial velocities are plotted against total ASF(ΔRS2) (○), ASF(ΔRS) (●), ASF(4M-ΔRS) (□), ASF(RRM1) (△), and ASF(RRM2) (▲) and fit to true K_I values of 170 ± 60, 180 ± 20, 200 ± 30, 1600 ± 400 and 6300 ± 1900 nM, respectively. The dotted line shows relative initial velocities for ASF/SF2 taken from Fig 4B. (C) Double reciprocal plot of initial velocity versus varying ASF/SF2 concentration using 0 nM (●), 400 nM (▲) and 800 nM (■) ASF(ΔRS), respectively. (D) Start-trap experiments. SRPK1 (1 μM) is pre-equilibrated with 250 nM of ASF(ΔRS2) and then allowed to react with 100 μM ^{32}P-ATP in the absence (○) and presence (start-trap) (●) of 30 μM kdSRPK1 added at the time of reaction start. In control experiments (trap-start), kdSRPK1 is prior to reaction start (▲) and fit to a linear function with a slope of 1.3 sites/min.

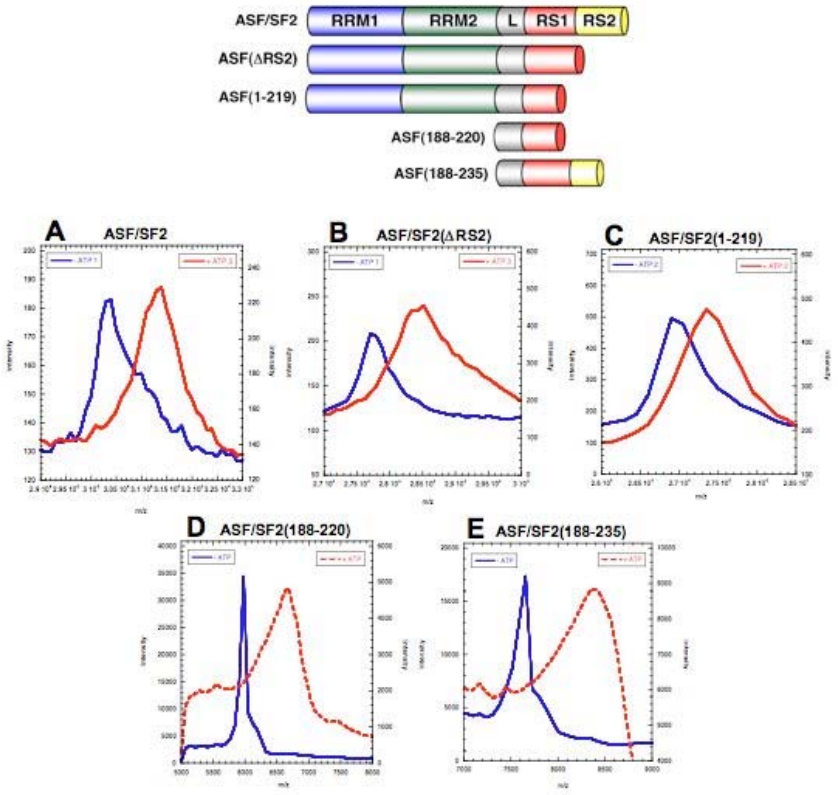

Figure 4.8 The effects of C-terminal and bilateral deletions on ASF/SF2 phosphorylation endpoints by SRPK1. All constructs have a N-terminal His tag: (A) The full length ASF/SF2 construct had a mass shift from 30,400 to 31,500 Da., consistent with ~14 phosphorylation sites. (B) The ASF(ΔRS2) construct had a mass shift from 27,800 to 28,700 Da., consistent with ~12 phosphorylation sites. (C) The ASF(1-219) construct had a mass shift from 26,900 to 27,600 Da., consistent with ~9 phosphorylation sites. (D) The ASF(188-220) construct had a mass shift from 5,980 to 6,690 Da., consistent with ~9 phosphorylation sites. (E) The ASF(188-235) construct had a mass shift from 7,640 to 8,500 Da., consistent with ~11 phosphorylation sites.

RRM2 interface based on the X-ray structure (Ngo et al., 2008). The high affinity of this mutant construct, ASF(4M-ΔRS), suggests that the contacts inRRM2are flexible and/or the RRM1 directly interfaces with SRPK1 (Figure 4.8B). Overall, the C-terminal deletion studies reveal that ASF/SF2 presents two separable modules (RRM1–RRM2 and the RS domain) that can independently bind SRPK1 with high affinity, yet the separate domains within the RRM1–RRM2 module can function cooperatively in enhancing substrate binding.

5. Docking Groove in SRPK1 Controls Initiation of Processive Phosphorylation

Since the RS domain confers high-affinity binding and commitment to about three processive phosphorylation steps (Figures 4.2 and 4.4), we wished to address whether specific charged residues in the docking groove that contact the RS1 portion serve to initiate the processive reaction. We made six charge-to-alanine mutations in the docking groove of SRPK1 (Figure 4.10A).While four of these residues directly interact with N′-RS1 (D564, E571, D548, and K615), two are nearby and are anticipated to interact with RS1 (E558 and E557). These mutations result in a modified kinase [SRPK1(6M)]with impaired catalytic power. In single-turnover kinetics, the initial fast-phase rate and amplitude for SRPK1(6M) are about fourfold (4 versus 1 min^{-1}) and twofold (12 versus 6 sites) lower than those for wild type (Figure 4.10B). Despite these kinetic changes, SRPK1(6M) incorporated the same amount of 32P in ASF/SF2 after 25min as wt-SRPK1 in single turnover progress curves (data not shown), suggesting that mutation does not impact phosphoryl content. In competition

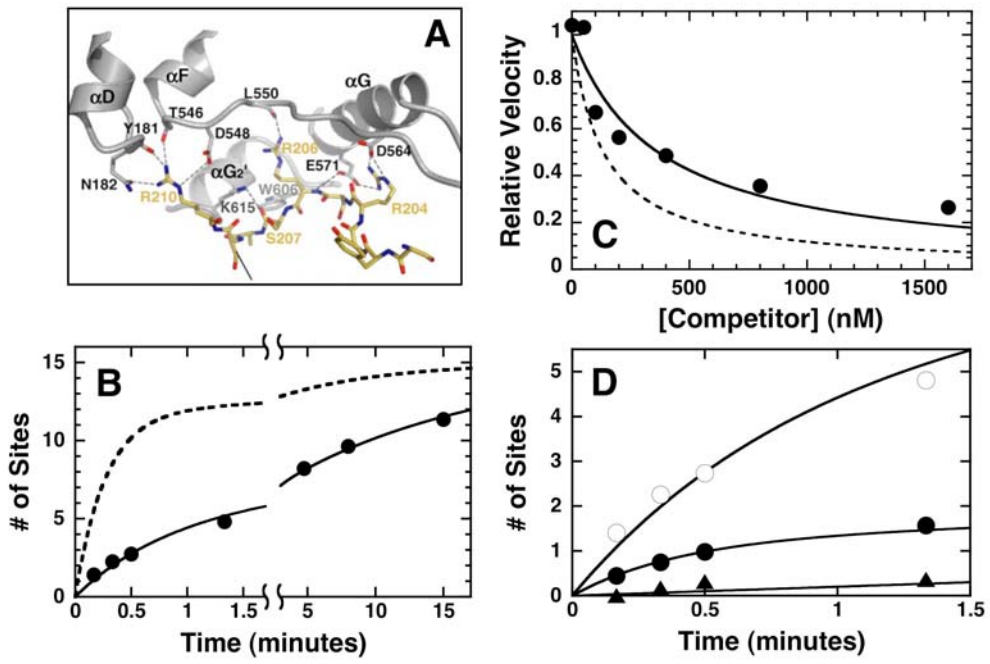

Figure 4.9 Effects of docking groove mutations on phosphorylation kinetics. (A) Docking groove in SRPK1. Residues from N'-RS1 are shown in gold. (B) Single turnover kinetics. SRPK1(6M) (3 mM) is preequilibrated with ASF/SF2 (250 nM) and then mixed with 100 mM 32P-ATP. The curve is fit to a double exponential function with rate constants and amplitudes of 1 min-1 and 5.5 sites and 0.07 min-1 and 9.5 sites. Kinetic data for wild-type SRPK1 are taken from Fig. 3A and are displyed as a dotted line. (C) Binding affinity. Competition experiments are performed using 50 nM ASF(ΔRRM2), varying amounts of ASF/SF2 and 15 nM SRPK1(6M). A true K_I of 240 ± 50 nM for ASF/SF2 to SRPK1(6M) is obtained using equation (1). The dotted line shows the inhibitor plot for wild-type SRPK1 and ASF/SF2 taken from Fig. 4B. (D) Start-Trap Experiment. SRPK1(6M) (3 mM) and ASF/SF2 (250 nM) are preequilibrated before 100 mM 32P-ATP is added in the absence (○) and presence (●) of 60 mM kdSRPK1 at the time of start. In the trap-start experiments, kdSRPK1 is added to the enzyme-substrate complex before addition of 32P-ATP. The amplitude is lowered from 5.6 sites in the absence to 1.2 sites in the presence of kdSRPK1. The slope of the trap-start experiment is 0.2 sites/min.

assays, we found that docking site mutation reduced binding affinity by only two fold (Figure 4.10C). To determine whether the docking groove affects the phosphorylation mechanism, start– trap experiments were performed. In these assays, we found that SRPK1(6M) phosphorylates ASF/SF2 using a strictly distributive mechanism (Figure 4.10D). The phosphorylation of only one site in the presence of kdSRPK1 relative to the trap–start control is likely the result of slow exchange in the unphosphorylated substrate relative to forward catalysis. However, after the first site is phosphorylated, the SR protein dissociates and is trapped by kdSRPK1. These findings suggest that the docking groove, while not important for overall phosphoryl content or binding affinity, plays a vital role in controlling the initiation of efficient processive phosphorylation.

D. Discussion

SRPK1 catalyzes a highly specialized multi-site phosphorylation reaction that is essential for the localization of SR proteins in the nucleus and subsequent splicing function.30 Prior studies indicate that the serine-specific protein kinase SRPK1 places these phosphates in the RS domain of ASF/SF2 using a regiospecific, directional, and processive mechanism (Aubol et al., 2003; Ma et al., 2008; Velazquez-Dones et al., 2005). Recent crystallographic data now illustrate that protein–protein interactions help SRPK1 to initiate this phosphorylation reaction near the RS1/RS2 boundary (Figure 4.1). While these same interactions are likely to support the processive component, it is not clear how static contacts with the RS domain and RRMs function dynamically to thread the long Arg-Ser chain through the SRPK1 binding channel. We

showed previously using ATP-dependent cross-linking experiments that the RS domain moves in the binding channel as a function of phosphorylation (Ngo et al., 2008). These studies show that while the N′-RS1 is initially bound in the docking groove at the start (Figure 4.1), this segment moves out of the groove as a function of C-terminal-to-N terminal phosphorylation. This process not only requires movement of the RS domain but also induces changes in secondary structure within ASF/SF2. In place of N′-RS1, β4 of RRM2, which we label as linker (L), unfolds and moves into the docking groove for the phosphorylation of residues at the N-terminal end of RS1. In this present study, we address how protein–protein interactions, including contacts with the RRMs and the RS domain (Figure 4.1B), may accommodate such a 'gliding' RS domain as the reaction progresses from an unphosphorylated state to a hyper-phosphorylated state.

1. SRPK1 Uses an Atypical Docking Mechanism for ASF/SF2 Recognition

The SRPK1-ASF/SF2 complex is unusually stable (K_d~100 nM) compared to most kinase–substrate pairs. While the present structure is incomplete (Figure 4.1), interactions with RRM2 are well-defined and bury nearly 1100 Å of surface area or about 20% more than that for the N′-RS1 docking groove on SRPK1. These observations suggest that polypeptide regions outside the immediate phosphorylation segment in RS1 may contribute significantly to high affinity. Indeed, many protein kinases use distal contacts far from the immediate phosphorylation segment to enhance binding affinity. For example, the transcription factor substrates for the MAP kinases are not phosphorylated without the presence of amino acids 50–100 residues

away from the site of phosphorylation (Kallunki et al., 1996; Kallunki et al., 1994; Yang et al., 1999). Thus, the kinase domain may be presented with several individual binding modules from the protein substrate that cooperatively enhance substrate recognition. This simple model contrasts with that for SRPK1 where a silent high-affinity binding module far from the local phosphorylation segment in RS1 is not optimally recruited in the initial recognition step. Using a large series of N-terminal and C-terminal deletion constructs, we showed that while the RS domain binds as well as the full-length ASF/SF2, the separate RRM1–RRM2 module has the capacity to form a high affinity complex with SRPK1 similar to that for the separate RS domain (Figures 4.2 and 4.8). In fact, the intrinsic high affinity of this RRM1–RRM2 module is likely to be responsible for the unusually stable binding observed in the charge-to-alanine RS domain block mutants and RS2-deleted substrate (Figures 4.5 and 4.8). In all, while ASF/SF2 does not require the RRM1–RRM2 module for initial recognition, these N-terminal domains appear to have an important function when the electropositive character of the RS domain is diminished. This binding feature of SRPK1 not only is very distinct from the classic docking site model but also appears to be an essential property for sequential processive phosphorylation of ASF/SF2, as we will discuss next.

2. Redundant Binding Modules Guide Processivity Through a Strain Mechanism

While the separate RRM1–RRM2 and RS domain modules in ASF/SF2 have high intrinsic binding affinities, the total energies are not realized in the enzyme–substrate complex, at least prior to phosphorylation. This phenomenon induces some

strain within the complex that we believe is important for processive phosphorylation in the presence of building repulsive charge. In our studies, we can gauge this strain and its dynamic utilization in start–trap experiments by observing an increase in the level of processivity from about three serines in the separate RS domain to eight serines upon the addition of the RRM1–RRM2 module (Figure 4.4). Processivity is achieved in SRPK1 by maintaining a high forward catalytic rate (k_f) and a low substrate dissociation rate (k_{off}). While SRPK1 uses contacts with the RS domain to support the initial processive events (i.e., $k_f/k_{off} \gg 1$), these contacts are insufficient to support a stable enzyme–substrate complex in later phosphorylation stages due to increased repulsive forces with the acidic docking groove of SRPK1 (i.e., $k_f/k_{off} \ll 1$). To keep the enzyme attached for future steps and to maintain a high k_f/k_{off}, strain energy stored in the complex is released upon initial RS domain phosphorylation as the RRM1–RRM2 module is recruited for enhanced binding. Although additive modules could also provide stability for initiation, they would not be expected to provide both the stability and the flexibility required for later processive steps. For example, if the two binding modules behaved in a purely additive manner, the K_d for the complex would likely be in the sub-picomolar range. This high affinity may fix the substrate too strongly in the active site and may not allow facile movement of the RS domain, resulting in a very low k_f. By using an apparently redundant binding module in the form of RRM1–RRM2, SRPK1 balances stability needed for processivity with flexibility needed to allow the requisite structural reorganizations in a lengthy phosphorylation reaction.

3. Model for Processive Phosphorylation

The kinetic data presented here allow us to speculate on howSRPK1 provides a stable yet flexible platform for the polyphosphorylation of the SR protein ASF/SF2. As shown in Figure 4.11, the processive component can be dissected into several events (steps 1–5). While the initial encounter complex is not fully optimal (step 1), it is sufficiently stable to permit the processive phosphorylation of the first three serines (step 2). It is likely that this initial modification then induces a structural change in the complex that allows further optimization of enzyme–substrate interactions (step 3). The nature of this reorganization is not understood but could involve adjustments in the RRM1–RRM2 and RS domain contacts, unfolding of β strand 4 in RRM2 (linker segment), and conformational changes in the kinase domain of SRPK1. As these events are critical for further processivity (step 4), the electropositive P+2 pocket in SRPK1 also helps to stabilize the later phosphorylation steps allowing rapid continued phosphorylation. Despite all these strategies to stabilize the phosphocomplex, after about eight steps, SRPK1 releases the incompletely modified SR protein and then relies on distributive steps to finish RS1 phosphorylation. Interestingly, while we can disrupt processive phosphorylation through RRM1–RRM2 deletion or docking groove mutation, neither alters the overall phosphoryl content of ASF/SF2, raising the question of why SRPK1 evolved such a processive mechanism. Although further studies are needed to address this question, we believe that processivity regulates the biological function of ASF/SF2 by influencing dynamic protein–protein interactions in the context of competing catalytic factors. The sequestration of early phospho-ASF/SF2 intermediates may help promote a unique folded state poised for interaction

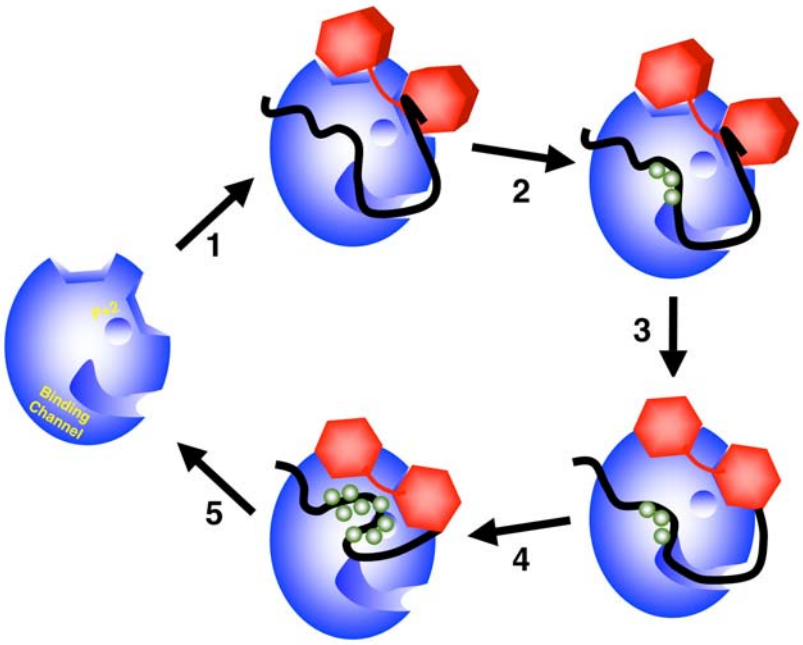

Figure 4.10 Model for processive phosphorylation of ASF/SF2. SRPK1 (blue) contains a binding channel for the RS domain (black line), the P+2 electropositive pocket, and binding surfaces for RRM1 and RRM2 (both in red). The processive cycle includes 5 steps that involve substrate recognition (1), initial processive phosphorylation of ~3 serines (2), rearrangement step to optimize contacts (3), continuation of processive phosphorylation of ~5 serines (4), and release of phospho-ASF/SF2. Phosphates are shown in green.

with nuclear transport proteins and/or may limit the activity of protein phosphatases that would readily lower phosphoryl content and potentially prohibit SR protein shuttling and splicing function.

E. Materials and Methods

1. Peptide Synthesis. Peptides were synthesized from L-amino acids using solid-phase N-(9-fluorenylmethoxycarbonyl) chemistry on an Applied Biosystems 433A synthesizer, purified on a C18 HPLC column, and analyzed by electrospray mass spectrometry at 215 and 225 nM absorbance for concentration determination.

2. Expression and Purification of Recombinant Proteins

All single-site and multisite mutations in ASF/SF2 and SRPK1 were generated by single or sequential polymerase chain reactions using the QuikChange™ mutagenesis kit and relevant primers (Stratagene, La Jolla, CA). C-terminal deletion constructs were made by inserting stop codons into the pET15b (N-terminal His tag) ASF/SF2 construct. N-terminal deletion constructs were generated by polymerase chain reaction amplification and subcloning into pET28a (C-terminal His tag). All mutations in SRPK1 were made from a wild-type vector containing an N-terminal His tag (pET15b). Unless otherwise designated, all SRPK1 and ASF/SF2mutants contain theN-terminalHis6 tag. A kinase inactive form of SRPK1 (kdSRPK1) was generated by replacing Lys at position 109 with Met and was previously described (Yeakley et

al., 1999). The synthesis of the cleavage vectorASF(5R1K) was described previously (Ma et al., 2008). The plasmids for wild-type and mutant forms of ASF/SF2 and SRPK1 were transformed into the BL21(DE3) Escherichia coli strain, and the cells were then grown at 37 °C in LB broth supplemented with 100 μg ml−1 ampicillin. Protein expression was induced with 0.4 mM IPTG at room temperature for 5 h. SRPK1 was purified by Ni-resin affinity chromatography using published procedures (Aubol et al., 2003). All ASF/SF2 constructs were refolded and purified using a previously published protocol (Velazquez-Dones et al., 2005).

3. Phosphorylation Reactions

The phosphorylation of wild-type and mutant forms of ASF/SF2 by SRPK1 was carried out in accordance with previously published procedures in the presence of 50 mM 3-(N-morpholino)propanesulphonic acid (pH 7.4), 10 mM free Mg^{2+}, 5 mg ml−1 bovine serum albumin, and [γ-^{32}P] ATP (600–1000 cpm pmol−1) at 23 °C.26 Reactions were typically initiated with the addition of [^{32}P]ATP (100 μM) in a total reaction volume of 10 μl and then were quenched with 10 μl of SDS-PAGE loading buffer. Each quenched reaction was loaded onto a 12% SDS-PAGE gel, and the dried gels were exposed with Kodak imaging film (Biomax MR). The protein bands corresponding to phosphorylated ASF/SF2 were excised and counted on the 32P channel in liquid scintillant. Control experiments, specific activity determination, and time-dependent product concentrations were determined as previously described (Aubol et al., 2003).

4. Mass Spectrometric Analyses

MALDI-TOF analyses were carried out using a PerSeptive Biosystems Voyager DE PRO spectrometer. Preparation of phosphorylated protein samples was typically carried out using SRPK1 (300 nM) and ASF/SF2 (1 μM) in the presence of 50 mM Tris–HCl (pH 7.4), 10 mM free Mg^{2+}, and 1 mM DTT at room temperature. Reactions were initiated with the addition of 1 mM ATP in a total volume of 100 μl. Reactions then were quenched with 5% acetic acid, desalted with Zip-tip C18, and eluted with 80% acetonitrile and 2% acetic acid for MALDI-TOF analysis. Unphosphorylated sample controls were prepared in the same manner, without ATP. The matrix solution consisted of 5 mg ml^{-1} α-cyano-4-hydroxy cinnamic acid in 1:1:1 acetonitrile/ethanol/0.52% trifluoroacetic acid. The final pH of the matrix solution was 2.0.

5. Data Analysis

Progress curve data for ASF/SF2 phosphorylation were plotted as ratios of incorporated phosphate to the total substrate concentration (number of sites) as a function of time and were fitted to a double-exponential function. Start–trap data were fitted to a single-exponential function followed by a linear function. The relative initial velocities for the competition data were fitted to Equation (1):

$$\frac{v_i}{v_o} = \frac{[S] + K_m}{[S] + K_m\left(1 + \frac{[I]}{K_I}\right)}$$

where v_i/v_o is the relative initial velocity (ratio of v in the presence of inhibitor to v in the absence of inhibitor), K_m is the Michaelis constant for the fixed substrate [ASF(ΔRRM1), ASF/SF2, or ASF/SF2-His], [S] is the total concentration of the fixed substrate, [I] is the total concentration of the competitive inhibitor, and K_I is the dissociation constant for the inhibitor. The relative initial velocities for the partial competitive data were fitted to Eq. (2):

$$\frac{v_i}{v_o} = \frac{[S] + K_m}{[S] + K_m\left[\frac{1 + [I]/K_I}{1 + [I]/\alpha K_I}\right]}$$

(Segel, 1975) where v_i/v_o, K_m, [S], and [I] are the same as in Eq. (1), and K_I and αK_I are the dissociation constants for the partial competitive inhibitor in the absence and in the presence of S (see Scheme 1).

The text of Chapter IV is a reprint of the material as it appears in *The Journal of Molecular Biology*, 2008, 382(4), 894-909, Hagopian, J.C., Ma, C.T., Meade, B.R., Albuquerque, C.P., Ngo, J., Ghosh, G., Jennings, P.A., Fu, X.D., Adams, J.A. The dissertation author was the primary researcher and author of this publication.

Chapter V

FT-ICRMS Analysis of SR Protein Phosphorylation by SRPK1

A. Abstract

We utilized high-resolution Fourier transform ion cyclotron resonance mass spectrometry (FT-ICRMS or FTMS), in collaboration with Dr. Pieter Dorrestein, to refine our understanding of ASF/SF2 splicing factor phosphorylation by SRPK1. We elucidated the source of a mysterious phospho-serine residue observed in a recent crystal structure of SRPK1ΔNS:ASF/SF2(ΔRRM1ΔRS2) solved in the presence of non-hydrolyzable AMP-PNP nucleotide. Crystallization conditions reproduced for FTMS analysis revealed partial phosphorylation of a single serine on the ASF/SF2(ΔRRM1ΔRS2) substrate, indicating the AMP-PNP stocks contained low levels of ATP. Kinetic experiments with SRPK1 and ASF/SF2ΔRRM1 revealed a biphasic reaction characterized by rapid phosphorylation of the initial 10 serines, followed by slow incorporation of 4 additional phosphates. Kinetic data with full length ASF/SF2 was also biphasic with fast incorporation of 10-12 phosphates, followed by slow phosphorylation of the final 3 serines. Unlike the single turnover experiments which indicate that SRPK1 catalyzes a semi-processive reaction, the distributive component dominates under steady-state turnover conditions. Analysis of full length ASF/SF2, in the absence of SRPK1, by gel-filtration chromatography and ultracentrifugation sedimentation illustrated the aggregated nature of this substrate in these reactions, and explains the shift in mechanism from semi-processivity previously described for heterodimeric complexes of SRPK1 and ASF/SF2 to a more distributive mechanism.

B. Introduction

The majority of human genes are known to have alternatively spliced isoforms (Modrek and Lee, 2002). RNA splicing takes place in the nucleus at a macromolecular complex called the spliceosome (Akker et al., 2001; Stojdl and Bell, 1999). While this complex is composed of several RNA and protein molecules, it is now understood that assembly of the spliceosome and selection of splice sites is directed by highly regulated phosphorylation of a family of splicing factors known as SR proteins (Fu, 1995). The SR proteins have a modular structure with N-terminal domains that bind nucleic acids called RNA recognition motifs (RRMs), and C-terminal RS domains with long stretches of arginine-serine dipeptide repeats modified by phosphorylation to meditate protein-protein interactions. The SRPK and Clk/Sty kinases catalyze RS domain phosphorylation of splicing factors *in vivo* (Colwill et al., 1996; Wang et al., 1999; Yun and Fu, 2000). The phosphorylation state of SR proteins influences spliceosome assembly, alternative splice site selection, SR protein localization, and mRNA metabolism (Koizumi et al., 1999; Lai et al., 2001). The influence of RS domain phosphorylation states on these critical cellular events highlights the importance of understanding the mechanics and dynamics of splicing factor phosphorylation and dephosphorylation.

We have extensively studied the catalytic properties of splicing factor AFS/SF2 phosphorylation by SRPK1. We reported that SRPK1 and ASF/SF2 bind as a high affinity complex with a K_D of approximately 60 nM (Hagopian et al., 2008; Velazquez-Dones et al., 2005). We have also demonstrated that the spacer domain of

SRPK1 does not significantly effect affinity or catalysis with ASF/SF2 (Ding et al., 2006)). A crystal structure of an SRPK1 spacer deleted construct in complex with ASF/SF2(ΔRRM1ΔRS2) was recently solved by our collaborators (Ngo et al., 2008). The structure revealed that three distinct regions of ASF/SF2 interact with SRPK1. Residues in the RRM2 of ASF/SF2 formed bonds with both the large and small lobes of SRPK1. The N-terminal segment of the RS domain of ASF/SF2 interacted with an acidic docking groove in the kinase adjacent to the active site. Finally, a floating phospho-serine made contacts with basic residues near the P+1 loop of SRPK1 (Ngo et al., 2008). The observation of a phospho-serine in the crystal structure was puzzling because the complex was soaked with a non-hydrolyzable analog of ATP (AMP-PNP). We will here describe our efforts to elucidate the source of this molecule in the SRPK1ΔNS:ASF/SF2(ΔRRM1ΔRS2) structure utilizing high-resolution FTMS.

The MALDI-TOF spectra of ASF/SF2 proteins phosphorylated by SRPK1 described in Chapters 3 and 4 are broad low-resolution peaks spanning more than 1,000 mass units. Phosphate incorporation was determined by measuring the centroid value shifts of these peaks following reactions with kinase in the presence of saturating concentrations ATP. As a result, the end-points of phosphorylation by the SR kinases are not very well defined. We utilized FTMS to refine the defined specificity of SRPK1 for ASF/SF2. FTMS is an extremely sensitive method of ion detection, that can be applied to study proteins and peptides with high mass accuracy and resolution (Marshall et al., 1998). Simply stated, FTMS instruments take ions generated at a source and accumulated in an ion trap into a cyclotron cell within a superconducting high field magnet that is cooled by liquid helium and nitrogen.

Excitation plates accelerate the ions into a circular motion within the cell governed by the Lorentz Force (see equation 1, where F is the Lorentz Force, B is the magnetic field strength, *z* is the charge of the ion, and v is the incident velocity of the ion). The frequency of ion rotation (ω_C) detected within the cell is a function of the mass to charge ratio (*m/z*) are described by equations 2 and 3.

$$F = zv \times B \qquad (1)$$

$$\omega_C = \frac{zB}{2\pi m} \qquad (2)$$

$$m/z = \frac{B}{2\pi\omega_C} \qquad (3)$$

The signals are deconvoluted by Fourier transform mathematical methods and ultimately converted to mass vs. intensity spectra (Marshall et al., 1998). We here report our results by FTMS analysis of ASF/SF2 phosphorylation with SRPK1.

C. Results

1. The Mysterious Phospho-Serine of the SRPK1ΔS:ASF/SF2(ΔRRM1ΔRS2)

Crystal Structure

The SRPK1ΔASF/SF2(ΔRRM1ΔRS2) crystal structure demonstrated that three discontinuous regions of ASF/SF2 interact with SRPK1. Residues in the RRM2 of ASF/SF2 formed bonds with both the large and small lobes of SRPK1, the N-terminal segment of the RS domain of ASF/SF2 interacted with an acidic docking groove in the kinase adjacent to the active site, and a phospho-serine dipeptide made contacts with basic residues near the P+1 loop of SRPK1 (Ngo et al., 2008). The observation of a

phospho-serine in the crystal structure was strange because the complex was formed with a non-hydrolyzable analog of ATP (AMP-PNP) (Figure 5.1).

To investigate the source of the phospho-serine residue, we designed experiments to test conditions and reagents used to generate crystals for X-ray analysis. Three distinct reaction conditions were studied. Buffer concentrations for all reactions were consistent with those used for crystallization, except that PEG 4000 was omitted. Reactions were incubated at room temperature for 1 hour, quenched with 5% acetic acid, and purified with C-18 Zip-Tips (Millipore). Mass spectrometric analyses of the reactions were performed by FTMS. Data were averaged with Qualbrowser and processed with Xtract (Xcalibur software package).

In the first reaction, 10 μM of the SRPK1ΔS: ASF/SF2(ΔRRM1ΔRS2) complex was reacted in the absence of AMP- PNP. FTMS analysis of this reaction revealed a high intensity peak at 13649.99 Da., corresponding to the unmodified molecular weight of the ASF/SF2(ΔRRM1ΔRS2) molecule in complex with SRPK1 (Figure 5.2A). In the second reaction, 10 μM of the SRPK1ΔS: ASF/SF2(ΔRRM1ΔRS2) complex was reacted in the presence of 2 mM AMP-PNP. This reaction contained nucleotide at concentrations used to create crystals, but the protein complex was diluted 10-fold relative to conditions used for crystallization. FTMS results showed 4 distinct mass states at 14128.80, 14209.77, 14289.75, and 14369.71 Da., corresponding precisely to the mass of the substrate with the addition of 6, 7, 8, and 9 phosphates (Figure 5.2B). The third reaction was a reproduction of crystallization conditions with 100 μM SRPK1ΔS: ASF/SF2(ΔRRM1ΔRS2) complex and 2 mM AMP-PNP. The FTMS spectra of this reaction had major peak at 13650.00 Da., the

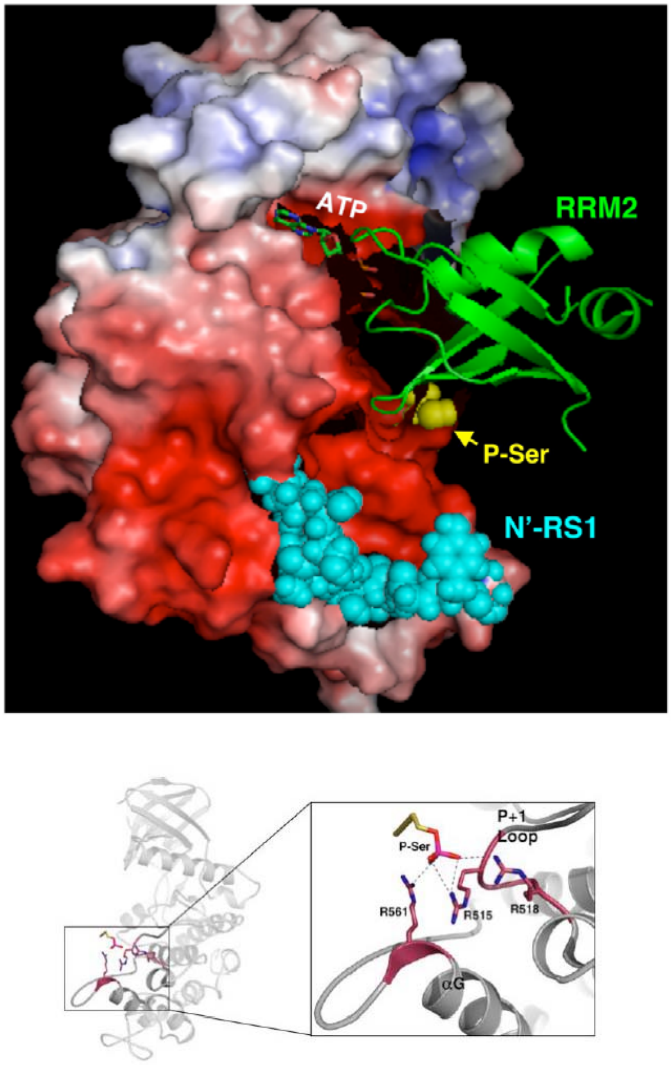

Figure 5.1 The SRPK1ΔS:ASF/SF2ΔRRM1 crystal structure generated in the presence of ATP analog AMP-PNP. The electrostatic surface of spacer deleted SRPK1, red represents negative charge and blue represents positive charge. Three distinct regions of ASF/SF2 interact with SRPK1. 1) Residues in RRM2 of ASF/SF2 formed bonds with SRPK1 (green). 2) The N-terminal segment of the RS domain of ASF/SF2 interacted with an acidic docking groove in the kinase (blue). 3) A phospho-serine residue made contacts with basic residues near the P+1 loop of SRPK1 (yellow above and detailed below) (Hagopian et al., 2008; Ngo et al., 2008).

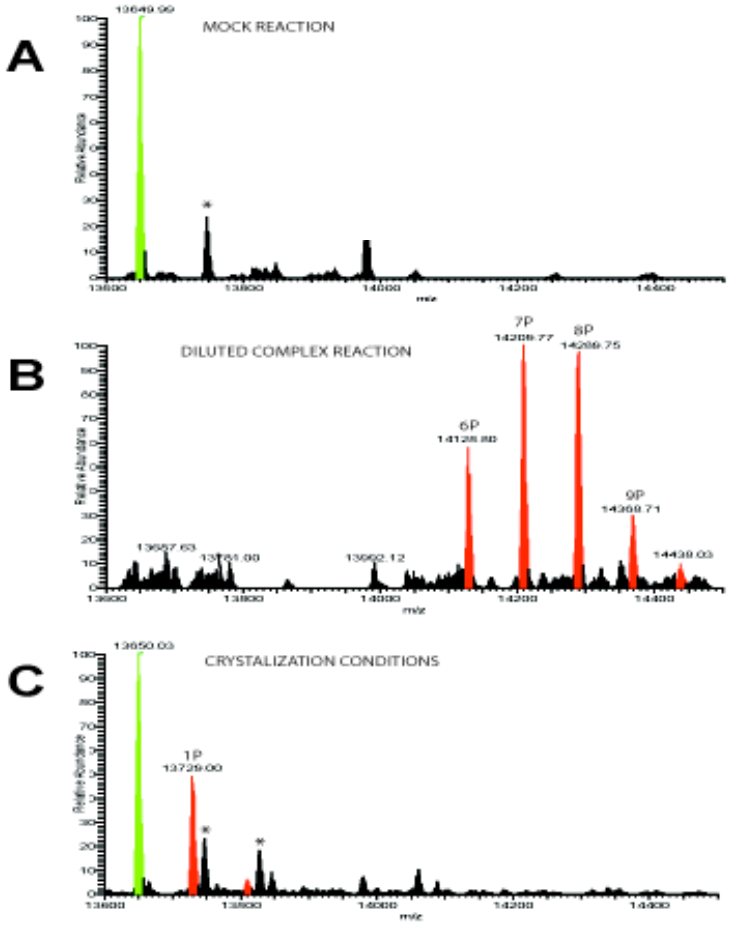

Figure 5.2 FTMS analysis of ASF/SF2 in the SRPK1ΔS:ASF/SF2ΔRRM1 complex used for co-crystallization with AMP-PNP. The reaction in (A) used 10 μM SRPK1ΔS:ASF/SF2ΔRRM1 complex and no AMP-PNP. The mass peak of unphosphorylated ASF/SF2ΔRRM1 is colored green. Inorganic phosphate adducts are labeled with an asterisk. There was no evidence of phosphorylation in this reaction. The reaction in (B) used 10 μM SRPK1ΔS:ASF/SF2ΔRRM1 complex and 2 mM AMP-PNP. This reaction maintained the nucleotide concentration used for crystallization, but diluted the relative complex concentration 10 fold. Mass peaks of ASF/SF2ΔRRM1 phosphorylation states are colored red and labeled. The robust phosphorylation profile indicated the AMP-PNP stock was indeed contaminated with ATP. The reaction in (C) used 100 μM complex and 2 mM AMP-PNP, similar to the crystallization conditions. In this case, the contaminating nucleotide was present in limiting amounts relative to substrate. This resulted in partial occupancy of a single phosphorylated species that is colored red and labeled in the figure. These results indicate the observed phospho-serine in our crystal structure corresponds to the single phosphorylation site in ASF/SF2ΔRRM1.

unmodified substrate, and a secondary peak at 13729.00 that was the result of a single phosphorylation. This partial occupancy of a single phosphorylated species indicates that the observed phospho-serine in our crystal structure corresponds to the initial phosphorylation site in ASF/SF2(ΔRRM1ΔRS2). The positive correlation between complex concentration and the extent of phosphorylation was clear evidence that the AMP-PNP stocks used in the crystallization reactions were contaminated with ATP.

2. Analysis of ASF/SF2ΔRRM1 Phosphorylation by SRPK1

Initial attempts to refine our definition of the endpoint of ASF/SF2 phosphorylation catalyzed by SRPK1 were conducted with truncated constructs of the splicing factor. Smaller proteins are easier to study by FTMS because the ion species generated at the source are distributed over a smaller number of charge states. As a result, the spectral envelope of smaller proteins more readily rises above background signal levels. In Chapter 4 we showed that removal of the RRMs of ASF/SF2 did not significantly change binding affinity with the kinase. However, the processive nature of ASF/SF2 phosphorylation became more distributive in the ASF/SF2ΔRRM1 construct.

A timecourse of phosphorylation was conducted with 300 nM SRPK1 and 3 μM ASFΔRRM1 in reactions containing 10 mM MOPS pH7.4 and 11 mM $MgCl$, initiated with 100 μM ATP. Reactions were quenched with 5% acetic acid at regular time intervals, and purified with C-18 Zip-Tips (Millipore). Zip-Tip protocol substituted 2% acetic acid for trifluoroacetic acid in all buffers to reduce ion suppression, washed with 5% methanol and 15% acetonitrile, and eluted with 80%

acetonitrile. RAW files of FTMS spectra were averaged in Qualbrowser and processed with Xtract (Xcalibur Software Package) The results of FTMS analysis of these timecourse samples are shown in Figure 5.3. Prior to reaction initiation with ATP, the ASF/SF2ΔRRM1 substrate spectra consists of a single high-intensity peak at 17085 mass units, the precise molecular weight of the unmodified protein. The spectra of the reaction quenched at 10 minutes reveals significant mass shifts with peaks at 17717, 17797, and 17876 mass units, consistent with the phosphorylation of 8, 9, and 10 sites respectively. At 20 minutes, ASF/SF2ΔRRM1 is phosphorylated at 9 to 12 sites, and the remainder of the reaction progresses very slowly until reaching a final endpoint of 14 phosphorylations and a molecular weight of 18191.

To investigate the fast phase of ASF/SF2ΔRRM1 phosphorylation by SRPK1, occurring within the first ten minutes of the reaction, we ran a secondary timecourse and quenched at regular intervals within this window. The 17085 mass peak remained unmodified for the first 4 minutes of the reaction. Subsequent timepoints from 6 to 10 minutes demonstrated rapid incorporation of up to 8 phosphates on ASF/SF2ΔRRM1 (Figure 5.4). Since the reaction was performed with substrate in excess of the enzyme concentration, the completion of phosphorylation by SRPK1 required multiple turnover of ASF/SF2ΔRRM1. Therefore, the observation of intermediate phosphorylation states was an indication of distributive multisite catalysis. Interestingly, there was a significant delay in the initial 4 minutes of the reaction. Because we do not observe such a lag in ^{32}P assays, we think that a single-turnover processive event may have occured within this time frame

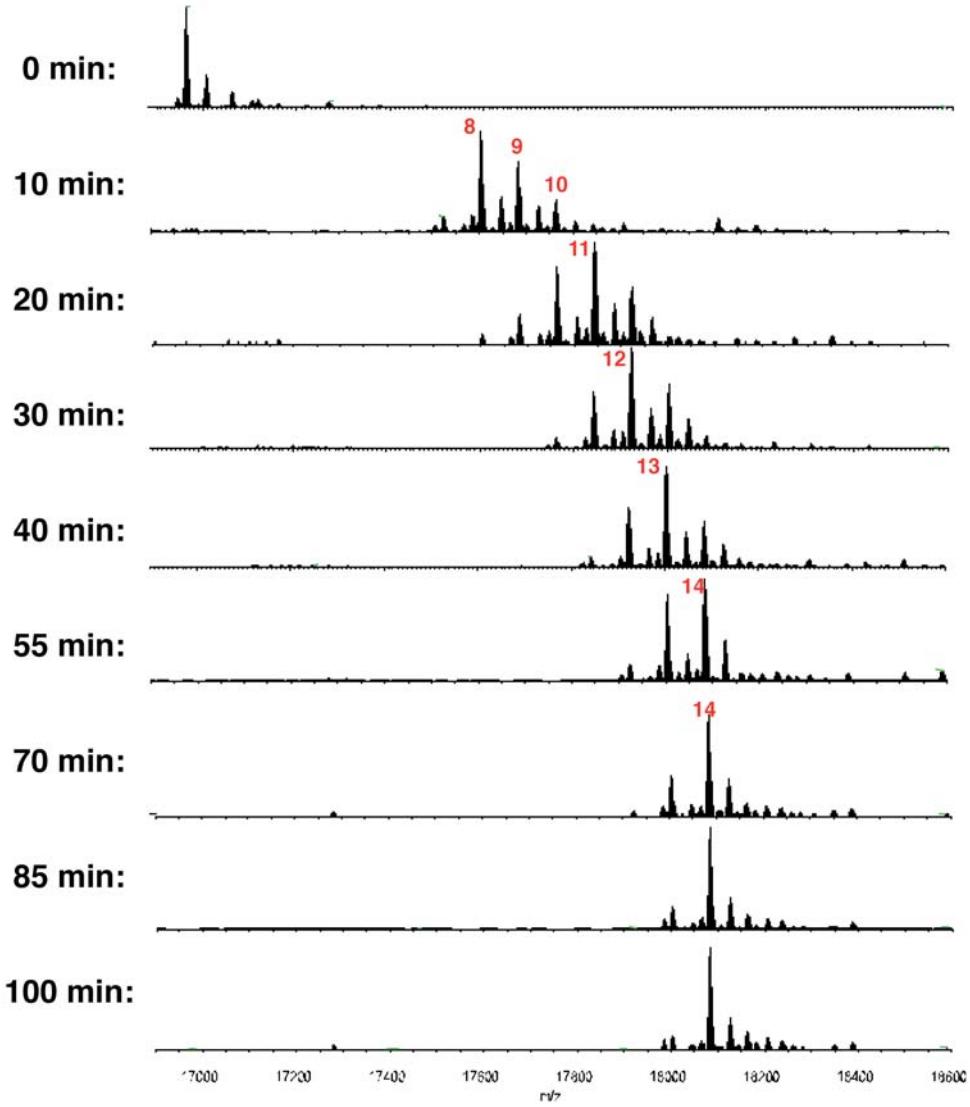

Figure 5.3 SRPK1 phosphorylates 14 residues in the RS domain of ASF/SF2ΔRRM1. The highly pure ASF/SF2ΔRRM1 FTMS spectra consists of a single high intensity peak at 17085 mass units, the precise molecular weight of the unmodified protein (0 min). The timecourse initiated by the addition of ATP displays clear biphasic kinetics with rapid incorporation of the initial 10 phosphates followed by slow transfer onto the final 4 phosphorylation sites. This experiment precisely defines the phosphorylation endpoint for SRPK1 catalysis with ASF/SF2ΔRRM1 of 14 phosphorylation sites.

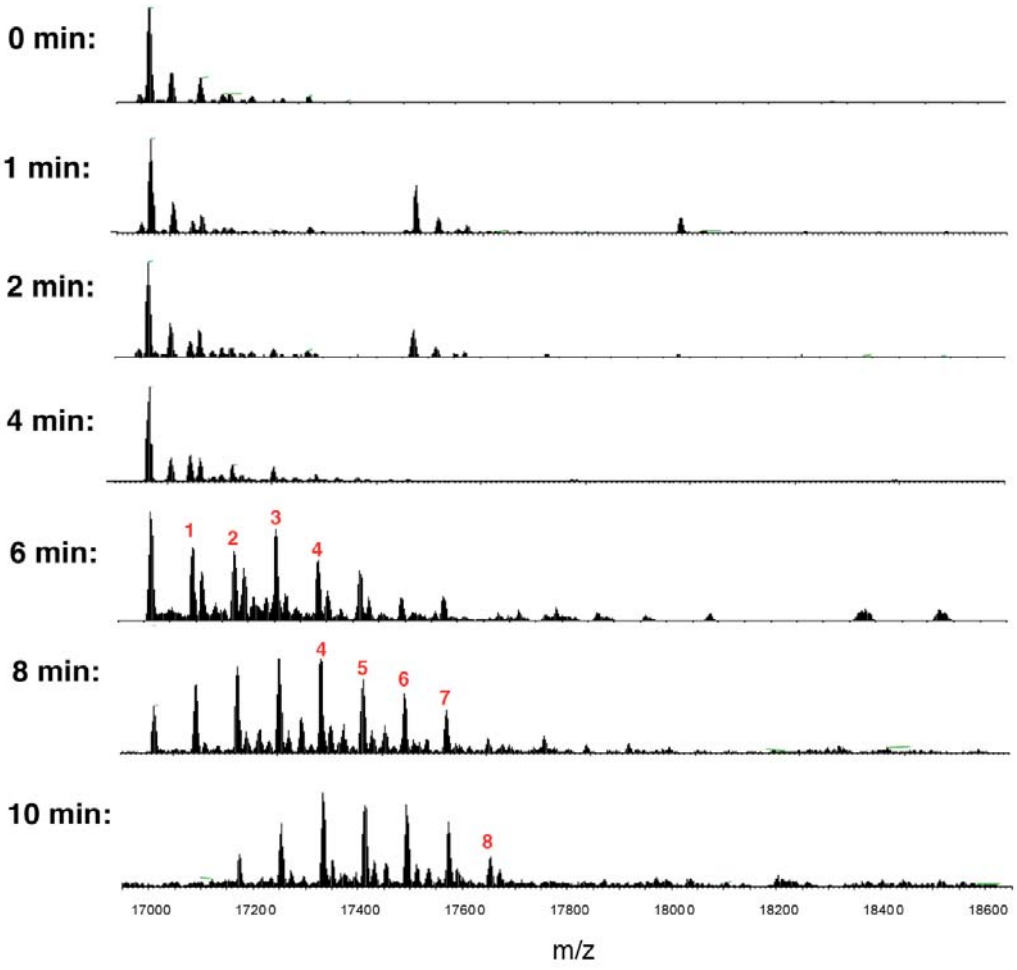

Figure 5.4 The fast phase of ASF/SF2ΔRRM1 phosphorylation by SRPK1. 300 nM SRPK1 was incubated with 3 μM ASF/SF2ΔRRM1 prior to reaction initiation with 100 μM ATP. The transfer of phosphates was significantly delayed, with no measurable phosphorylation occurring in the first 4 minutes of the reaction. This could possibly be due to a single-turnover processive event that was below detection limits for our system. From the 6 to 10 minute timepoints, the reaction displays rapid incorporation of up to 8 phosphates.

to yield product below the limits of detection for our system. Overall, the result was consistent with previous results that showed a shift toward distributive phosphorylation for the ASF/SF2ΔRRM1 construct in single-turnover start-trap experiments (Chapter 4).

3. Analysis of ASF/SF2 Phosphorylation by SRPK1.

To determine if the endpoint of ASF/SF2 phosphorylation by SRPK1 is consistent between single-turnover and multi-turnover reactions, we conducted a series of ^{32}P timecourses. 1μM ASF/SF2 was mixed with 0.01, 0.025, 0.05, 0.1, or 1 μM SRPK1 in reactions containing 10 mM MOPS pH 6.5, 11 mM $MgCl_2$, 3 mg/ml BSA, initiated with 300 μM ATP. Quantification was achieved using the SDS-PAGE assay described previously (Chapter 3). Figure 5.5 shows an enzyme dependent increase in velocity, with a common endpoint achieved in both single-turnover and multi-turnover reactions.

Studying full length ASF/SF2 protein posed a challenge for analysis by FTMS because the larger molecule has its signal distributed over many more charge states. After many failed attempts we finally managed to tune the FTMS and gather data on ASF/SF2 phosphorylation by SRPK1. Reaction buffer components and purification protocols were the same as described for ASFΔRRM1. However, because the signal to noise ratio was dramatically decreased, the Xtract processed data was not as clean as previously presented for ASFΔRRM1. 25 nM SRPK1 was reacted with 1 μM ASF/SF2 in reactions initiated with 100 μM ATP, quenched at regular intervals within

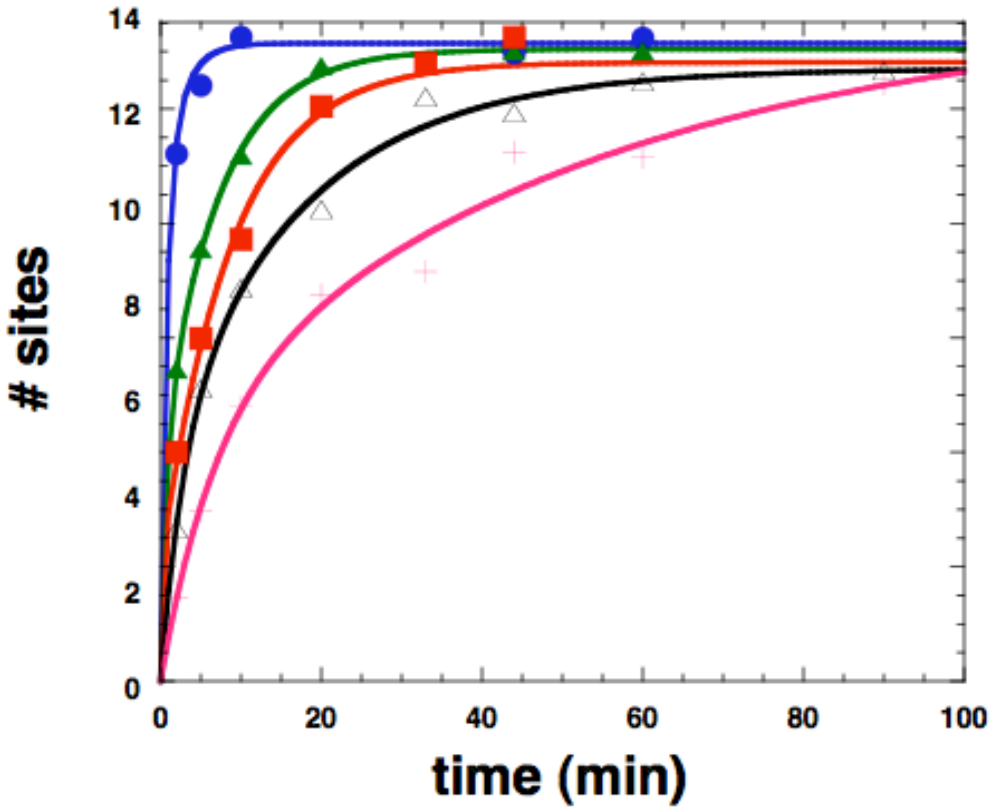

Figure 5.5 Common endpoints of single-turnover and multi-turnover ASF/SF2 phosphorylation by SRPK1. SRPK1 at 0.01 (+), 0.025 (Δ), 0.05 (■), 0.1 (▲), or 1 μM was reacted with 1 μM ATP. The endpoint of ASF/SF2 phosphorylation did not change as a function of enzyme concentration.

a one hour timecourse. Prior to the addition of ATP, the unmodified ASF/SF2 substrate is seen with a mass peak at 30377 Da. (Figure 5.6). Additional peaks observed in the 0 min spectra are non-covalent adducts of inorganic phosphate. What the data clearly demonstrates is that ASF/SF2 phosphorylation by SRPK1, similar to the deletion mutant, displays biphasic kinetics with rapid phosphorylation of the first 10 phosphates and slow incorporation of an additional 4-5 sites to achieve a clear end-point of catalysis by SRPK1 of 14-15 phosphates. Based on this data, we proposed to shift the model of the RS1 domain of ASF/SF2 (residues phosphorylated by SRPK1) from residue 219 to 228. The absence of intermediate phosphorylation states with 1-9 phosphates could be due to processive phosphorylation of ASF/SF2 by SRPK1 as described in single-turnover start-trap experiments. To determine if SRPK1 generates intermediates at the early stages of the reaction, we decreased the SRPK1 concentration to 2 nM and kept ASF/SF2 at 1 μM. Figure 5.7 shows averaged raw data prior to processing with Xtract for the 0 and 10 minute time points of the reaction initiated with 100 μM ATP. The +46 charge state of the unphosphorylated species is shown in green, and the expanded window displays the high-resolution distribution of isotopes that define the peak. The -18 peak likely corresponds to a dehydration, the +98 peak to an inorganic phosphate adduct, and the +42 peak is probably an acetylation. The +45 charge state can also be seen in this window. Because the 10 minute time point distributed the signal over multiple phosphorylation states, the signal dropped even further into the noise, but phosphorylated intermediates are clearly visible as indicated in red. This data is consistent with a distributive reaction for SRPK1 under steady-state conditions.

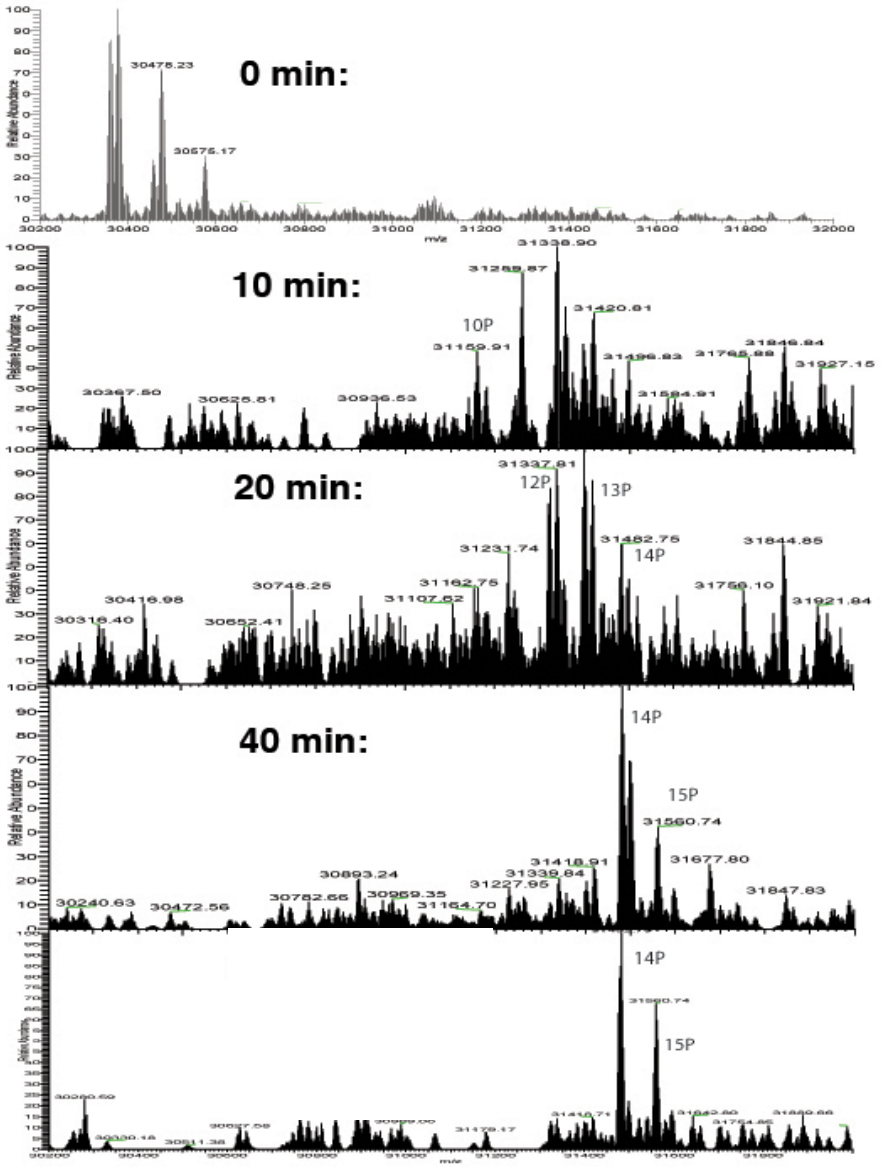

Figure 5.6 SRPK1 phosphorylates 14-15 residues in the RS domain of ASF/SF2. 25 nM SRPK1 was reacted with 1 μM ASF/SF2 in reactions initiated with 100 μM ATP, quenched at regular intervals within a one hour timecourse. The unmodified ASF/SF2 substrate has a mass of 30377 Da. (0 min). The phosphorylation timecourse shows biphasic kinetics. Within 10 minutes, SRPK1 has rapidly transferred 10-12 phosphates to ASF/SF2. A secondary slow phase is seen in the data for timepoints 20 thru 60 minutes, where slow incorporation of additional phosphates eventually yields an endpoint of the reaction with 14-15 phosphorylations.

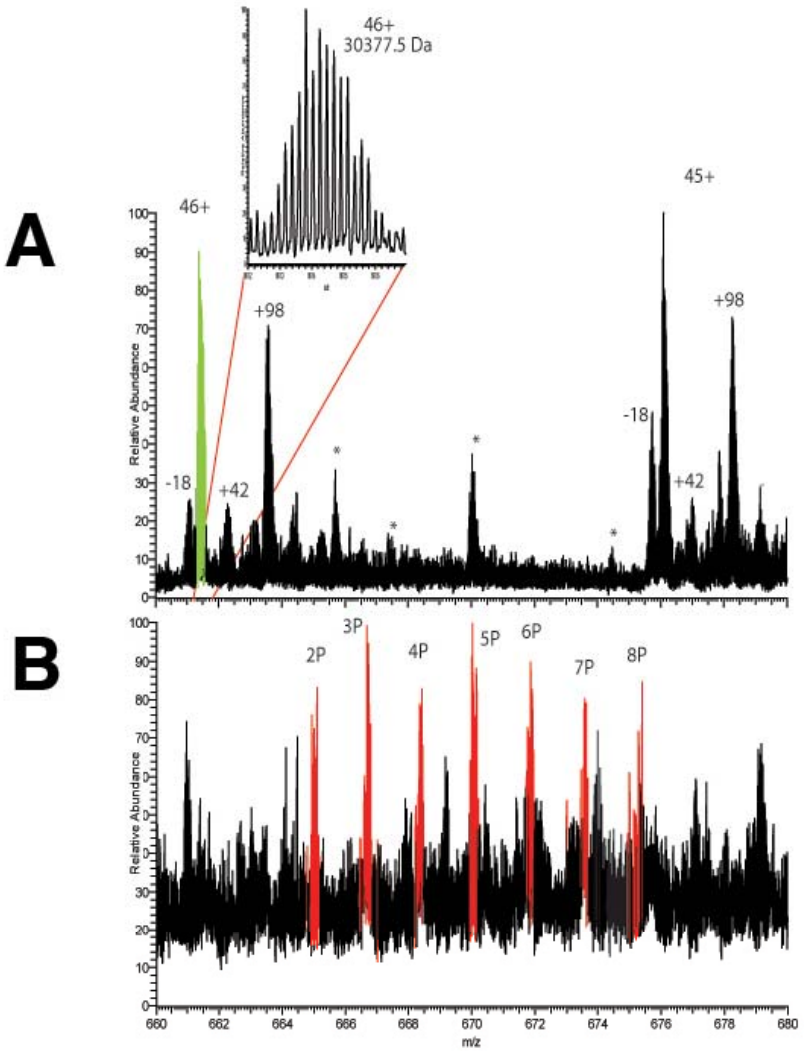

Figure 5.7 FTMS detection of ASF/SF2 phospho-intermediates with catalytic concentrations of SRPK1. Reactions with 2 nM of SRPK1 were incubated with 1 μM of ASF/SF2 and initiated with 100 μM ATP. A) Pre-ATP control. The +46 charge state of unphosphorylated ASF/SF2 is shown in green, and the expanded window displays the high-resolution distribution of isotopes that define the peak. The +45 charge state can also be seen in this window. B) 10 minute timepoint. Phosphorylated intermediates with 2 to 8 phosphates are clearly visible as indicated in red.

To provide support for the FTMS result, we needed to establish another means to identify intermediate phosphorylation states of ASF/SF2 by SRPK1. Phosphorylation of ASF/SF2 inhibits the migration of the protein through SDS-PAGE gels. Steady-state phosphorylation reactions separated by SDS-PAGE as a function of time would reveal intermediate migrating phosphorylation states for a distributive reaction. We conducted steady-state experiments and monitored the reaction progress of 1 μM ASF/SF2 phosphorylation by 25 nM SRPK1 on SDS-PAGE gels (Figure 5.8A). The fully phosphorylated ASF/SF2 product of single-turnover catalysis with SRPK was

compared with quenched time points of the steady-state reaction. If the reaction was fully processive, we would see a build up at the slow migrating position marked by the fully phosphorylated single-turnover control. What we observe is a time course characterized by a slow upward progression toward the endpoint control samples labeled with a red asterisk, consistent with a distributive mechanism (Figure 5.8A). Quantification of the data demonstrates the biphasic nature of the reaction consistent with the FTMS data (Figure 5.8B).

We hypothesized that the shift in mechanism observed for SRPK1 in the presence of excess concentrations of ASF/SF2 was due to a change in the physical state of the substrate in phosphorylation conditions used for FTMS experiments. These reactions were carried out at pH 6.5, with high concentrations of ASF/SF2 (μM), and lacked stabilizing buffer components incompatible with mass spectrometric analysis (BSA). We performed gel-filtration studies to compare ASF/SF2 solution

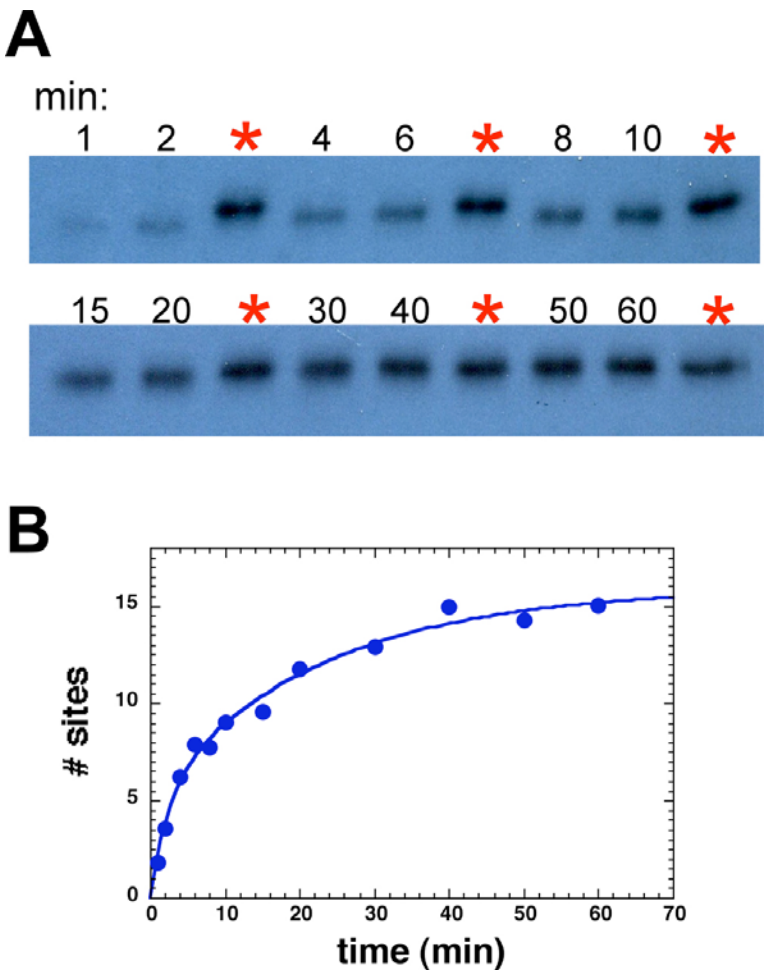

Figure 5.8 ^{32}P SDS-PAGE assay of ASF/SF2 Phosphorylation by SRPK1. A) Timecourse of 1 μM ASF/SF2 phosphorylation with 25 nM SRPK1 initiated with 100 μM ATP. The reaction was quenched at specified timepoints for SDS-PAGE analysis of migration behavior. Early timepoints in the phosphorylation reaction banded as fast migrating species relative to fully phosphorylated ASF/SF2 (*). Reaction progress resulted in the steady migration of ASF/SF2 toward the slow migrating endpoint consistent with distributive phosphorylation. B) Quantitative data for the timecourse visualized in (A), demonstrating biphasic kinetics consistent with FTMS analysis.

dynamics in buffers used to purify the protein with buffers used in the FTMS phosphorylation reaction. A Sephadex-200 column was equilibrated with either purification stock buffer (100 mM MOPS, pH2.2, 20 mM Tris-HCL, 300 mM NaCl, 4% Glycerol) or reaction buffer (10 mM MOPS, pH 6.5, 100 mM NaCl, 11 mM $MgCl_2$, 4% Glycerol) on a HPLC at 0.4 ml/min. Dilutions were made to generate 100 μL samples of 1 μM ASF/SF2 in these buffers. The samples were centrifuged at 13,000 rpm in a microcentrifuge and confirmed to contain soluble protein by A_{280} measurements. The samples were injected onto the Sephadex-200 column and monitored by A_{280} for elution profiles. The ASF/SF2 protein in purification buffer eluted from the column as a single peak at 40 minutes, consistent with a protein of approximately 30 kD as determined by analysis of molecular weight standards (Figure 5.9A). The majority of ASF/SF2 protein in reaction buffer was trapped on the column, with only a fraction eluting at 19 ml, indicating the protein may have self-associated to form large aggregates (Figure 5.9B). The relatively delayed retention time of the eluting material could be due to hydrophobic interations between the protein and the column.

To further characterize ASF/SF2 in the reaction conditions described above, we sent the sample to the Center for Analytical Ultracentrifugation of Macromolecular Assemblies (CAUMA) within the University of Texas Health Science Center in San Antonio, Texas. 1 μM ASF/SF2 samples in the reaction buffer described above were centrifuged for 30 minutes at 13,000 rpm in a micro-centrifuge and determined to contain soluble protein with absorbance of 0.35 at 230 nm. The sample was then

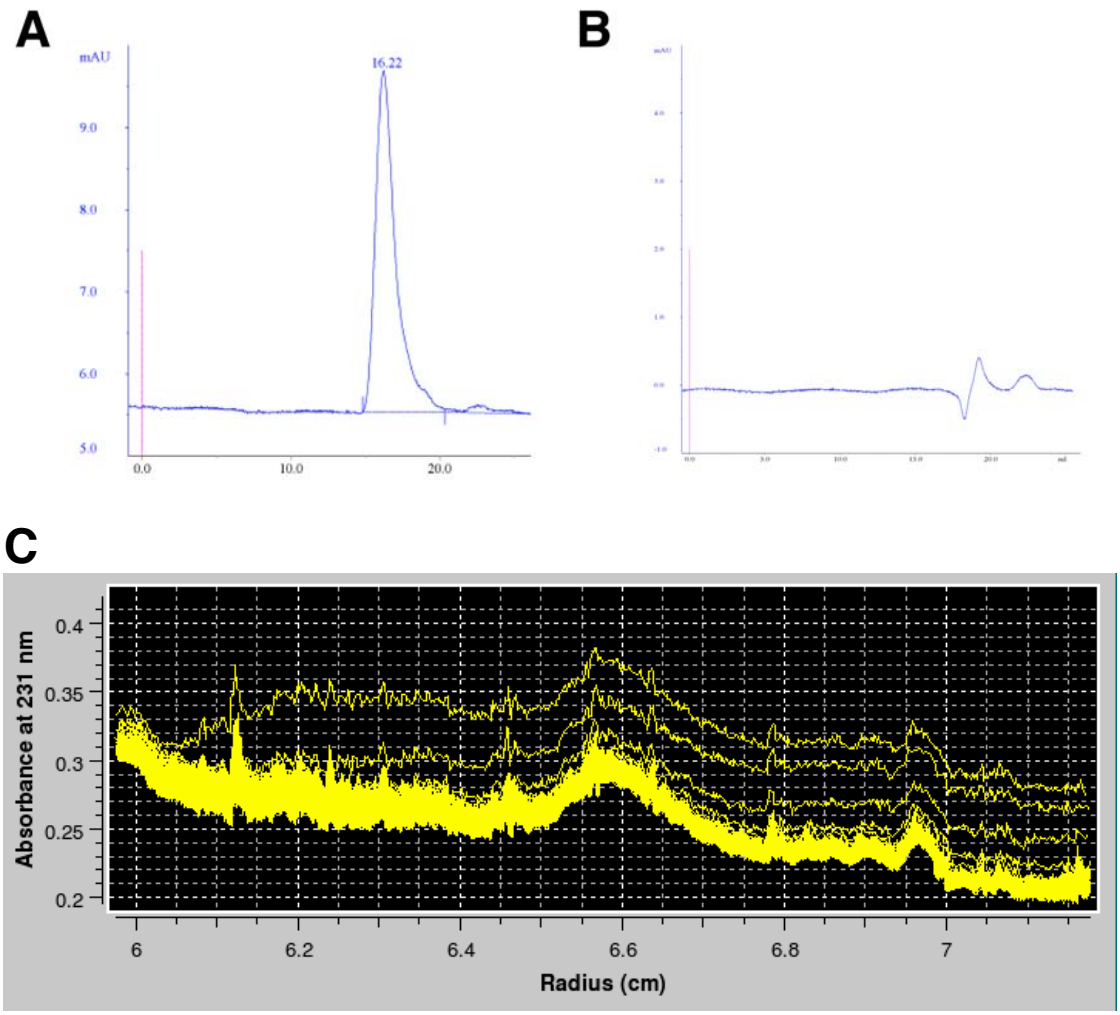

Figure 5.9 ASF/SF2 forms soluble aggregates in reaction conditions used for FTMS analysis. A,B) HPLC gel-filtration analysis on Sephadex-200 column (0.4 ml/min flow rate). A) 1μM ASF/SF2, in low pH buffer used for protein purification, eluted as a single peak at 16 ml, consistent with a protein of approximately 30 kD. B) 1μM ASF/SF2, in FTMS reaction buffer conditions, was primarily lost on the column with a fraction eluting at 19 ml C) Analytical ultracentrifugation of 1μM ASF/SF2 in FTMS reaction buffer conditions centrifuged at 20,000 rpm sedimented rapidly in the first few scans of the run due to significant aggregation.

centrifuged at 20,000 rpm on a Beckman Optima XLI/A analytical ultracentrifuge equipped with UV absorption optics. The sample was determined to contain large soluble aggregates with the leading edge of the absorption boundary rapidly migrating to the bottom of the cell in the first few scans of the experiment (Figure 5.9C).

D. Discussion

1. Understanding the SRPK1ΔS: ASF/SF2(ΔRRM1ΔRS2) Phospho-serine

An interesting feature of the SRPK1ΔS: ASF/SF2(ΔRRM1ΔRS2) complex structure was the presence of a phospho-serine residue at a basic site near the P+1 loop of the kinase (Ngo et al., 2008). Since no ATP was introduced throughout the course of purification and crystallization, it raised the question as to how the phospho-serine is produced and from what component of the complex this peptide is derived. We reasoned that trace amounts of ATP, sufficient to partially phosphorylate the substrate, might be present in the AMP-PNP stock used for crystallization. Indeed, FTMS analysis confirmed that, under crystallization conditions, one serine of ASF/SF2(ΔRRM1ΔRS2) is phosphorylated. Since density was seen in the structure for the N-terminal portion of the RS domain, this initial phosphorylation event did not take place on any of these residues. The linear distance between R210, the last substrate residue seen in the structure, and the positively charged surface where the phospho-serine binds suggests that the serine that underwent phosphorylation is located at the C-terminus of the ASF/SF2(ΔRRM1ΔRS2) construct. This observation is consistent with recent biochemical experiments that show SRPK1 initiates directional phosphorylation of ASF/SF2 from C’ to N’ (Ma et al., 2008). Our

collaborators hypothesize that binding of the phosphorylated residue by the kinase prevents backtracking of the phosphorylated product to maintain directional catalysis (Ngo et al., 2008).

2. Insights Gained by FTMS Analysis of ASF/SF2 Phosphorylation by SRPK1

We observed biphasic kinetics in steady-state phosphorylation experiments with SRPK1 and ASF/SF2. The rapid phosphorylation of the first 10-12 phosphates fits the current model that SRPK1 initiates phosphorylation at the C-terminus (Ma et al., 2008). This fast phase of phosphorylation by SRPK1 may represent the stretch of serines that extend from the docking site to the active site of the kinase. Recent data shows that C-terminal initiation is maintained in the steady-state (Chen-Ting Ma, pers. comm.). The crystal structure of SRPK1ΔS with ASF/SF2ΔRRM1ΔRS2 shows an acidic pathway that extends from the docking motif in the C-terminal lobe of the kinase to the active site (Ngo et al., 2005; Ngo et al., 2008). The current model based on this structural and directionality data suggests the initial phosphorylation event prevents movement towards the C-terminus, but allows rapid progression of phosphorylation toward the N-terminus. Further data supporting this model comes from more recent observations in single-turnover studies showing partial processivity of 50-60% of the total number of serines on ASF/SF2 phosphorylated by SRPK1 (Figure 4.4).

We observed a shift in kinetic mechanism of SRPK1 in single-turnover versus steady-state conditions. This shift was induced by changes in the physical state of the substrate in the two distinct conditions. It is important to point out that conditions

used in multi-turnover FTMS and SDS-PAGE experiments were quite different from steady-state conditions used to measure affinity in Chapter 4. The concentration of ASF/SF2 that induced aggregation was much higher than the dynamic range which defined the nano-molar affinity of the substrate. We have never observed aggregation of ASF/SF2 at nano-molar concentrations. Furthermore, the presence of BSA at 3 mg/ml was critical for the stability of ^{32}P assays, and absolutely incompatible with mass spectrometric and optical analyses of this system. Factors influencing the physical state of ASF/SF2 and resulting mechanisms of phosphorylation by SRPK1 are modeled in Figure 5.10. Processive phosphorylation has been shown for the refolded heterodimeric complex of SRPK1ΔS:ASF/SF2 (Aubol et al., 2003) and ASF/SF2 substrate stabilized by excess SRPK1 in single-turnover reactions (Velazquez-Dones et al., 2005). When ASF/SF2 is adjusted to reaction conditions in the presence of catalytic concentrations of SRPK1, the splicing factor is free to self-associate to form oligomeric complexes, a conclusion supported by gel filtration and sedimentation data (Figure 5.9). ASF/SF2 indeed forms soluble aggregates in the reaction conditions that yielded the distributive mechanism. It is fascinating that SRPK1 is capable of rapid and complete phosphorylation of these ASF/SF2 aggregates. Contacts on ASF/SF2 critical for SRPK1 processivity are likely masked in the aggregated state, resulting in the distributive mechanism observed in FTMS and SDS-PAGE experiments. Indeed, we have shown in single-turnover experiments that processivity is significantly diminished in the absence of the ASF/SF2 RRMs.

While we observe an apparent distributive build up of phospho-intermediates using wild-type and ASF/SF2(ΔRRM1), it is possible that this phase may reflect only

one component of the reaction. It is conceivable that SRPK1 catalyzes both processive and distributive reactions in the steady-state, but the SRPK1 bound phospho-intermediates resulting from the processive component may have reduced affinity for zip tips used for purification. Furthermore, the highly phosphorylated species generated by a processive mechanism may fly less efficiently than the minimally phosphorylated molecules produced in a distributive manner. This could occur because the mass spectrometer is ran in positive ion mode. We have some indirect evidence that a processive component may be lost in the mass spectrometric experiment. We observe a 4 minute lag in the time-dependent generation of phospho-intermediates in the steady-state (Figure 5.4). There is no such lag in the corresponding ^{32}P experiment (Figure 5.8B). However, we see a rapid rise in phospho-product in this time frame. Such findings suggest that an important initial phase of the reaction is missing in the mass spectrometric assay, but not in the steady-state radiometric assay. Until this can be resolved, it is very likely that this phase reflects the processive component of the reaction.

Aggregation of ASF/SF2 and other SR proteins has been well documented in the literature. SR proteins form aggregated structures in the nucleus called nuclear speckles that are thought to be adjacent to active sites of transcription (Hall et al., 2006). We have shown that cell-cycle signaling events induce spacer-mediated translocation of SRPK1 to the nucleus (Ding et al., 2006). Therefore, SRPK1 phosphorylation of aggregated substrates in the nucleus has important biological relevance. Phosphorylation by SRPK1 induces redistribution of SR proteins from speckles *in vivo* (Colwill et al., 1996; Yeakley et al., 1999), and prevents aggregation

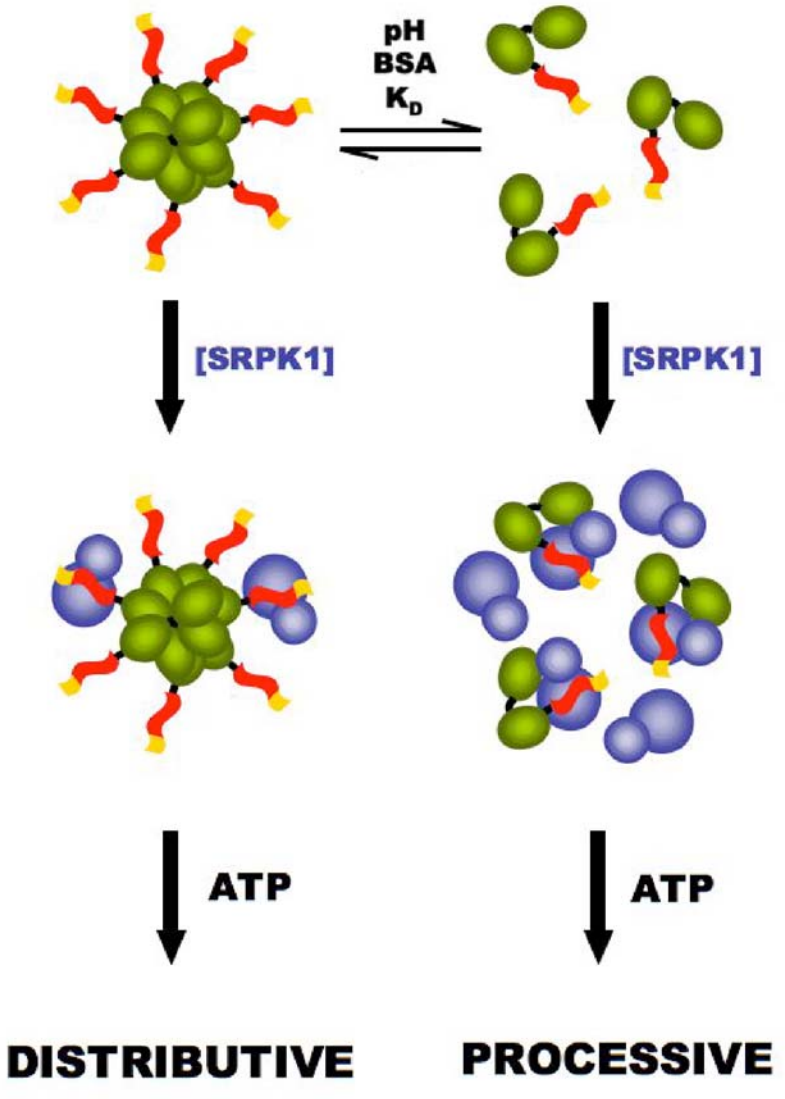

Figure 5.10 Modeling the shift in mechanism observed for SRPK1 phosphorylation of ASF/SF2. The physical state of ASF/SF2 is proposed to exist in equilibrium between an aggregated and monomeric state that is influenced by its own dissociation constant, pH, and the presence of stabilizing proteins like BSA. In addition, SRPK1 can function as a chaperone for ASF/SF2 to form heterodimeric complexes that can be co-purified at high concentrations. SRPK1 recognition of monomeric ASF/SF2 results in processive phosphorylation in reactions initiated with ATP. SRPK1 that encounters ASF/SF2 aggregates can't make all of the contacts needed for processivity. However, the kinase can phosphorylate the RS domain in a rapid distributive manner that induces dissociation.

in vitro (Nikolakaki et al., 2008). Expression of ASF/SF2 and other SR proteins in bacteria is difficult because the proteins precipitate at high concentration and neutral pH. We purify ASF/SF2 in refolded heterodimeric complexes with SRPK1, or maintained in low pH buffer to prevent precipitation. The processive result with the complex and single-turnover conditions represent the reaction catalyzed by the heterodimeric complex. Heterodimeric complexes may form between SRPK1 and ASF/SF2, as it is translated by the ribosome in the cytoplasm, prior to the transfer of phosphates in a processive manner that induces translocation to the nucleus. The processive reaction would prevent ASF/SF2 recognition of intermediate phosphorylation states by opposing catalytic factors such as phosphatases in the cytoplasm. On the other hand, a distributive mechanism of ASF/SF2 phosphorylation in the nucleus would generate intermediate states of the splicing factor in a manner that would permit concentration dependent competitive recognition events to fine tune regulation and function of these critical splicing factors.

The text of Chapter V is, in part, a reprint of the material as it appears in *Molecular Cell*, 2008, 29(5), 563-76, Ngo, J.C., Giang, N., Chakrabarti, S., Ma, C.T., Huynh, N., Hagopian, J.C., Dorrestein, P.C., Fu X.D., Adams, J.A., Ghosh, G. The dissertation author was a collaborative researcher and co-author of this publication.

Chapter VI

Future Directions

A. Arginine-Serine Repeat Domains Function as Cell Penetrating Peptides

The observations that RS repeat peptides bind with high affinity to SRPK1 (Chapter 4) motivated us to explore these molecules further. It is well documented that positively charged peptides can penetrate the plasma membrane of mammalian cells by endocytosis. The positive charge of arginine rich peptides such as TAT (trans-activator of TAR) induces binding to the surfaces of cells, and subsequent uptake by micropinocytosis into vesicles within the cytoplasm of the cell (Wadia et al., 2004). In addition, cell penetrating peptides such as TAT can carry fusion passenger proteins along with them into cells at concentrations capable of effecting cellular function (Wadia and Dowdy, 2003). Passengers carried across the plasma membrane by TAT can eventually reach the nucleus as well. When incubated in cell media with floxed-promoter-GFP expression transgenic cells, TAT fused Cre-recombinase will traverse the plasma membrane and eventually the nuclear membrane to induce GFP expression (Gump and Dowdy, 2007). We hypothesized that our RS domain peptides could function in a similar manner considering their structural similarity to TAT.

To explore the cell penetrating potential of our RS repeat peptides we performed another synthesis with a final FITC conjugation step to generate fluorescent peptides labeled on their C-terminus. The (RS)8-FITC and (RS)16-FITC peptides were compared directly to TAT-FITC in cell transduction assays. H1299 cells were treated with 1, 5, 10, 25, and 50 μM of TAT-FITC, (RS)8-FITC or (RS)16-FITC for 1 hour incubations in serum free media. Following the incubation the cells were washed extensively and treated with trypsin to remove any peptides bound to the surface of the cells. FACS analysis of the washed cells showed that both (RS)8-FITC and (RS)16-

FITC efficiently traversed the membrane of H1299 cells (Figure 5.1). Surprisingly, these peptides penetrated cells with greater efficiency than TAT-FITC at all concentrations studied.

Because current research is implicating SRPK1 and SR proteins in cancer and other disease states, these proteins have become targets for therapeutic intervention. The unique acidic pocket in the C-terminal lobe of SRPK1 may provide a means for allosteric regulation the kinase. Since they function as high-affinity inhibitors of SRPK1, it could be possible to modulate SRPK1 activity in cells transduced with SR protein peptides. Furthermore, it would be interesting to test if full length SR proteins in cell culture media could be transported to the cytoplasm of cells by micropinocytosis. Phosphorylation of the SR peptides would likely inhibit their uptake into cells due to repulsion of negative charge at the cell surface. The regulation of cell penetrating peptide function by phosphorylation and dephosphorylation could provide a mechanism for targeted delivery of fusion passenger molecules.

B. Expression, Purification, and Analysis of Additional SR Protein Family Members.

An important future goal of our group is to study SRPK1 and Clk/Sty kinetics and regiospecifictiy with other SR protein family members of ASF/SF2. I have cloned several SR protein genes into bacterial expression plasmids (see Chapter 2). Some of these proteins were expressed and purified using methods similar to those used for ASF/SF2. To confirm the purified proteins functioned as substrates for

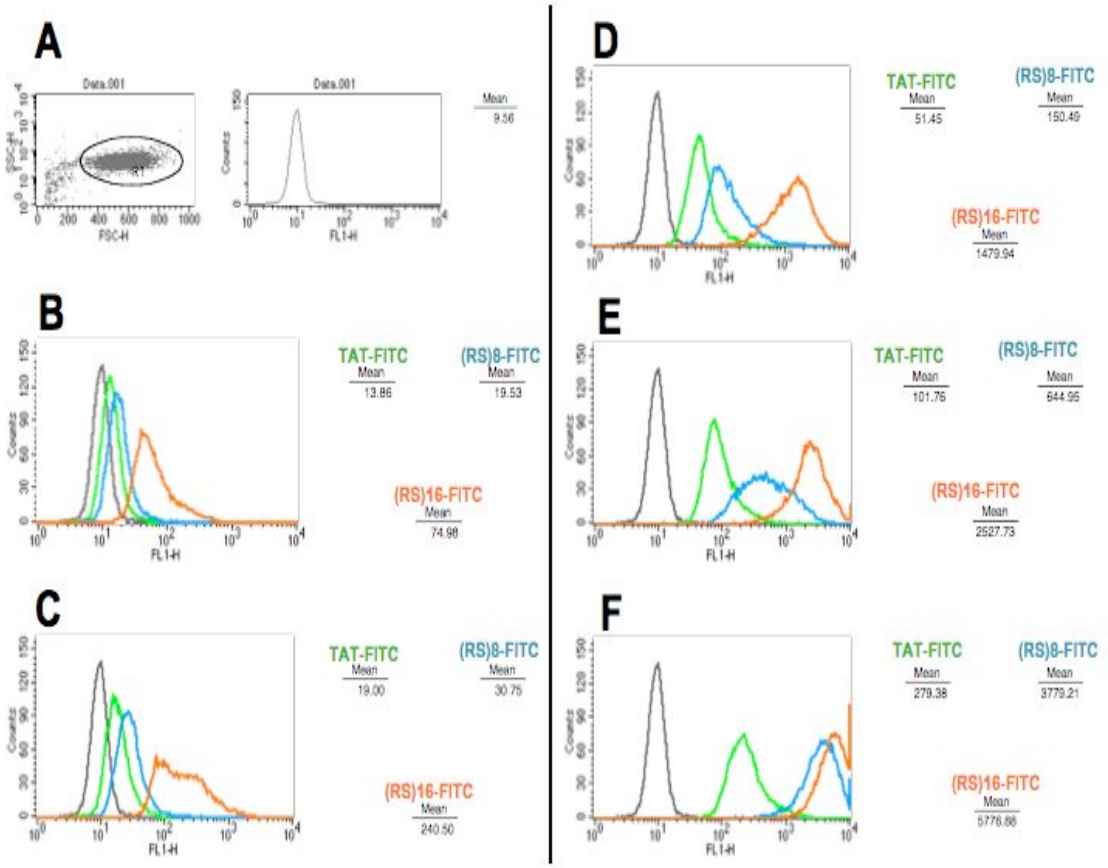

Figure 6.1 RS peptides function as cell penetrating peptides. H1299 cells were treated with increasing concentrations of TAT-FITC, (RS)8-FITC or (RS)16-FITC for 1 hour incubations in serum free media prior to trypsin wash and FACS analysis. (A) FACS data, untreated cells were used as a control. All three peptides were studied at 1 μM (B), 5 μM (C), 10 μM (D), 25 μM (E) and 50 μM (F). Mean values of filtered fluorescence intensities (FL1-H) are shown.

splicing kinases, I performed simple ^{32}P-ATP phosphorylation assays for SDS-PAGE analysis. The results of the purification and phosphorylation of these proteins are shown in Figure 6.2.

Although the SR-like kinases hTra2α and hTra2β expressed very well in *E. coli*. The SR proteins SC35 and SRp38 had low yields, most likely due to the abundance of rare Arg codons in the very large RS domains of these protein, despite being expressed in codon plus cells (Expression Technologies, plus4RA). We are very interested in SC35 considering recent research by our group reporting the critical role this protein plays in transcriptional elongation (Lin et al., 2008). Despite low yields, the SC35 protein from plus4RA cells is of the expected molecular weight, and is phosphorylated by SRPK1 (Figure 6.2). This protein should be suitable for single-turnover analysis with SR protein kinases.

Additional methods with SC35 would require more protein. The utilization of bacculovirus expression systems for the recombinant over-expression of SR proteins is considered by some to be a “gold-standard” method due to the enhanced solubility of SR proteins yielded at high-concentrations following purification. An important consideration when using insect cells for recombinant over-expression is the increased potential for post-translational modifications. These alterations can affect the function of proteins in experimental applications. We utilized MALDI-TOF MS (Figure 6.3A) and FTMS (Figure 6.3B) to characterize bacculovirus expressed His-SC35 protein (provided by Dr. Kristen Lynch). The FTMS spectra show the bacculovirus SC35 is heavily modified by multiple phosphorylations, with 10 different phosphorylation

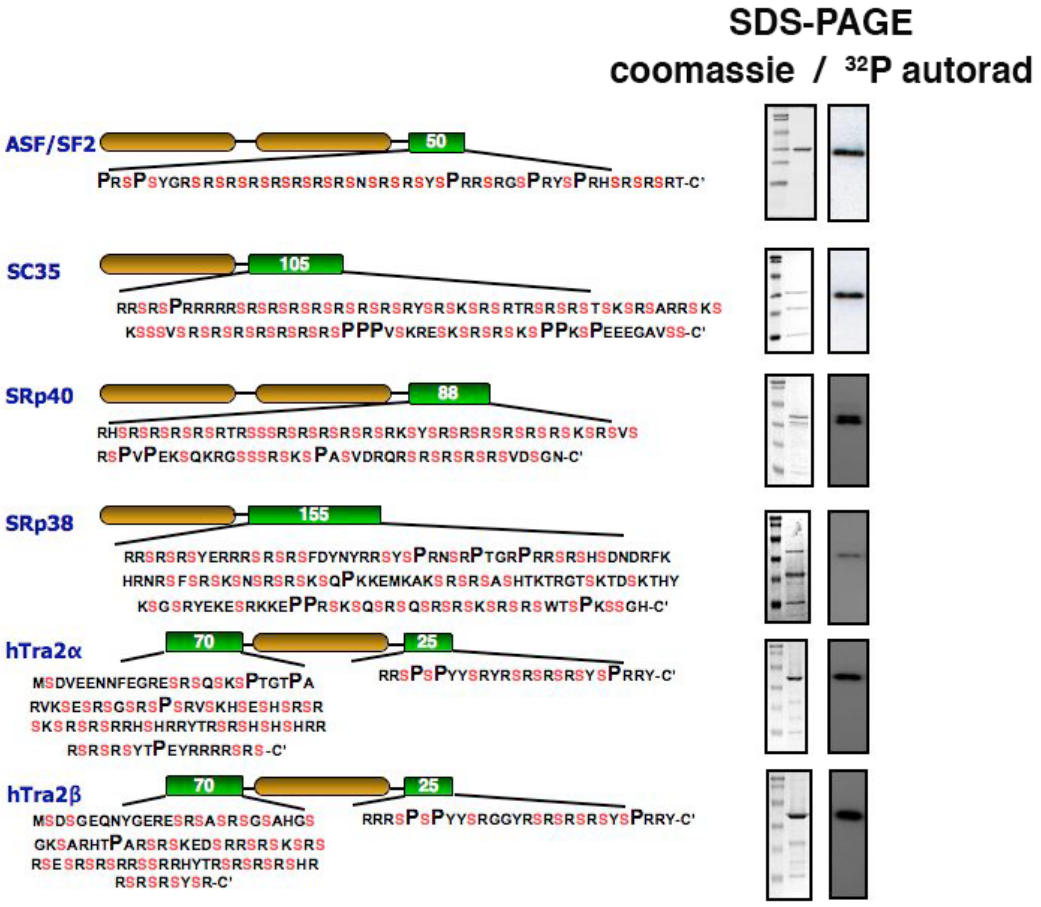

Figure 6.2 Preliminary expression and SRPK1 phosphoryation of several SR proteins. The SR-like proteins hTra2α and hTra2β expressed very well in *E. coli*. The SR proteins SC35 and SRp38 had very low yields, most likely due to the abundance of rare Arg codons in the very large RS domains of these proteins.

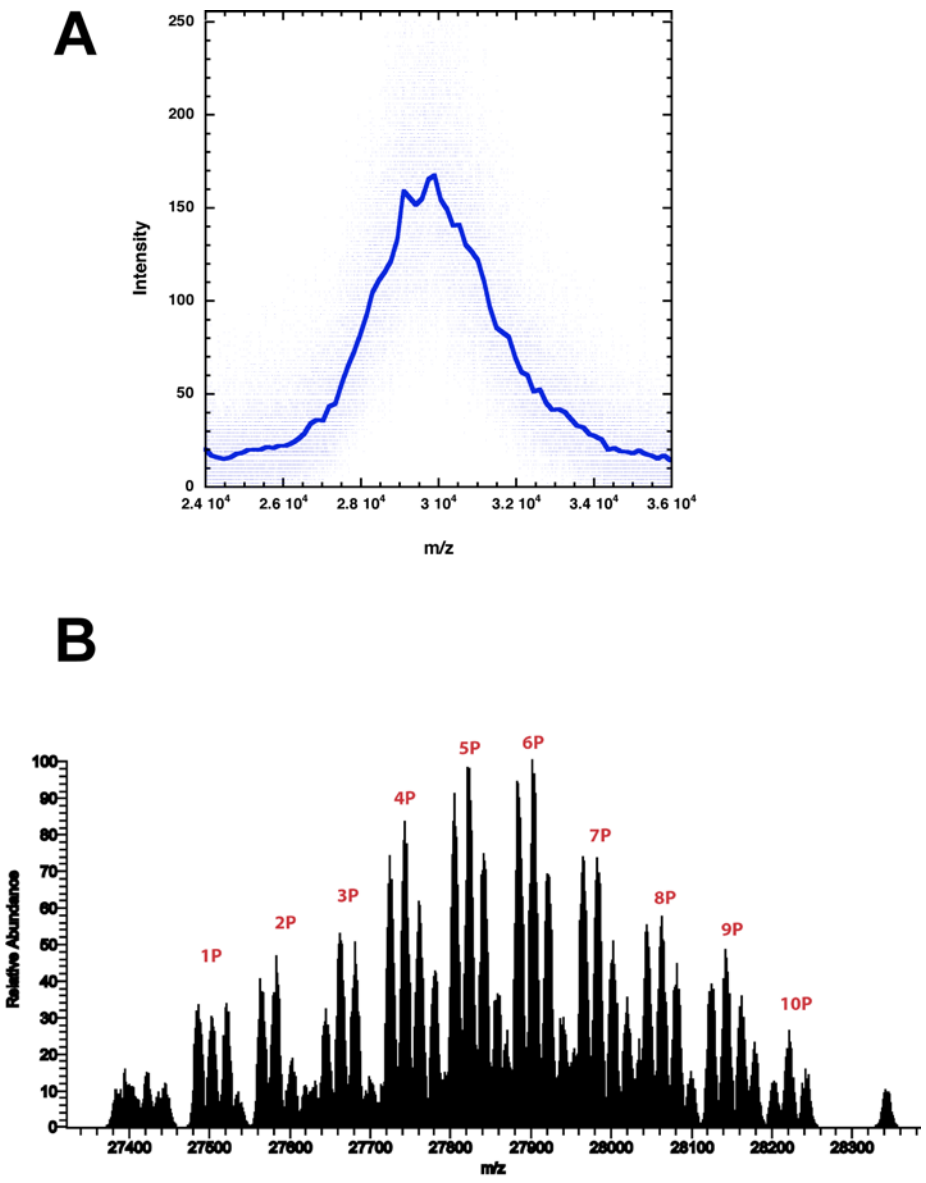

Figure 6.3 His-SC35 purified from bacculovirus expression system. A) MALDI-TOF spectra show a broad low-resolution peak. B) The FTMS spectra demonstrates clearly that the protein has significant post-translational modifications, including a distribution of phosphorylation states from 1 to 10 phosphates. The phosphorylated nature of SR proteins expressed in insect cells should be considered in cell biological experiments using this material.

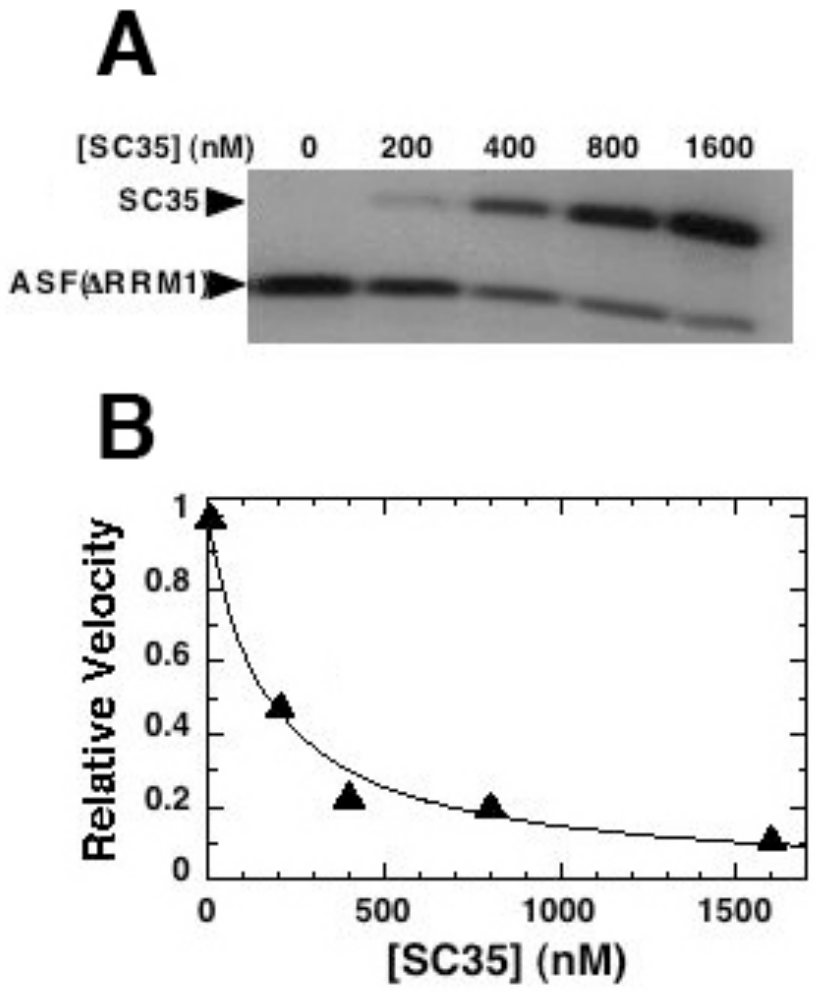

Figure 6.4 Competition assay with SRPK1 and Bacculovirus His-SC35. (A) Autoradiograph of SDS-PAGE gel. 50 nM of ASF(ΔRRM1) was monitored in competition reactions with varying concentrations of SC35 as described previously. (B) The relative velocity data of ASF(ΔRRM1) phosphorylation as a function of SC35 concentration was fit to generate a true K_I value of 160 nM for SRPK1.

states each separtated by 80 mass units. The extensive phosphorylation observed for bacculovirus SC35 may explain the enhanced solubility of SR proteins expressed in insect cells. We studied the affinity of bacculovirus SC35 in competition experiments with ASF/SF2ΔRRM1. Results of this assay showed that phosphorylated His-SC35 maintains a high-affinity for SRPK1 (K_I = 160 nM) (Figure 6.4). Because we desire to study SC35 as an unmodified substrate, the heavily phosphorylated nature of bacculovirus SC35 is problematic. We do not expect to be able to completely dephosphorylate the material with additional purification steps, considering the fact that SC35 is reported to be very resistant to dephosphorylation by phosphatases (Lin et al., 2005). A better strategy may be to mutate the rare Arg codons of the SC35 gene to ones more commonly used for *E. coli.* proteins.

Chapter VII

Conclusion

This has been an investigation into the mechanics of SR protein phosphorylation by the splicing kinases SRPK1 and Clk/Sty. Critical aspects of RNA metabolism such as constitutive and alternative splicing, mRNA export, and transcription are controlled by the SR protein family of splicing factors. SR proteins are carefully regulated by phosphorylation in vivo. SR protein localization and recruitment to and from active sites of transcription and translation in the cell are regulated by phosphorylation and dephosphorylation events that influence protein-protein interactions. The SR proteins and the kinases that regulate them have been increasingly implicated in disease states including cancer. Therefore, detailed understanding of SR kinase catalysis with SR proteins is necessary to elucidate biological mechanisms of regulation.

The finding that spacer deleted SRPK1 processively phosphorylates its substrate ASF/SF2 (Aubol et al., 2003) has implications for the biological activity of this splicing factor in mammalian cells. We have reproduced this result with full-length independently purified components in a novel efficient start-trap system that utilizes a catalytically inactive form of the kinase. The development of this assay was a significant advance for the study of mulit-site phosphorylation. Although the peptide trap based start-trap experiment was functional with the SRPK1ΔS:ASF/SF2 complex, the peptide inhibitor trap system used had several significant limitations that motivated us to develop a more efficient trapping system for additional investigations of processive phosphorylation by splicing kinases. We utilized the trapping potential of kinase-inactive mutant enzymes. A conserved lysine residue in the active site that is critical for ATP binding is commonly mutated in cell biological systems to study

phenotypic effects of catalytically inactive forms of protein kinases. Mutation of this residue did not alter substrate recognition by the kinase mediated by external docking interactions. Because the kinase-inactive trap interacted with the substrate at the same contact points as the active kinase, trapping in the start-trap assa resulted in complete displacement of the kinase. Finally, because all protein kinases can have a single lysine residue mutated in their active site to generate a kinase-inactive enzyme, this trapping system was applied to investigate the processive nature of polyphosphorylation by other kinases, namely Clk/Sty. The kinase-dead trap was effective at 50 μM for both SRPK1 and Clk/Sty. The processive result obtained for SRPK1ΔS purified as a complex with ASF/SF2 was corroborated for independently purified wild-type SRPK1 and ASF/SF2 in start-trap assays using kinase-inactive SRPK1. Clk/Sty was found to processively phosphorylate the entire RS domain of ASF/SF2. For Clk/Sty an early phospho-intermediate was populated in the active site before conversion to the fully phosphorylated form. This early form is generated at a faster rate than the fully mature species, thus, establishing two identifiable blocks of Clk/Sty modification. Interestingly, Clk/Sty is capable of switching between these two phosphorylation blocks without dissociating from the SR protein. We believe that processivity regulates the biological function of ASF/SF2 by influencing dynamic protein–protein interactions in the context of competing catalytic factors. The sequestration of early phospho-ASF/SF2 intermediates may help promote a unique folded state poised for interaction with nuclear transport proteins and/or may limit the activity of protein phosphatases that would readily lower phosphoryl content and potentially prohibit SR protein shuttling and splicing function.

We used single-turnover kinetic methods to demonstrate nano-molar affinity for both SRPK1 and Clk/Sty with ASF/SF2. This tight binding is very unique for protein kinases, and certainly contributes to their processive catalytic properties. It is clear that the spacer in SRPK1 plays a key regulatory role. Our collaborators have reported signal induced translocation of SRPK1 that is mediated by its spacer domain. Our kinetic analysis indicates that removal of the spacer did not significantly alter catalysis or affinity of kinase-substrate complex. This observation did not support a proposed model that SRPK1 translocation was mediated by a "piggy-back" mechanism via ASF/SF2. The current hypothesis is that additional protein factors, stimulated by signalling events, interact with the spacer domain of SRPK1 to facilitate nuclear import.

To investigate the unusual high affinity of SRPK1 for its substrate, we analyzed multiple domains of ASF/SF2 by developing a competitive inhibition assay from which equilibrium dissociation constants could be determined in the form K_I. The single-turnover method for K_D determination used by our lab was very labor intensive and had limitations for the study of substrates phosphorylated in a semi or non-processive manner. The competition assay was an efficient method to analyze the binding affinities of proteins independent of kinetic mechanism. Using a large series of deletion and mutant constructs, we showed that the RS domain binds as well as full-length ASF/SF2, and that the RRM1–RRM2 module itself has the capacity to form a high affinity complex with SRPK1. While the separate RRM1–RRM2 and RS domain modules have high intrinsic binding affinities, the total energies are not realized in the enzyme–substrate complex, at least prior to phosphorylation. This phenomenon

induces some strain within the complex that we believe is important for processive phosphorylation in the presence of building repulsive charge.

The kinetic data presented here allow us to speculate on how SRPK1 provides a stable yet flexible platform for the polyphosphorylation of the SR protein ASF/SF2. The processive component of ASF/SF2 phosphorylation can be dissected into several events in the following model. While the initial encounter complex is not fully optimal, it is sufficiently stable to permit the processive phosphorylation of the first three serines. It is likely that this initial modification then induces a structural change in the complex that allows further optimization of enzyme–substrate interactions. The nature of this reorganization is not understood but could involve adjustments in the RRM1–RRM2 and RS domain contacts, unfolding of β strand 4 in RRM2 (linker segment), and conformational changes in the kinase domain of SRPK1. As these events are critical for further processivity, the electropositive P+2 pocket in SRPK1 also helps to stabilize the later phosphorylation steps allowing rapid continued phosphorylation. Despite all these strategies to stabilize the phospho-complex, after about eight steps, SRPK1 releases the incompletely modified SR protein and then relies on distributive steps to finish RS1 phosphorylation. The absence of additive thermodynamics in the context of SRPK1 interaction with full-length ASF/SF2 indicates that the kinase utilizes sub-optimal recognition of its substrate during catalysis to allow the flexibility required for poly-phosphorylation of the RS domain.

We used high-resolution FT-ICRMS to refine our definition of the endpoint of ASF/SF2 phosphorylation by SRPK1. We showed that SRPK1 phosphorylates 14-15 residues of ASF/SF2, and that this endpoint did not change for RRM deletion

constructs. Based on this data, we proposed to shift the model of the RS1 domain of ASF/SF2 (residues phosphorylated by SRPK1) from residue 219 to 228. We demonstrated a clear biphasic reaction in which the initial 10 phosphorylations are incorporated within a fast phase followed by a slow phase to achieve the final endpoint. In single turnover conditions, an unaggregated enzyme-substrate complex displays processive kinetics. We demonstrated mechanistic changes that reflect enzyme kinetics with an aggregated substrate, potentially relevant to the phosphorylation of ASF/SF2 in nuclear speckles. The aggregated state of ASF/SF2 was induced by high concentrations at neutral pH, the lack of stabilizing buffer components (3 mg/ml BSA), and the absence of equal molar concentrations of SRPK1. Most significantly, we showed that the phospho-serine observed in the SRPK1ΔNS:ASF/SF2ΔRRM1 crystal structure was due to ATP contaminated AMPPNP. Therefore, we proved that this phospho-serine represented the initial phosphorylation step of the multi-site reaction with the ASF/SF2 substrate. The phospho-serine was bound to basic residues in a pocket defined as the P+2 pocket. Considering the observed density in the structure for the N-terminal portion of the RS domain, and the linear distance between R210 and the positively charged surface where the phospho-serine binds the serine that underwent phosphorylation was located at the C-terminus of the ASF/SF2(ΔRRM1ΔRS2) construct. This observation is consistent with recent biochemical experiments that show SRPK1 initiates directional phosphorylation of ASF/SF2 from C' to N' (Ma et al., 2008). Therefore, the P+2 binding of phospho-serine explains the directional nature of ASF/SF2 phosphorylation

by preventing backtracking and enhancing affinity of the substrate as serines sequentially slide through the active site of SRPK1.

Future work will involve the study of additional SR proteins. The use of bacculoviral expression systems generates SR proteins that are heavily modified by phosphorylation. Bacterial expression is more desirable for our purposes to generate protein in a state that is free of post translational modifications. To get the lab moving in this direction, I have cloned multiple SR protein family members, and their RS domains, from mammalian constucts into bacterial expression plasmids.

References

Akker, S.A., Smith, P.J., and Chew, S.L. (2001). Nuclear post-transcriptional control of gene expression. J Mol Endocrinol 27, 123-131.

Allemand, E., Gattoni, R., Bourbon, H.M., Stevenin, J., Caceres, J.F., Soret, J., and Tazi, J. (2001). Distinctive features of Drosophila alternative splicing factor RS domain: implication for specific phosphorylation, shuttling, and splicing activation. Mol Cell Biol 21, 1345-1359.

Aubol, B.E., Chakrabarti, S., Ngo, J., Shaffer, J., Nolen, B., Fu, X.D., Ghosh, G., and Adams, J.A. (2003). Processive phosphorylation of alternative splicing factor/splicing factor 2. Proc Natl Acad Sci U S A 100, 12601-12606.

Ben-David, Y., Letwin, K., Tannock, L., Bernstein, A., and Pawson, T. (1991). A mammalian protein kinase with potential for serine/threonine and tyrosine phosphorylation is related to cell cycle regulators. EMBO J 10, 317-325.

Black, D.L. (2000). Protein diversity from alternative splicing: a challenge for bioinformatics and post-genome biology. Cell 103, 367-370.

Blaustein, M., Pelisch, F., Tanos, T., Munoz, M.J., Wengier, D., Quadrana, L., Sanford, J.R., Muschietti, J.P., Kornblihtt, A.R., Caceres, J.F., et al. (2005). Concerted regulation of nuclear and cytoplasmic activities of SR proteins by AKT. Nat Struct Mol Biol 12, 1037-1044.

Blencowe, B.J. (2000). Exonic splicing enhancers: mechanism of action, diversity and role in human genetic diseases. Trends Biochem Sci 25, 106-110.

Bouton, A.H., Riggins, R.B., and Bruce-Staskal, P.J. (2001). Functions of the adapter protein Cas: signal convergence and the determination of cellular responses. Oncogene 20, 6448-6458.

Brook, J.D., McCurrach, M.E., Harley, H.G., Buckler, A.J., Church, D., Aburatani, H., Hunter, K., Stanton, V.P., Thirion, J.P., Hudson, T., et al. (1992). Molecular basis of myotonic dystrophy: expansion of a trinucleotide (CTG) repeat at the 3' end of a transcript encoding a protein kinase family member. Cell 69, 385.

Buxton, J., Shelbourne, P., Davies, J., Jones, C., Van Tongeren, T., Aslanidis, C., de Jong, P., Jansen, G., Anvret, M., Riley, B., et al. (1992). Detection of an unstable fragment of DNA specific to individuals with myotonic dystrophy. Nature 355, 547-548.

Caceres, J.F., and Krainer, A.R. (1993). Functional analysis of pre-mRNA splicing factor SF2/ASF structural domains. EMBO J 12, 4715-4726.

Cao, W., Jamison, S.F., and Garcia-Blanco, M.A. (1997). Both phosphorylation and dephosphorylation of ASF/SF2 are required for pre-mRNA splicing in vitro. RNA 3, 1456-1467.

Chew, S.L., Liu, H.X., Mayeda, A., and Krainer, A.R. (1999). Evidence for the function of an exonic splicing enhancer after the first catalytic step of pre-mRNA splicing. Proc Natl Acad Sci U S A 96, 10655-10660.

Colwill, K., Feng, L.L., Yeakley, J.M., Gish, G.D., Caceres, J.F., Pawson, T., and Fu, X.D. (1996a). SRPK1 and Clk/Sty protein kinases show distinct substrate specificities for serine/arginine-rich splicing factors. J Biol Chem 271, 24569-24575.

Colwill, K., Pawson, T., Andrews, B., Prasad, J., Manley, J.L., Bell, J.C., and Duncan, P.I. (1996b). The Clk/Sty protein kinase phosphorylates SR splicing factors and regulates their intranuclear distribution. EMBO J 15, 265-275.

Coovert, D.D., Le, T.T., McAndrew, P.E., Strasswimmer, J., Crawford, T.O., Mendell, J.R., Coulson, S.E., Androphy, E.J., Prior, T.W., and Burghes, A.H. (1997). The survival motor neuron protein in spinal muscular atrophy. Hum Mol Genet 6, 1205-1214.

Cyert, M.S. (2001). Regulation of nuclear localization during signaling. J Biol Chem 276, 20805-20808.

D'Souza, I., Poorkaj, P., Hong, M., Nochlin, D., Lee, V.M., Bird, T.D., and Schellenberg, G.D. (1999). Missense and silent tau gene mutations cause frontotemporal dementia with parkinsonism-chromosome 17 type, by affecting multiple alternative RNA splicing regulatory elements. Proc Natl Acad Sci U S A 96, 5598-5603.

Dahmus, M.E. (1996). Reversible phosphorylation of the C-terminal domain of RNA polymerase II. J Biol Chem 271, 19009-19012.

Dajani, R., Fraser, E., Roe, S.M., Young, N., Good, V., Dale, T.C., and Pearl, L.H. (2001). Crystal structure of glycogen synthase kinase 3 beta: structural basis for phosphate-primed substrate specificity and autoinhibition. Cell 105, 721-732.

Ding, J.H., Zhong, X.Y., Hagopian, J.C., Cruz, M.M., Ghosh, G., Feramisco, J., Adams, J.A., and Fu, X.D. (2006). Regulated cellular partitioning of SR protein-specific kinases in mammalian cells. Mol Biol Cell 17, 876-885.

Du, C., McGuffin, M.E., Dauwalder, B., Rabinow, L., and Mattox, W. (1998). Protein phosphorylation plays an essential role in the regulation of alternative splicing and sex determination in Drosophila. Mol Cell 2, 741-750.

Duncan, P.I., Stojdl, D.F., Marius, R.M., Scheit, K.H., and Bell, J.C. (1998). The Clk2 and Clk3 dual-specificity protein kinases regulate the intranuclear distribution of SR proteins and influence pre-mRNA splicing. Exp Cell Res 241, 300-308.

Duyster, J., Baskaran, R., and Wang, J.Y. (1995). Src homology 2 domain as a specificity determinant in the c-Abl-mediated tyrosine phosphorylation of the RNA polymerase II carboxyl-terminal repeated domain. Proc Natl Acad Sci U S A 92, 1555-1559.

Faustino, N.A., and Cooper, T.A. (2003). Pre-mRNA splicing and human disease. Genes Dev 17, 419-437.

Fiol, C.J., Wang, A., Roeske, R.W., and Roach, P.J. (1990). Ordered multisite protein phosphorylation. Analysis of glycogen synthase kinase 3 action using model peptide substrates. J Biol Chem 265, 6061-6065.

Fischer, D.C., Noack, K., Runnebaum, I.B., Watermann, D.O., Kieback, D.G., Stamm, S., and Stickeler, E. (2004). Expression of splicing factors in human ovarian cancer. Oncol Rep 11, 1085-1090.

Frame, S., Cohen, P., and Biondi, R.M. (2001). A common phosphate binding site explains the unique substrate specificity of GSK3 and its inactivation by phosphorylation. Mol Cell 7, 1321-1327.

Fu, X.D. (1995). The superfamily of arginine/serine-rich splicing factors. RNA 1, 663-680.

Fu, X.D., and Maniatis, T. (1990). Factor required for mammalian spliceosome assembly is localized to discrete regions in the nucleus. Nature 343, 437-441.

Fu, Y.H., Pizzuti, A., Fenwick, R.G., Jr., King, J., Rajnarayan, S., Dunne, P.W., Dubel, J., Nasser, G.A., Ashizawa, T., de Jong, P., et al. (1992). An unstable triplet repeat in a gene related to myotonic muscular dystrophy. Science 255, 1256-1258.

Fukuhara, T., Hosoya, T., Shimizu, S., Sumi, K., Oshiro, T., Yoshinaka, Y., Suzuki, M., Yamamoto, N., Herzenberg, L.A., and Hagiwara, M. (2006). Utilization of host SR protein kinases and RNA-splicing machinery during viral replication. Proc Natl Acad Sci U S A 103, 11329-11333.

Ghigna, C., Giordano, S., Shen, H., Benvenuto, F., Castiglioni, F., Comoglio, P.M., Green, M.R., Riva, S., and Biamonti, G. (2005). Cell motility is controlled by SF2/ASF through alternative splicing of the Ron protooncogene. Mol Cell 20, 881-890.

Ghigna, C., Moroni, M., Porta, C., Riva, S., and Biamonti, G. (1998). Altered expression of heterogenous nuclear ribonucleoproteins and SR factors in human colon adenocarcinomas. Cancer Res 58, 5818-5824.

Graveley, B.R. (2000). Sorting out the complexity of SR protein functions. RNA 6, 1197-1211.

Graveley, B.R. (2001). Alternative splicing: increasing diversity in the proteomic world. Trends Genet 17, 100-107.

Gui, J.F., Lane, W.S., and Fu, X.D. (1994a). A serine kinase regulates intracellular localization of splicing factors in the cell cycle. Nature 369, 678-682.

Gui, J.F., Tronchere, H., Chandler, S.D., and Fu, X.D. (1994b). Purification and characterization of a kinase specific for the serine- and arginine-rich pre-mRNA splicing factors. Proc Natl Acad Sci U S A 91, 10824-10828.

Gump, J.M., and Dowdy, S.F. (2007). TAT transduction: the molecular mechanism and therapeutic prospects. Trends Mol Med 13, 443-448.

Gunthert, U., Hofmann, M., Rudy, W., Reber, S., Zoller, M., Haussmann, I., Matzku, S., Wenzel, A., Ponta, H., and Herrlich, P. (1991). A new variant of glycoprotein CD44 confers metastatic potential to rat carcinoma cells. Cell 65, 13-24.

Guo, Y., Ma, J., Wang, J., Che, X., Narula, J., Bigby, M., Wu, M., and Sy, M.S. (1994). Inhibition of human melanoma growth and metastasis in vivo by anti-CD44 monoclonal antibody. Cancer Res 54, 1561-1565.

Gutfreund, H. (1995). Kinetics for the life sciences: receptors, transmitters and catalysts (Cambridge, Cambridge University Press).

Hagiwara, M. (2005). Alternative splicing: a new drug target of the post-genome era. Biochim Biophys Acta 1754, 324-331.

Hagopian, J.C., Ma, C.T., Meade, B.R., Albuquerque, C.P., Ngo, J.C., Ghosh, G., Jennings, P.A., Fu, X.D., and Adams, J.A. (2008). Adaptable molecular interactions guide phosphorylation of the SR protein ASF/SF2 by SRPK1. J Mol Biol 382, 894-909.

Hall, L.L., Smith, K.P., Byron, M., and Lawrence, J.B. (2006). Molecular anatomy of a speckle. Anat Rec A Discov Mol Cell Evol Biol 288, 664-675.

Hannink, M., and Donoghue, D.J. (1985). Lysine residue 121 in the proposed ATP-binding site of the v-mos protein is required for transformation. Proc Natl Acad Sci U S A 82, 7894-7898.

Hong, M., Zhukareva, V., Vogelsberg-Ragaglia, V., Wszolek, Z., Reed, L., Miller, B.I., Geschwind, D.H., Bird, T.D., McKeel, D., Goate, A., et al. (1998). Mutation-specific functional impairments in distinct tau isoforms of hereditary FTDP-17. Science 282, 1914-1917.

Howell, B.W., Afar, D.E., Lew, J., Douville, E.M., Icely, P.L., Gray, D.A., and Bell, J.C. (1991). STY, a tyrosine-phosphorylating enzyme with sequence homology to serine/threonine kinases. Mol Cell Biol 11, 568-572.

Huang, Y., Gattoni, R., Stevenin, J., and Steitz, J.A. (2003). SR splicing factors serve as adapter proteins for TAP-dependent mRNA export. Mol Cell 11, 837-843.

Huang, Y., and Steitz, J.A. (2001). Splicing factors SRp20 and 9G8 promote the nucleocytoplasmic export of mRNA. Mol Cell 7, 899-905.

Huang, Y., and Steitz, J.A. (2005). SRprises along a messenger's journey. Mol Cell 17, 613-615.

Huang, Y., Yario, T.A., and Steitz, J.A. (2004). A molecular link between SR protein dephosphorylation and mRNA export. Proc Natl Acad Sci U S A 101, 9666-9670.

Jamison, S.F., Pasman, Z., Wang, J., Will, C., Luhrmann, R., Manley, J.L., and Garcia-Blanco, M.A. (1995). U1 snRNP-ASF/SF2 interaction and 5' splice site recognition: characterization of required elements. Nucleic Acids Res 23, 3260-3267.

Jeffery, D.A., Springer, M., King, D.S., and O'Shea, E.K. (2001). Multi-site phosphorylation of Pho4 by the cyclin-CDK Pho80-Pho85 is semi-processive with site preference. J Mol Biol 306, 997-1010.

Jiang, Z.H., and Wu, J.Y. (1999). Alternative splicing and programmed cell death. Proc Soc Exp Biol Med 220, 64-72.

Kallunki, T., Deng, T., Hibi, M., and Karin, M. (1996). c-Jun can recruit JNK to phosphorylate dimerization partners via specific docking interactions. Cell 87, 929-939.

Kallunki, T., Su, B., Tsigelny, I., Sluss, H.K., Derijard, B., Moore, G., Davis, R., and Karin, M. (1994). JNK2 contains a specificity-determining region responsible for efficient c-Jun binding and phosphorylation. Genes Dev 8, 2996-3007.

Karni, R., de Stanchina, E., Lowe, S.W., Sinha, R., Mu, D., and Krainer, A.R. (2007). The gene encoding the splicing factor SF2/ASF is a proto-oncogene. Nat Struct Mol Biol 14, 185-193.

Karni, R., Hippo, Y., Lowe, S.W., and Krainer, A.R. (2008). The splicing-factor oncoprotein SF2/ASF activates mTORC1. Proc Natl Acad Sci U S A 105, 15323-15327.

Kohtz, J.D., Jamison, S.F., Will, C.L., Zuo, P., Luhrmann, R., Garcia-Blanco, M.A., and Manley, J.L. (1994). Protein-protein interactions and 5'-splice-site recognition in mammalian mRNA precursors. Nature 368, 119-124.

Koizumi, J., Okamoto, Y., Onogi, H., Mayeda, A., Krainer, A.R., and Hagiwara, M. (1999). The subcellular localization of SF2/ASF is regulated by direct interaction with SR protein kinases (SRPKs). J Biol Chem 274, 11125-11131.

Komeili, A., and O'Shea, E.K. (1999). Roles of phosphorylation sites in regulating activity of the transcription factor Pho4. Science 284, 977-980.

Krainer, A.R., Conway, G.C., and Kozak, D. (1990). The essential pre-mRNA splicing factor SF2 influences 5' splice site selection by activating proximal sites. Cell 62, 35-42.

Krainer, A.R., and Maniatis, T. (1985). Multiple factors including the small nuclear ribonucleoproteins U1 and U2 are necessary for pre-mRNA splicing in vitro. Cell 42, 725-736.

Krawczak, M., Reiss, J., and Cooper, D.N. (1992). The mutational spectrum of single base-pair substitutions in mRNA splice junctions of human genes: causes and consequences. Hum Genet 90, 41-54.

Lai, M.C., Lin, R.I., and Tarn, W.Y. (2001). Transportin-SR2 mediates nuclear import of phosphorylated SR proteins. Proc Natl Acad Sci U S A 98, 10154-10159.

Lai, M.C., and Tarn, W.Y. (2004). Hypophosphorylated ASF/SF2 binds TAP and is present in messenger ribonucleoproteins. J Biol Chem 279, 31745-31749.

Lewis, L.A., Chung, C.D., Chen, J., Parnes, J.R., Moran, M., Patel, V.P., and Miceli, M.C. (1997). The Lck SH2 phosphotyrosine binding site is critical for efficient TCR-induced processive tyrosine phosphorylation of the zeta-chain and IL-2 production. J Immunol 159, 2292-2300.

Li, X., and Manley, J.L. (2005). Inactivation of the SR protein splicing factor ASF/SF2 results in genomic instability. Cell 122, 365-378.

Lin, C.L., Bristol, L.A., Jin, L., Dykes-Hoberg, M., Crawford, T., Clawson, L., and Rothstein, J.D. (1998). Aberrant RNA processing in a neurodegenerative disease: the cause for absent EAAT2, a glutamate transporter, in amyotrophic lateral sclerosis. Neuron 20, 589-602.

Lin, S., Coutinho-Mansfield, G., Wang, D., Pandit, S., and Fu, X.D. (2008). The splicing factor SC35 has an active role in transcriptional elongation. Nat Struct Mol Biol 15, 819-826.

Lin, S., Xiao, R., Sun, P., Xu, X., and Fu, X.D. (2005). Dephosphorylation-dependent sorting of SR splicing factors during mRNP maturation. Mol Cell 20, 413-425.

Liu, H.X., Chew, S.L., Cartegni, L., Zhang, M.Q., and Krainer, A.R. (2000). Exonic splicing enhancer motif recognized by human SC35 under splicing conditions. Mol Cell Biol 20, 1063-1071.

Ma, C.T., Velazquez-Dones, A., Hagopian, J.C., Ghosh, G., Fu, X.D., and Adams, J.A. (2008). Ordered multi-site phosphorylation of the splicing factor ASF/SF2 by SRPK1. J Mol Biol 376, 55-68.

Madhusudan, Trafny, E.A., Xuong, N.H., Adams, J.A., Ten Eyck, L.F., Taylor, S.S., and Sowadski, J.M. (1994). cAMP-dependent protein kinase: crystallographic insights into substrate recognition and phosphotransfer. Protein Sci 3, 176-187.

Mahadevan, M., Tsilfidis, C., Sabourin, L., Shutler, G., Amemiya, C., Jansen, G., Neville, C., Narang, M., Barcelo, J., O'Hoy, K., et al. (1992). Myotonic dystrophy mutation: an unstable CTG repeat in the 3' untranslated region of the gene. Science 255, 1253-1255.

Marshall, A.G., Hendrickson, C.L., and Jackson, G.S. (1998). Fourier transform ion cyclotron resonance mass spectrometry: a primer. Mass Spectrom Rev 17, 1-35.

Matsuda, M., Mayer, B.J., Fukui, Y., and Hanafusa, H. (1990). Binding of transforming protein, P47gag-crk, to a broad range of phosphotyrosine-containing proteins. Science 248, 1537-1539.

Mayer, B.J., Hirai, H., and Sakai, R. (1995). Evidence that SH2 domains promote processive phosphorylation by protein-tyrosine kinases. Curr Biol 5, 296-305.

McClure, W.R., and Chow, Y. (1980). The kinetics and processivity of nucleic acid polymerases. Methods Enzymol 64, 277-297.

Mermoud, J.E., Cohen, P., and Lamond, A.I. (1992). Ser/Thr-specific protein phosphatases are required for both catalytic steps of pre-mRNA splicing. Nucleic Acids Res 20, 5263-5269.

Misteli, T., Caceres, J.F., Clement, J.Q., Krainer, A.R., Wilkinson, M.F., and Spector, D.L. (1998). Serine phosphorylation of SR proteins is required for their recruitment to sites of transcription in vivo. J Cell Biol 143, 297-307.

Misteli, T., and Spector, D.L. (1999). RNA polymerase II targets pre-mRNA splicing factors to transcription sites in vivo. Mol Cell 3, 697-705.

Modrek, B., and Lee, C. (2002). A genomic view of alternative splicing. Nat Genet 30, 13-19.

Muraki, M., Ohkawara, B., Hosoya, T., Onogi, H., Koizumi, J., Koizumi, T., Sumi, K., Yomoda, J., Murray, M.V., Kimura, H., et al. (2004). Manipulation of alternative splicing by a newly developed inhibitor of Clks. J Biol Chem 279, 24246-24254.

Ngo, J.C., Chakrabarti, S., Ding, J.H., Velazquez-Dones, A., Nolen, B., Aubol, B.E., Adams, J.A., Fu, X.D., and Ghosh, G. (2005). Interplay between SRPK and Clk/Sty kinases in phosphorylation of the splicing factor ASF/SF2 is regulated by a docking motif in ASF/SF2. Mol Cell 20, 77-89.

Ngo, J.C., Giang, K., Chakrabarti, S., Ma, C.T., Huynh, N., Hagopian, J.C., Dorrestein, P.C., Fu, X.D., Adams, J.A., and Ghosh, G. (2008). A sliding docking interaction is essential for sequential and processive phosphorylation of an SR protein by SRPK1. Mol Cell 29, 563-576.

Nikolakaki, E., Drosou, V., Sanidas, I., Peidis, P., Papamarcaki, T., Iakoucheva, L.M., and Giannakouros, T. (2008). RNA association or phosphorylation of the RS domain prevents aggregation of RS domain-containing proteins. Biochim Biophys Acta 1780, 214-225.

Nolen, B., Yun, C.Y., Wong, C.F., McCammon, J.A., Fu, X.D., and Ghosh, G. (2001). The structure of Sky1p reveals a novel mechanism for constitutive activity. Nat Struct Biol 8, 176-183.

Padgett, R.A., Grabowski, P.J., Konarska, M.M., Seiler, S., and Sharp, P.A. (1986). Splicing of messenger RNA precursors. Annu Rev Biochem 55, 1119-1150.

Patwardhan, P., Shen, Y., Goldberg, G.S., and Miller, W.T. (2006). Individual Cas phosphorylation sites are dispensable for processive phosphorylation by Src and anchorage-independent cell growth. J Biol Chem 281, 20689-20697.

Pellicena, P., and Miller, W.T. (2001). Processive phosphorylation of p130Cas by Src depends on SH3-polyproline interactions. J Biol Chem 276, 28190-28196.

Prasad, J., Colwill, K., Pawson, T., and Manley, J.L. (1999). The protein kinase Clk/Sty directly modulates SR protein activity: both hyper- and hypophosphorylation inhibit splicing. Mol Cell Biol 19, 6991-7000.

Prasad, J., and Manley, J.L. (2003). Regulation and substrate specificity of the SR protein kinase Clk/Sty. Mol Cell Biol 23, 4139-4149.

Proudfoot, N.J., Furger, A., and Dye, M.J. (2002). Integrating mRNA processing with transcription. Cell 108, 501-512.

Resing, K.A., and Ahn, N.G. (1997). Protein phosphorylation analysis by electrospray ionization-mass spectrometry. Methods Enzymol 283, 29-44.

Reynolds, A.B., Kanner, S.B., Wang, H.C., and Parsons, J.T. (1989). Stable association of activated pp60src with two tyrosine-phosphorylated cellular proteins. Mol Cell Biol 9, 3951-3958.

Roscigno, R.F., and Garcia-Blanco, M.A. (1995). SR proteins escort the U4/U6.U5 tri-snRNP to the spliceosome. RNA 1, 692-706.

Ruest, P.J., Shin, N.Y., Polte, T.R., Zhang, X., and Hanks, S.K. (2001). Mechanisms of CAS substrate domain tyrosine phosphorylation by FAK and Src. Mol Cell Biol 21, 7641-7652.

Sacco-Bubulya, P., and Spector, D.L. (2002). Disassembly of interchromatin granule clusters alters the coordination of transcription and pre-mRNA splicing. J Cell Biol 156, 425-436.

Sakai, R., Iwamatsu, A., Hirano, N., Ogawa, S., Tanaka, T., Mano, H., Yazaki, Y., and Hirai, H. (1994). A novel signaling molecule, p130, forms stable complexes in vivo with v-Crk and v-Src in a tyrosine phosphorylation-dependent manner. EMBO J 13, 3748-3756.

Sanford, J.R., Gray, N.K., Beckmann, K., and Caceres, J.F. (2004). A novel role for shuttling SR proteins in mRNA translation. Genes Dev 18, 755-768.

Segel, I.H. (1975). Enzyme Kinetics: Behavior and Analysis of Rapid Equilibrium and Steady-State Enzyme Systems (New York, Wiley).

Sharp, P.A. (1985). On the origin of RNA splicing and introns. Cell 42, 397-400.

Shen, H., and Green, M.R. (2004). A pathway of sequential arginine-serine-rich domain-splicing signal interactions during mammalian spliceosome assembly. Mol Cell 16, 363-373.

Shen, H., Kan, J.L., and Green, M.R. (2004). Arginine-serine-rich domains bound at splicing enhancers contact the branchpoint to promote prespliceosome assembly. Mol Cell 13, 367-376.

Stickeler, E., Kittrell, F., Medina, D., and Berget, S.M. (1999). Stage-specific changes in SR splicing factors and alternative splicing in mammary tumorigenesis. Oncogene 18, 3574-3582.

Stojdl, D.F., and Bell, J.C. (1999). SR protein kinases: the splice of life. Biochem Cell Biol 77, 293-298.

Tanner, S., Shu, H., Frank, A., Wang, L.C., Zandi, E., Mumby, M., Pevzner, P.A., and Bafna, V. (2005). InsPecT: identification of posttranslationally modified peptides from tandem mass spectra. Anal Chem 77, 4626-4639.

Velazquez-Dones, A., Hagopian, J.C., Ma, C.T., Zhong, X.Y., Zhou, H., Ghosh, G., Fu, X.D., and Adams, J.A. (2005). Mass spectrometric and kinetic analysis of ASF/SF2 phosphorylation by SRPK1 and Clk/Sty. J Biol Chem 280, 41761-41768.

Venables, J.P. (2006). Unbalanced alternative splicing and its significance in cancer. Bioessays 28, 378-386.

Wadia, J.S., and Dowdy, S.F. (2003). Modulation of cellular function by TAT mediated transduction of full length proteins. Curr Protein Pept Sci 4, 97-104.

Wadia, J.S., Stan, R.V., and Dowdy, S.F. (2004). Transducible TAT-HA fusogenic peptide enhances escape of TAT-fusion proteins after lipid raft macropinocytosis. Nat Med 10, 310-315.

Wang, H.Y., Arden, K.C., Bermingham, J.R., Jr., Viars, C.S., Lin, W., Boyer, A.D., and Fu, X.D. (1999). Localization of serine kinases, SRPK1 (SFRSK1) and SRPK2 (SFRSK2), specific for the SR family of splicing factors in mouse and human chromosomes. Genomics 57, 310-315.

Wang, H.Y., Lin, W., Dyck, J.A., Yeakley, J.M., Songyang, Z., Cantley, L.C., and Fu, X.D. (1998). SRPK2: a differentially expressed SR protein-specific kinase involved in mediating the interaction and localization of pre-mRNA splicing factors in mammalian cells. J Cell Biol 140, 737-750.

Wu, J.Y., and Maniatis, T. (1993). Specific interactions between proteins implicated in splice site selection and regulated alternative splicing. Cell 75, 1061-1070.

Wu, J.Y., Tang, H., and Havlioglu, N. (2003). Alternative pre-mRNA splicing and regulation of programmed cell death. Prog Mol Subcell Biol 31, 153-185.

Xiao, S.H., and Manley, J.L. (1997). Phosphorylation of the ASF/SF2 RS domain affects both protein-protein and protein-RNA interactions and is necessary for splicing. Genes Dev 11, 334-344.

Xiao, S.H., and Manley, J.L. (1998). Phosphorylation-dephosphorylation differentially affects activities of splicing factor ASF/SF2. EMBO J 17, 6359-6367.

Yang, S.H., Galanis, A., and Sharrocks, A.D. (1999). Targeting of p38 mitogen-activated protein kinases to MEF2 transcription factors. Mol Cell Biol 19, 4028-4038.

Yeakley, J.M., Tronchere, H., Olesen, J., Dyck, J.A., Wang, H.Y., and Fu, X.D. (1999). Phosphorylation regulates in vivo interaction and molecular targeting of serine/arginine-rich pre-mRNA splicing factors. J Cell Biol 145, 447-455.

Yun, C.Y., and Fu, X.D. (2000). Conserved SR protein kinase functions in nuclear import and its action is counteracted by arginine methylation in Saccharomyces cerevisiae. J Cell Biol 150, 707-718.

Yun, C.Y., Velazquez-Dones, A.L., Lyman, S.K., and Fu, X.D. (2003). Phosphorylation-dependent and -independent nuclear import of RS domain-containing splicing factors and regulators. J Biol Chem 278, 18050-18055.

Zerbe, L.K., Pino, I., Pio, R., Cosper, P.F., Dwyer-Nield, L.D., Meyer, A.M., Port, J.D., Montuenga, L.M., and Malkinson, A.M. (2004). Relative amounts of antagonistic splicing factors, hnRNP A1 and ASF/SF2, change during neoplastic lung growth: implications for pre-mRNA processing. Mol Carcinog 41, 187-196.

Zhu, J., and Krainer, A.R. (2000). Pre-mRNA splicing in the absence of an SR protein RS domain. Genes Dev 14, 3166-3178.

Zhu, J., Mayeda, A., and Krainer, A.R. (2001). Exon identity established through differential antagonism between exonic splicing silencer-bound hnRNP A1 and enhancer-bound SR proteins. Mol Cell 8, 1351-1361.